A STATISTICAL FRAMEWORK FOR THE ANALYSIS OF THE NEURAL CONTROL OF MOVEMENT WITH AGING AND OTHER CLINICAL APPLICATIONS

A Dissertation
Presented to
The Academic Faculty

by

Ashley Nzinga Johnson

In Partial Fulfillment
of the Requirements for the Degree
Doctor of Philosophy in the
School of Electrical and Computer Engineering

Georgia Institute of Technology
May 2012

A STATISTICAL FRAMEWORK FOR THE ANALYSIS OF THE NEURAL CONTROL OF MOVEMENT WITH AGING AND OTHER CLINICAL APPLICATIONS

Approved by:

Dr. Minoru Shinohara, Advisor
School of Applied Physiology
Georgia Institute of Technology

Dr. George J. Vachtsevanos,
Co-Advisor
School of Electrical and Computer
Engineering
Georgia Institute of Technology

Dr. Bonnie H. Ferri
School of Electrical and Computer
Engineering
Georgia Institute of Technology

Dr. Ayanna M. Howard
School of Electrical and Computer
Engineering
Georgia Institute of Technology

Dr. William D. Hunt
School of Electrical and Computer
Engineering
Georgia Institute of Technology

Dr. Lewis A. Wheaton
School of Applied Physiology
Georgia Institute of Technology

Date Approved: March 2, 2012

This milestone is dedicated to my grandparents, Mr. and Mrs. Roy and Elizabeth Ross and Dr. and Mrs. Leonard W. and Annie Ruth Johnson, my maternal and paternal grandparents, respectively.

PREFACE

"There is no royal road to knowledge. [So] always strive to better your best!"

-Dr. Leonard W. Johnson

ACKNOWLEDGEMENTS

I am where I am in life because of God. Thank you Lord for blessing me with the talent, perseverance, focus, discernment, support, experiences, people and love necessary to achieve my goal.

Throughout this journey I have been inspired by so many people and events. To each of you I say thank you from the bottom of my heart, a few words of encouragement have taken me a long way. To my advisor, Dr. Minoru Shinohara, thank you for your support and the opportunity to work under your guidance. I have gained a wealth of knowledge on everything from setting up a new lab, to conducting scientific research, to publishing a manuscript. To my co-advisor, Dr. George Vachstevanos, thank you for your guidance and working with me to merge two fields of research. I would like to thank my committee members, Dr. Bonnie Ferri, Dr. Ayanna Howard, Dr. William Hunt, and Dr. Lewis Wheaton, for providing thoughtful feedback to help improve my research.

Thank you to those individuals that assisted with recruitment of subjects, in particular Dr. Christopher Hertzog from Georgia Institute of Technology for assistance with elderly subjects and Dr. Steve Wolf from Emory University for assistance with stroke subjects. A special thank you to Dr. Teresa Snow for being so generous with offering your statistical advice. Thank you to Shikhar Vohra and Vasiliy Buharin for assistance with data collection, and daily conversations ranging from data to life after grad school. Dr. Tammy McCoy and Tiara Jeter, thank you for assisting me with editing the dissertation.

The completion of my dissertation would not have been possible without the generous financial support from multiple people and organizations, in particular I would

like to acknowledge the Ford Foundation Pre-doctoral Fellowship, National Research Council (Division of the National Academy of Sciences), SURE, NSF-funded Student and Teacher Enhancement Partnership, NSF-funded Facilitating Academic Careers in Engineering and Science, Internal Business Machines, Inc., Georgia Engineering Foundation, School of Electrical and Computer Engineering, and the Georgia Institute of Technology President's Fellowship. A special thank you to Ms. Wanda Pierson and the Georgia Space Consortium.

Thank you to the many individuals that have supported me and served as positive models, in particular Dean Gary May, Dr. Raheem Beyah, Dr. Comas Haynes, Dr. Keith Oden, Dr. Christal Gordon, Dr. Tammy McCoy, Akibi Archer, Brett Matthews, Dr. Jacqueline Fairley, Dr. Otis Smart, Dr. Sekou Remy, Dr. Ayanna Howard, Dr. Donna Llewellyn, Dr. Marion Usselman, Jill Auerbach, Dr. Leyla Conrad, and Dr. Felicia Benton-Johnson. Dr. Smart, I appreciate the candid feedback you provided each step of the way. Thank you for the insight provided by Etta Pitman, Jacqueline Trappier, Tasha Torrence, Marylou Mycko and Christopher Malbrue. Thank you to the BGSA for the kinship provided over the years.

I have made so many lifelong friends throughout my time at Georgia Tech and I am so proud of all that we have accomplished. I look forward to continuing to celebrate our many accomplishments: Calvin King, Nicholas Brown, Akibi Archer, Dr. Tammy McCoy, Dr. Mela Johnson, Dr. Shara McClendon, Dr. Dimitri Hughes, Dr. Saunya Williams, Dr. Adaora Okwo, Dr. Clarence Wardell and Dr. Christianna Taylor. To the women of WPSG and my accountability partner, Dr. Benetta Johnson, your helpful suggestions have always been right on time, thank you for your support and ability to find the positive in challenging situations. To my mentor and friend Dr. Jacqueline Fairley, your journey and success continues to inspire me. Thank you for exposing me to this area of research and supporting me each step of the way.

Thank you to my undergraduate professors and mentors from Florida A&M University that encouraged me to attend graduate school and have continued to be supportive, in particular Dr. Shaundra Bryant Daily, Dr. Wanda Eugene, and Dr. Makola Abdullah.

Last, but certainly not least I would like to thank my family and friends. From day one, each of you have been supportive of my goals and celebrated with me each step of the way. Words cannot express just how grateful I am for each of you. I share this milestone with each of you: Annie Ruth Johnson, Amanda Walker, Lonnie Walker, W. Gerard Best, Antoinette Johnson, Sherilynn Kimble, Gay Brown, Allison Young, Lynette Vaughn, Tiara Jeter, Cemere' James, Sharonda Eggleton, Kayelyn Richardson, Tiffany McEntyre, Karen White, Shaquita Rahming Ridley, Dr. Twyla Thompson, and Crystal Moore Mitchell. Thank you to my spiritual family at St. Paul's Episcopal Church, in particular Fr. Robert Wright. To my fiance', Vincent Long, your patience, prayers, and comedic relief were second to none. I thank God for your special role in my love. To my father, Ronald Johnson, thank you for helping me to remember that life is a marathon and not a sprint. My PhD is just one of my many accomplishments in life. Thank you for the numerous "out of the box"' life lessons you have taught me. To my heart, my mother, Brenda Johnson Best, I do not have enough words to express all of my thanks for your sacrifice and support leading to this point. I share this moment with you. Although some of my grandparents are not here in the flesh, I would be remiss if I did not acknowledge the legacy and culture they set for hard work and attaining an education.

TABLE OF CONTENTS

LIST OF TABLES

LIST OF FIGURES

SUMMARY

The objective of this research is to develop a methodology to understand the neural control of movement with aging and applications to the stroke population. The number of Americans age 65 or older will double to ∼70 million in the next 25 years. Without in-depth research and sophisticated technologies to understand the mechanisms involved in normal neuromuscular aging, America will struggle to care for this maturing population. Research in this area will not only benefit the aging population, but the findings from healthy individuals can then be extrapolated to investigate clinical populations with disorders influencing their neural control of movement, specifically stroke patients. One in six people over the age of 55 will suffer from a stroke, with over 1.1 million elderly (>65 years) Americans reporting impairment of motor function post-stroke [108].

The work in this dissertation focuses on tasks requiring a level of fine motor control in the upper extremity because activities involved in daily living require some level of fine motor control (e.g., dressing, bathing, preparing a meal), and the ability to perform such tasks can degrade with age and post-stroke. In the controlled experiments, tasks were selected that represent the multiple modalities that might be involved in performing a task for daily living (e.g., unilateral motor, bilateral motor, and motor cognitive). To address the research statement of developing a methodology to interpret the neural control of movement with aging and stroke populations, the project was divided into four parts. The first portion considers the aspect of the neural control of movement with a focus on task. The second portion incorporated task in the context of healthy aging. While the first two parts took more of a statistical

approach, the third portion models the neural control of movement with aging taking a data mining approach. Lastly, the fourth portion investigates the neural control of movement in the stroke population.

The methodological approach incorporated traditional features from the physiology community (corticomuscular coherence and power spectral density) with the addition of features from time, frequency, and information theory domains. Additionally, the use of cepstral analysis was modified toward this application to analyze electroencephalogram and electromyogram signals. Optimal features for distinguishing between young and elderly adults were obtained using forward, backward, and branch-and-bound feature selection algorithms. The inclusion and optimization of cepstral features significantly improved classification accuracy. Additionally, classification of young and elderly adults using Gaussian Mixture Models with Minimum Classification Error improved overall accuracy values.

Contributions from the dissertation include demonstration of the change in correlated activity between muscle and brain with fine motor simple and complex dual tasks; demonstration of the application and optimization of cepstral analysis for analysis of muscle and brain activity; a quantitative feature library for characterizing the neural control of movement with aging under three task conditions; and a methodology for the selection and classification of features to characterize the neural control of movement. Additionally, the dissertation provides functional insight for the association of features with tasks, aging, and clinical conditions. The results of the work are significant because the automated investigation of the neural control of movement with aging is not well established for the physiology community. From these contributions, future potential contributions are: 1) a methodology for physiologists to analyze and interpret data; 2) a computational tool to provide early detection of neuromuscular disorders in healthy populations; 3) a methodology for assessing the status and rehabilitation of patient populations.

CHAPTER I

INTRODUCTION

1.1 Problem Definition

According to the National Institute on Aging (NIA) Health Disparities Strategic Plan for 2009-2013, the number of Americans age 65 or older (∼35 million) will double in the next 25 years [98]. The NIA has stated that one of the challenges for the 21st Century is to better understand the aging process "to make these added years as healthy and productive as possible" [98]. As a result, the NIA aims to "understand the mechanisms involved in normal brain aging; the role of cognition in everyday functioning; protective factors for sensory, motor, emotional, and cognitive function; and the pathogenesis of Alzheimer's Disease and other neurodegenerative disorders of aging within health disparity populations" [98]. With this in mind, sophisticated technologies are necessary to advance research in this domain. Methodologies proven successful for healthy adults can then be extrapolated to investigate clinical populations with disorders influencing their neural control of movement. This rationale is supported by one of the goals of the National Institute of Neurological Disorders and Stroke (NINDS) goals to "understand how the normal brain and nervous system develop and work, and what goes wrong in disease" [99]. With this knowledge, the second goal is to "translate basic and clinical discoveries into better ways to prevent and treat neurological disorders."

This work creates a methodology for understanding the neural control of movement with aging, using both statistical and data mining approaches, with applications to clinical populations. The work employs features from the time, frequency, and information theory domains, in addition to the novel application of cepstral analysis,

to provide functional insight to the neural control of movement with aging. In addition, the data mining approach uses optimization of classification schemes specifically aimed at minimizing classification error, to improve electroencephalogram (EEG) and electromyogram (EMG) analysis. This research is the first of its kind to create a methodology for understanding the neural control of movement during fine motor tasks with aging using data mining methodologies adding value to previous work. A long range goal of the research is to provide a computational tool for physiologist to analyze and interpret data, with the ultimate goal being a tool to provide early detection of neuromuscular disorders in healthy populations.

1.2 Research Aims

Aim 1: Modulation of the Neural Control of Movement with Task

Approach: Determine how the neural control of movement (EEG and EMG) are influenced by unilateral motor task and concurrent motor tasks (bilateral motor and motor cognitive) utilizing classical features of coherence, power spectral density and coefficient of variation. In addition, assess the potential association between the frequency and time domain features.

Test the modulation of the neural control of movement with two tasks:

1. Simple task
2. Complex task

Hypothesis: Corticomuscular coherence would decrease with an additional motor or cognitive task because attention is divided from the primary motor task.

Aim 2: Neural Control of Movement with Aging

Approach: Determine the influence of aging on the features in Aim 1 using a unilateral motor task and concurrent motor tasks (additional motor and non-motor).

Test the modulation of the neural control of movement between young and elderly adults using the complex task from Aim 1.

Hypothesis: Beta-band corticomuscular coherence in elderly adults will be lower in the beta band and greater in the alpha band when compared to young adults during dual tasks, due to greater influences of divided attention.

Aim 3: Model the Neural Control of Movement

Approach: Develop a set of features that best distinguish between aging (young and elderly) during unilateral and concurrent motor/cognitive tasks.

1. Determine the appropriate parameters for feature extraction.

2. Determine the optimal subset of features from time, frequency, and information theory domains. Test automatic speech recognition features (cepstrum) for application to EEG and EMG and signal classification.

3. Classify selected features to provide proof of concept for a methodology and computational tool to be used by physiologists in practical applications.

Aim 4: Neural Control of Movement Post-Stroke

Approach: Apply the methodology of data preparation, feature selection, and classification to motor stroke data to validate the proposed methodology and suggest how it may be applied to future clinical applications.

Hypothesis: Stroke subjects will exhibit beta-band corticomuscular coherence during the unilateral motor task (however less than the control group) and a decrease in coherence with an additional motor or cognitive task. Additionally, despite recovery, frequency, automatic speech recognition and time domain features will be attenuated due to neural plasticity in the stroke population.

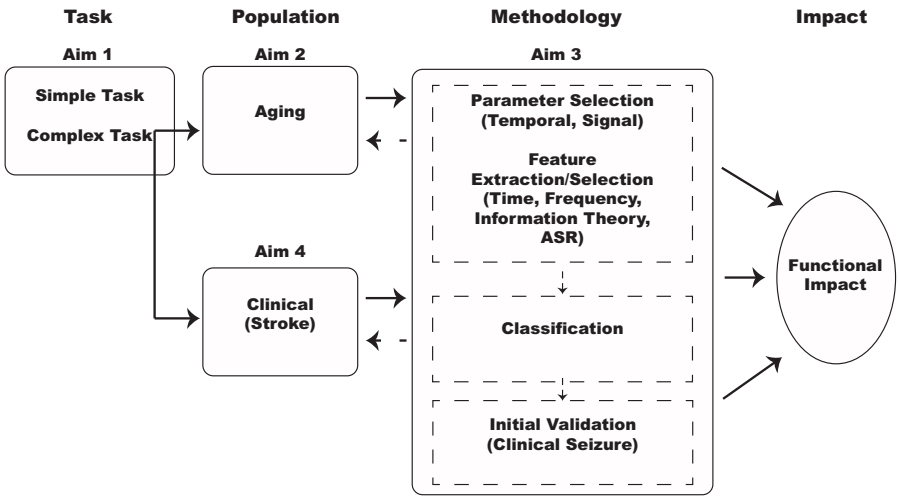

Figure 1: Research Overview.

1.3 Organization of the Study

The remaining portions of the dissertation are organized into seven chapters and appendices. Chapter 2 provides a review of relevant literature addressing the general background and motivation for the dissertation work. The experimental approach to address the research statement is presented in Chapter 3. The next three chapters address Aims one through three. Within each of these chapters, the aim is reiterated, the specific methodology is explained, followed by results and discussion of the findings. The work from chapters 4, 5, and 6 is extended in Chapter 7 and applied to a clinical population (stroke) by considering the influence of task and the potential application of the methodology. A summary and integration of the dissertation findings, and suggestions for future work are discussed in the final chapter.

CHAPTER II

BACKGROUND

2.1 Physiological Signals

Electroencephalogram. Activity of the brain can be measured in a variety of ways, such as with electroencephalogram (EEG), magnetoencephalogram (MEG), and functional magnetic resonance imaging (fMRI). MEG measures the magnetic fields generated by the electrical activity in the brain. Based on Maxwell's equations, any electrical current will produce an orthogonally-oriented magnetic field. MEG measures this field to find the locations of the neuronal sources in the brain. In comparison to EEG, MEG has good spatial and temporal resolution, but it is very expensive. Despite MEG and EEG being sensitive to different cortical sources (MEG to tangential dipole sources in the sulci and EEG to sources in the cortical gyri) [97], the use of EEG to investigate functional aspects of cortical activity during voluntary movement in humans is comparable to the use of MEG [44]. As opposed to EEG, fMRI provides an indirect measure of brain electrical activity by measuring the change in blood flow [51]. Active regions of the brain require more oxygen; therefore, fMRI provides a comparison of the blood oxygen levels in different regions of the brain. The temporal resolution of fMRI is approximately seconds, whereas the temporal resolution of EEG is milliseconds. Simplicity and reliability are advantages of EEG. Most importantly, the availability, cost, and non-invasiveness make EEG a feasible tool for university research settings.

Conventional measurement of EEG via scalp surface electrodes is based on the International 10-20 System of Electrode Placement defined by H. Jasper in 1958 [54]. The name of the system (10-20) is based on the distances for placement of

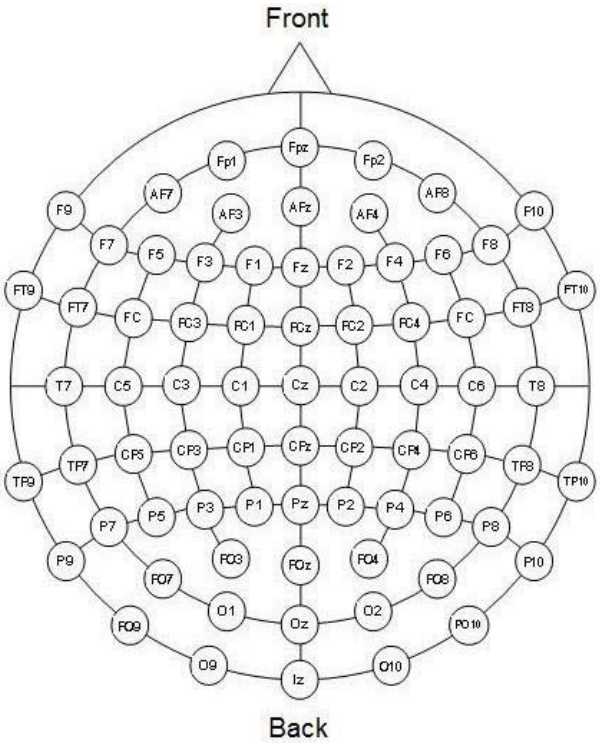

Figure 2: Standard 64-channel EEG channel layout (International 10-20 system) modified from [54].

the electrodes. Distances from the outer limits of the scalp in both longitudinal and transversal planes are divided into segments with a length of 10% and 20% of the total measured distance (Figure 2). The outer limits of the scalp are based on the nasion, inion, and the preaurical points of the earlobes.

EEG electrodes on the scalp record activity from a large number of neurons in underlying regions of the brain. The source of the activity is associated with post-synaptic potentials as opposed to action potentials, but the fundamental source-field relations are the same [104]. The assumed source of current causing the fluctuating scalp potential is primarily the pyramidal neurons and their synaptic connections to deeper layers of the cortex. Contributions from interneurons and glial cells to the EEG are small in comparison to the pyramidal neurons because their cells are not oriented in parallel, and their dendrites are not perpendicular to the cortical surface

like pyramidal neurons. The fluctuating scalp potential is a result of the reciprocal interaction of excitatory and inhibitory postsynaptic potentials. Excitatory postsynaptic potentials increase internal potentials, and inhibitory postsynaptic potentials decrease internal potentials [97]. The membrane potentials of groups of neurons are generating a small electrical field that changes over time.

EEG signal activity is predominately within the frequency range of 0.5 to 55 Hz. This spectrum can be partitioned into several frequency bands characterizing brain activity. The main EEG frequency bands are delta (≈0.5 - 4 Hz), theta (≈4 - 7 Hz), alpha (≈8 - 14 Hz), beta (≈15 - 32 Hz), and gamma (≈33 - 55 Hz). The dissertation primarily focused on the beta range of frequencies because beta-band rhythms are related to movement planning and production with activity localized around 20 Hz in the motor cortex [145, 3, 95].

Electromyogram. Electromyography is a method of monitoring the bioelectrical signals generated by the activity of skeletal muscles. The recording of the signals is called the electromyogram (EMG). Surface EMG is a non-invasive way to measure the composite of all muscle fiber action potentials occurring in the muscle under the skin where the surface electrode is placed (Figure 3). The action potentials are independent and occur at somewhat random intervals.

2.2 Task

The aim of the NIA is critical because the majority of everyday motor tasks necessitate the use of bimanual movements or concurrent cognitive processing. Compared with a simple unimanual movement, the involvement of additional tasks, such as additional contralateral movement or cognitive processing, accompanies divided attention and decreases the quality of motor performance in healthy individuals and often more so in elderly adults and patients with movement disorders (stroke) [56, 79, 7, 37, 146, 138, 49]. In particular, an additional task degrades fine motor performance such as motor

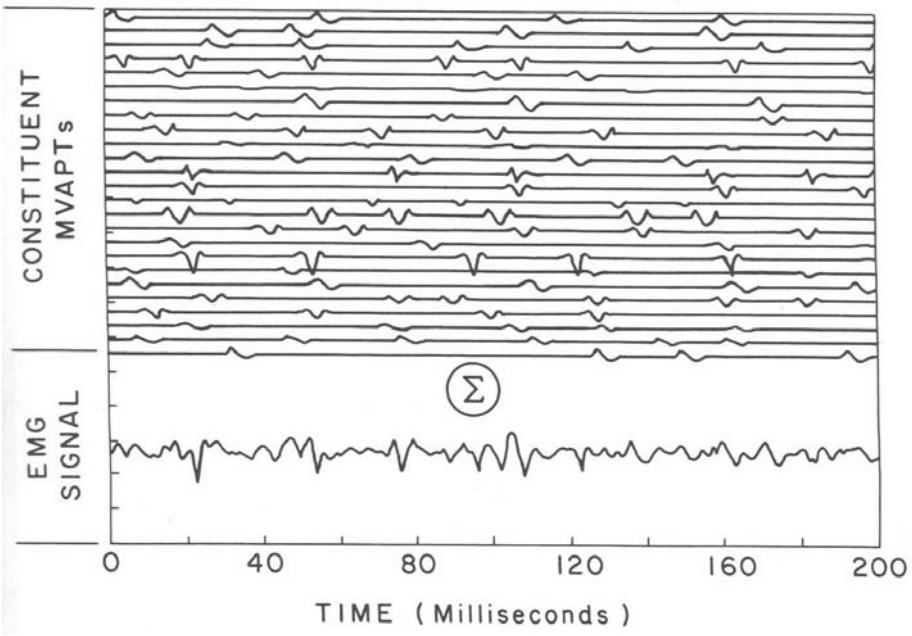

Figure 3: EMG signal formed from the linear summation of motor unit action potentials ([4], page 81).

steadiness and accuracy [146, 138]. Divided or reduced attention to a motor task influences neural activity, such as motor unity activity [114] and increased cortical activation of the supplementary motor area (17) and areas controlling higher-order processing (23). Recent studies imply that attention or fine motor performance may be associated with the amount of coherent activity between the motor cortex and muscle in the beta-band frequency range [76, 82].

The current method of determining corticomuscular coupling in the physiology community is using coherence analysis. Corticomuscular coherence between EMG in a contracting muscle and EEG or MEG in the contralateral hemisphere represents the synchronized oscillatory discharges of corticospinal cells [2, 20, 73] during muscle contraction. This synchronized oscillatory activity is dominant within the beta band for motor tasks [20, 44, 72, 87]. Alpha-band corticomuscular coherence is not dominant during motor tasks; however, significant peaks of corticomuscular coherence have been observed within the alpha band in some motor tasks requiring a distribution of

attention to the task [33, 77] and rapid movements of the wrist [21]. Alterations in the magnitude of corticomuscular coherence are regarded as the net result of multiple factors. Corticomuscular coherence appears to be influenced by task characteristics [33, 72, 77, 88], immobilization [82], muscle [43, 130], and visuo-motor learning [101]. However, the influence of advanced aging on and the functional significance of corticomuscular coherence are unclear.

Compared with the simple unilateral tasks, the influence of an additional task on beta-band coherence is rarely examined. One study [77] showed that, when a subject performed high-precision hand motor task with a concurrent cognitive task, the percentage of trials showing significant beta band coherence decreased from 23% to $\approx 12\%$. Another study [74] showed that the temporal profile of coherence between the right motor cortex and left hand performing steady contraction was modulated by the concurrent right-hand movement. Despite the fact that beta band coherence is susceptible to many factors as stated above, there is no study that systematically examines the influence of distinct types of additional tasks, cognitive and motor, on beta band coherence under the same condition for the performing hand.

2.3 Population

2.3.1 Aging

Advanced aging often degrades fine motor performance that can be attributed to several factors including age-associated alterations in information processing, motor neuron organization, and neuromotor activity [27, 113, 118, 116, 119]. While it is commonly accepted that with advanced age comes reductions in cognitive demanding tasks [22]; there are cases when elderly adults do not exhibit significant reductions and show signs of improvement as they progress through elderly age [19]. With this in mind, the ability to classify someone as young or elderly should not be taken for granted or assumed simply because their age is available. Measures of biological

changes with age provide the necessary information for understanding senescence.

While neural activity during motor tasks is often altered in elderly adults compared with young adults in various aspects including EMG power [42, 124, 131], EEG power [113, 133], and motor unit discharge strategies such as coherence [115, 116, 118], the effects of aging on corticomuscular coherence have been observed from childhood to middle age only [42, 53]. During a unilateral task, corticomuscular coherence within the beta band increased with development and aging from childhood (0 years old) to middle age (35 and 59 years old [42, 53], but not to senior age (55-80 years old) [42]. Alpha-band corticomuscular coherence during unilateral task was observed within elderly adults (55-80 years old) in more cases than within young adults (21-35 years old), but no significant difference was reported on the magnitude of coherence [42]. Hence, the current knowledge from only a few studies for elderly adults is that there is no significant change in the magnitude of corticomuscular coherence post-adulthood (>60 years old) although alpha band corticomuscular coherence might increase at senior age.

The execution of a task requiring divided attention degrades performance and often more so in elderly adults [7, 49, 138]. In particular, divided attention with dual tasks induces greater changes in neuromuscular activity [107] and task performance in elderly than young adults [86, 138] likely because elderly adults have less attentional resources or require more attention for performing a task [135]. Considering these more responsive neuromotor characteristics with regard to attention in elderly than young adults, corticomuscular coherence in elderly adults would be less in the beta band and greater in the alpha band compared with young adults if they perform tasks requiring substantial divided attention.

2.3.2 Stroke

A stroke occurs when regular blood flow to the brain is interrupted, causing a lack of oxygen which subsequently results in brain cells dying and potentially permanent damage (infarction) [64]. There are two major types of stroke, ischemic and hemorrhagic. An ischemic stroke occurs when blood flow to a portion of the brain is interrupted because of a blockage within a blood vessel. Hemorrhagic strokes occur when a blood vessel ruptures and bleeds within a particular area of the brain. The majority of strokes are ischemic in nature, therefore ischemic strokes were evaluated in the current work. According to a 2007 report from the American Heart Association Statistics Committee and Stroke Statistics Subcommittee, 87% of all strokes are ischemic in nature [108]. Additionally, one in six people over the age of 55 will suffer from a stroke, with over 1.1 million elderly (>65 years) Americans reporting impairment of motor function post-stroke [108]. Impairment of motor function may take the form of hemiparesis or hemiplegia of the upper limbs. Recovery of hand motor function is important for regaining control of tasks involved in daily living such as buttoning a shirt, opening a jar, or tying a shoe lace.

The residual motor deficits in elderly individuals are greater in comparison to young individuals at least six months post-stroke [69]. It is well known that brain neural plasticity changes following stroke to compensate for degenerated hemispherical areas [55]. Current research has shown decreased beta-band corticomuscular coherence of the affected side compared with the unaffected side in distal muscles of well-recovered patients with a subcortical infarction [89], and decreased beta- and gamma-band corticomuscular coherence during reaching in poorly recovered patients [29]. Cortico-cortical coherence research has also shown that while dominant beta band left hemisphere networks are responsible for praxis preparation of hand movements in healthy subjects, coherence is absent in the left hemisphere of stroke patients [141].

2.4 Feature Analysis

Feature extraction is the process of computing quantitative information (features) over a sliding window of data points, yielding a new time series of scalar quantities. This process reduces the data size, which decreases computation time, thus computational costs. Traditional pattern classification includes the following modules: preprocessing, feature extraction, feature selection, and classification [24]. Feature extraction and selection are considered one of the most important modules [71, 24] because if an extracted feature has low separation between groups, then the classifier will consequently demonstrate poor discrimination of the groups. If the computational demands of a classifier depend upon the performance of the features that it processes, it is more efficient to select quality features prior to classification to avoid unnecessary complex processing.

Feature selection algorithms aim to select a subset of features that reduce the feature space dimensionality and maximize the separation between classes [24]. Given a set of M features, the selection algorithm chooses a subset of size m <M, which optimizes the objective function *J(.)*. Optimization occurs by minimizing classification error or maximizing class separation. Objective functions are commonly optimized using two methods: filters or wrappers. Filters evaluate subsets based on interclass distance, statistical dependence or information content without the use of a classifier [13]. Wrappers evaluate subsets using classifiers based on their predictive accuracy. While filters are computationally less demanding, they tend to have lower classification accuracies and select large subsets as the optimal solution. Another form of feature selection is the transformation of features into lower dimensional space in order to reduce the number of correlated features. The challenge with feature transformation is the ability to functionally explain the reduced feature set or fused feature. Chapter 6 provides a comparison of forward feature selection, backward feature selection, and branch and bound selection.

As alluded to, analysis in this area is dominated by the coherence and power spectral density features, with periodic inclusion of time domain features (mean, standard deviation, and coefficient of variation). While these features have provided significant insight, other features more appropriate for characterizing age-dependent changes in biological data have the potential to provide more information. Features involving genetic algorithms have also been applied to biological data; however, after the fusion of features, the functional implications can no longer be explained by physiologists. A medium between traditional features from physiologists and high-order features is desired, in conjunction with tools for selecting and classifying these features. The stochastic and non-linear nature of the EEG and EMG signals suggests that the inclusion of information theory and non-linear features might provide more information to the nature of the characteristic changes with advanced aging [80]. The challenge with non-linear features is the high computational demand making the use of non-linear features a challenge for real-time applications.

Another feature set that has the potential to provide more information on the energy and frequency content, and not conflict with the statistical assumptions of the signals, are automatic speech recognition (ASR) features, the real cepstrum, and Mel Frequency Cepstral Coefficients (MFCC). The real cepstrum is the inverse Fourier transform of the real logarithm of the magnitude of the Fourier transform of a signal. MFCCs are short-term frequency based features obtained by calculating the discrete Fourier transform of a specified window, extracting the log of the amplitude spectrum ignoring the phase component, then converting the latter to a Mel spectrum, and finally computing the Discrete Cosine Transform. The real cepstrum and MFCCs have long been applied to speech signals [106] and more recently for music modeling [81]. Despite both speech and EEG signals having significant spectral characteristics the application of automatic speech recognition (ASR) features for biological data is only recently being investigated. Preliminary research has looked at the application of

the cepstrum to extracellular neural spike detection [117] and neonatal EEG signals for seizure detection [128]. These works have only considered computing the real cepstrum and lack examination of the application and interpretation of the results.

2.5 Classification

Classification uses feature characteristics to assign a class label to an unknown segment [134]. Learning occurs as the classifier uses a training set to estimate unknown parameters and optimize the function representing the classification error [24]. The dissertation utilized a supervised learning approach where the class labels for each feature window were provided for training.

To the author's knowledge, aging research on the classification of young and elderly adults has been limited to gait and balance analysis using support vector machines (SVMs) [8]. Automatic classification of gait patterns in young and elderly adults was reported with a maximum of 90% classification accuracy using a support vector machine [8]. The research has focused on identifying features to reflect gait degeneration in hopes of understanding falls in young and elderly adults. Features reflecting complexity and variability have been considered; however, biological signals were not include.

In alignment with being prepared to care for the aging population of the United States and the world, other aging research classified tasks of daily living using sensor data in smart homes with SVMs [34]. The dissertation builds upon this body of literature by considering classification of young and elderly adults during fine motor upper extremity motor tasks with the inclusion of biological data.

CHAPTER III

EXPERIMENTAL DESIGN

3.1 Experimental Overview

The neural control of movement can encompass numerous motor tasks. The dissertation focused on tasks requiring a level of fine motor control in the upper extremity because activities involved in daily living often require some level of fine motor control (e.g., dressing, bathing, preparing a meal). In the controlled experiments, tasks were selected that represent the multiple modalities that might be involved in performing a task for daily living. Examples include, the use of one hand to brush teeth (unilateral motor), two hands to open a jar or get dressed (bilateral motor), and the use of a hand and cognitive processing to receive and count change after making a purchase (motor cognitive). To address the research statement of developing a methodology to interpret the neural control of movement with aging and stroke populations, the project was broken into four parts. The first portion considered the neural control of movement primarily focusing on task. The second portion incorporated task in the context of healthy aging. The third portion developed a methodology to assess the change in the neural control of movement with aging. Lastly, the fourth portion investigated the neural control of movement in the stroke population by drawing upon the techniques and findings from the previous portions of the work.

The neural control of movement with task dependence was assessed using two levels of task difficulty. The first study considered the neural control of movement with a simple task, where for the dual task involving two motor modalities each were synchronized. The dual task involved a motor and cognitive aspect with a longer time duration for cognitive processing in comparison to the second study. The second

study increased the difficulty of the additional tasks by modulating the timing and synchronicity of the additional task. The change to an asynchronous and dynamic task was used to increase task difficulty [111].

This chapter provides an overview of the recruitment of subjects and collection of data for the study.

3.2 Subject Recruitment

Healthy right-hand dominant adults were recruited from the campus of Georgia Institute of Technology and the surrounding Atlanta area.

- Aim 1
  - Simple Task: Young adults (n=10), mean age: 27.1 ± 4.0 yrs; 5 females and 5 males
  - Complex Task: Young adults (n=10) 24.9 ± 7.1 yrs; 6 females and 4 males
- Aim 2
  - Young adults (n=16), mean age: 23.9 ± 5.8 yrs; 10 females and 6 males
  - Elderly adults (n=13), mean age: 69.2 ± 4.7 yrs; 7 females and 6 males
- Aim 3
  - Young adults (n=10), mean age: 24.9 ± 7.1 yrs; 6 females and 4 males
  - Elderly adults (n=10), mean age: 70.3 ± 4.2 yrs; 4 females and 6 males

Subjects were comprised of individuals who were free from high- or low-blood pressure, pregnancy, arthritis in their hands, history of neurological disorder, diabetes, skin allergies, and medication use that might influence motor control and/or neurological function. These factors were considered exclusion criteria because of their potential to erroneously influence EEG and/or EMG recordings. In addition, another constraint

in this investigation is the risk of population bias by choosing to sample only healthy older adults not having ailments typically associated with the aging process. Although this factor is acknowledged, the current research is focused on the effects of healthy aging to create a baseline for future research studies.

Subjects were instructed to refrain from caffeine and nicotine 2-3 hours prior to the experiment to control for varying levels of anxiety or awareness. Before beginning each experiment, hand dominance and cognitive state were measured according to the Edinburgh Handedness Inventory [100] (Appendix A) and a modified Mini-Mental State Exam (MMSE) [35] (Appendix B), respectively. Each subject's written consent was obtained prior to the experiment in accordance with the Institutional Review Board (IRB) of the Georgia Institute of Technology.

Additionally, approval was obtained from the Georgia Institute of Technology Institutional Review Board (IRB) for the collection of 3 right-hemispheric stroke subjects over the age of 40 years for the purpose of showing application to a patient population in Aim 4 (n=3, age: 51.7 ± 9.1 yrs, 2 females, 1 male). All subjects were right hand dominant. Subjects were physically and cognitively healthy with no history of neurological disorder outside of stroke. In addition, subjects with no hand movement, more than minimal neglect, uncontrolled high- or low-blood pressure, arthritis in their hands, skin allergies, or taking medications that affect motor control (outside of ones for the stroke) were excluded from the study. Lastly, stroke subjects were included if they met the following criteria: at least 6 months post-stroke, demonstrated spontaneous recovery, and have minimum neglect of the impaired upper extremity. Stroke subjects were recruited with the assistance of Dr. Steve Wolf and colleagues at Emory University.

3.3 Experimental Setup

All experiments were conducted in the Centennial Research Building on the campus of the Georgia Institute of Technology. Subjects were seated in an electrically shielded, dimly-lit room with their hands and forearms pronated and supported in rigid vacuum foam pads (Figure 4). The left and right shoulders were abducted at approximately 35°. The index finger was placed in a finger splint with all interphalangeal joints extended. All other fingers were fixed to a platform with Velcro straps. The metacarpophalangeal joint was in the neutral position such that the index finger was level with a force transducer during the measurement. Contraction intensity for the motor tasks was based on the subject's maximal voluntary contraction (MVC) force. Visual feedback of target and actual force levels was displayed on the monitor for all tasks. Performance of all motor task utilized the experimental setup designed by the author (Figure 4).

MVC.

Prior to the experimental tasks, maximal voluntary contraction (MVC) was performed to obtain the maximum abduction force independently exerted by the right and left index fingers. The MVC task consisted of a gradual increase in force from zero to maximum over 3 s, with the maximal force held for 2 to 3 s. The task was conducted by abducting the index finger and pulling on a rigid piece connected to a force transducer (21.3-21.4 N/V; Model 34, Honeywell, Ohio, USA). Subjects were verbally encouraged to achieve maximal force while the force exerted by the index finger was visually displayed on a monitor in front of the subjects. Three to four trials were performed, excluding trials not within 5% of maximal force of each other.

Recordings

EMG.

Figure 4: Experimental setup for young adults.

Surface EMG was recorded from the first dorsal interosseous (FDI) muscle on the left and right hands during the motor tasks. The FDI muscle was selected because it is responsible for approximately 93% of the abduction force exerted by the index finger [18]. Electrical recordings are accurate and reliable because the muscle has a small mass [68] that is isolated, thus when recording the abduction force from the FDI muscle there is limited interference from surrounding muscles. The intensity of steady contraction tasks was $\leq 10\%$ of the MVC force for all experiments, which is an intensity commonly used during activities of daily living [70].

The ActiveTwo Biosemi electrode system (Biosemi, Amsterdam, The Netherlands) was used to obtain EMG. This system is equipped with a miniature preamp adjacent to each electrode to reduce the contamination of electrical noise. To further reduce electrical noise contributions, a battery powered A/D box digitizes the signals and transfers them to a computer through a fiber optic connection. One active Ag-AgCl EMG electrode (diameter: 4 mm) was placed over the belly of the muscle and the other was attached to the skin over the base of the proximal phalanx of the index finger. A reference electrode was placed on the radial styloid process on the dorsal surface of the hand.

EEG.

Cortical EEG signals were recorded using the international 10-20 electrode placement method from C3 (left motor cortex) and C4 (right motor cortex) referenced to Cz. An EEG electrode cap was placed on the subject's head to assist with collection (Figure 4). The electro-oculogram (EOG) generated from blinks and eye movement was recorded from three facial electrodes: one ∼1 cm to the left of the left eye, one ∼1 cm to the right of the right eye, and one in between the left and right eyebrows. EEG and EOG were also obtained with the ActiveTwo Biosemi electrode system. The ground signal was recorded from a scalp electrode in the center of the EEG electrode array. The ActiveTwo system uses a gain of least significant bit equal to 31.25 nV, with a 1% gain accuracy. All bioelectric signals were digitized on a computer using ActiView software (Biosemi, Amsterdam, The Netherlands) and sampled at 2048 samples/s.

Force.

Force generated by index finger abduction was sensed by the transducer connected to an amplifier (Transbridge 4M, World Precision Instruments, Sarasota, Florida, USA). Target and actual forces were digitized at 2048 samples/s, in parallel with electrophysiological data, using an analogue-to-digital converter (Power 1401, Cambridge Electronic Design, Cambridge, UK). The force and electrophysiological data were synchronized with the concurrent recording of the synchronization pulse.

3.4 Preprocessing of Data

Care was taken to provide a comfortable and relaxed experimental environment within an electrically shielded room. To account for movement and electrodermal artifacts, portions of the body not involved in the task were constrained, and the subject was provided specific instruction not to move. The electrodermal artifacts are seen

particularly in the EEG signal, although they are also observed in EMG as very low-frequency signals typically in the range of 0.25 to 0.5 Hz. While the amplitude of electrodermal artifacts may impact the EEG, these artifacts can be easily removed with a high-pass filter because of their localization in the low frequency range [1]. Electrodermal artifacts were also accounted for by requesting that subjects wash their hair the night before testing to ensure a clean scalp and by maintaining a comfortable temperature in the laboratory. Electrodes were treated with salt water prior to all experiments to maintain optimal impedance levels. Preprocessing consisted of preparing the signals for analysis. Data during the steady phases of force (10-s period) were used for analysis. EOG data was monitored in real-time for excessive eye blinks. Trials with excessive eye blinks (> 5 blinks per 12 seconds) were excluded and subjects were asked to repeat the trial.

The data was filtered using a 4th-order butterworth filter for Aims 1 and 2, and 10th-order butterworth filter for Aims 3 and 4. In both cases, the specified filter parameters for the stop and passbands were verified. The butterworth filter was selected for the flat passband and for being monotonic overall. While the monotonicity is a trade-off for the rolloff steepness, a higher order can increase the rolloff steepness. A concern for the use of an infinite impulse response (IIR) filter versus a finite-impulse response (FIR) filter is the potential non-linear phase distortion. This is a concern for real-time systems where all of the data is not available prior to filtering. In the case of the present work, all analysis is performed offline using script written in MATLAB (Mathworks, Natick, MA, USA) thus all data is available prior to filtering. Also, the Matlab function 'filtfilt' was used and it is a zero-phase digital filter, thus accounting for the potential non-linear phase distortion with IIR filters.

The EEG and EMG signals were analyzed using a bipolar configuration to minimize the common mode artifact. The EEG signal was band-pass filtered (5-200 Hz) and detrended. This removes the baseline drift DC voltage that is sometimes present

in EEG and EMG signals. These steps also remove any high frequency noise not containing relevant information. A rectified EMG signal was obtained from the bipolar EMG that was band-pass filtered (10-500 Hz), full-wave rectified, and detrended. The EMG signal was rectified prior to power and coherence analysis according to the literature [44, 87, 112, 17] to reflect the timing and firing pattern of grouped motor units [92, 143]. Recent studies have questioned the appropriateness of rectified EMG for frequency analysis [93, 126]. The argument is that rectified EMG introduces a strong non-linearity, and the process is not based on neurophysiological properties. While the results in [126] showed suppressed coherence and power in certain frequency bands, the results were all based on simulations. The author of the present work investigated and presented a direct comparison of rectifying and not rectifying the EMG signal [57] and a statistical difference was not observed. It is of note that further research might continue to investigate the process of rectification to form a consensus.

CHAPTER IV

NEURAL CONTROL OF MOVEMENT WITH TASK

The neural control of movement was assessed using two levels of task difficulty. The first study considered how the neural control of movement was effected by simple tasks, and the second study increased the difficulty of the additional tasks by modulating the timing and synchronicity of the additional tasks.

Aim 1: Modulation of the Neural Control of Movement with Task

Approach: Determine how the neural control of movement (EEG and EMG) is influenced by unilateral motor task and concurrent motor tasks (additional motor and non-motor) utilizing classical features of coherence, power spectral density, and coefficient of variation. In addition, assess the potential association between the frequency and time domain features.

Test the modulation of the neural control of movement with two tasks:

1. Simple task
2. Complex task

Hypothesis: Corticomuscular coherence would decrease with an additional motor or cognitive task because attention is divided from the primary motor task.

4.1 First Study Methodology: Neural Control of Movement Simple Task

Subjects were instructed to keep their head straight and minimize the number of extraneous movements, including eye blinks, during the actual trial for all tasks.

Instructions were provided to wait for a signal on the screen to begin the trial. The experimenter counted down from three to one to ensure the subject was prepared for the trial. After a 2-s delay, a red box turned green indicating to the subject to begin the trial.

Five tasks were performed: unilateral abduction of the right index finger (unilateral motor task); unilateral abduction of the left index finger (unilateral motor task); cognitive task involving arithmetic and memory (cognitive task); concurrent cognitive-motor task with the right finger (motor-cognitive task); and bilateral motor-motor task with the left and right index fingers (motor-motor task). The unilateral motor task with the left hand and independent cognitive task were included to yield control values for comparison to additional motor and cognitive tasks.

Motor tasks. The motor tasks involved abduction of the index finger. A light-weight compliant spring (stiffness: 0.8 N/mm, mass: 0.24 g) was attached to the finger-splint between the ulnar side of the index finger at the distal interphalangeal joint and a force transducer (9.1-9.2 N/V; Model 31, Honeywell, Ohio, USA). Thus, when the index finger was abducted, the spring would pull on the force transducer. The spring was used because the primary feature of interest, corticomuscular coherence, is more evident with the addition of compliance in the transmission of force [72]. Subjects were instructed to exert force matching 5% and 10% of their MVC force by abducting the index finger of the left and right hands independently or concurrently (Figure 5). Each level was matched for 10 s with 2 s for ramping to the next level continuously (order: 5%, 10%, 5%, 10%; 48 s for one trial) (Figure 6). Subjects were instructed to keep their finger fully extended in a finger splint and level during the motor tasks. The same experimental procedures were used for left and right hand tasks.

Cognitive tasks. During the cognitive task, subjects were asked to solve four mathematical problems (2-digit addition and subtraction) and remember the answers until

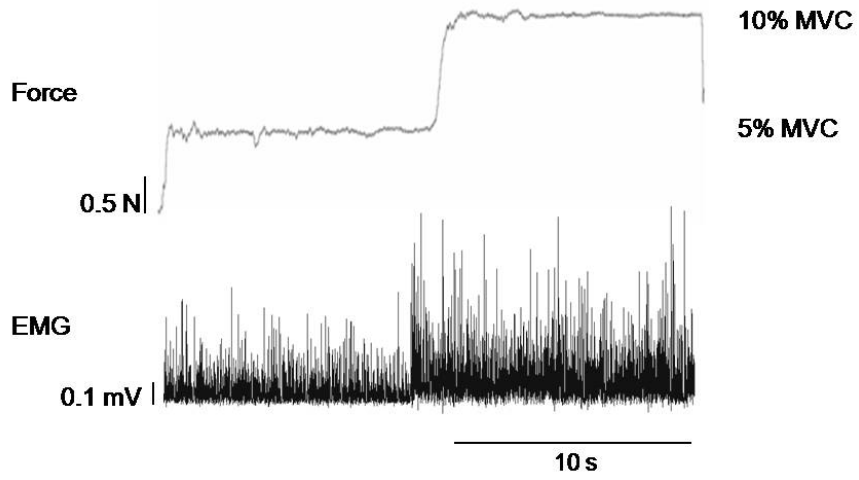

Figure 5: Representative recordings of force and rectified EMG in the first dorsal interosseus muscle during the unilateral motor task performed by the right hand. The first 5% and 10% MVC levels are shown.

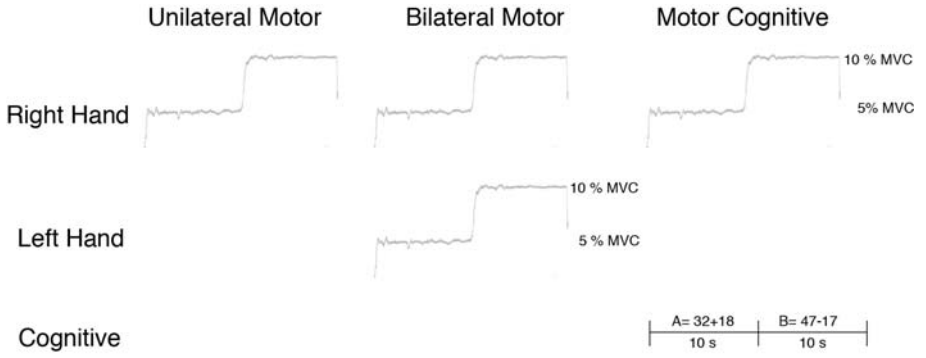

Figure 6: Simple task. Unilateral motor, bilateral motor, and motor cognitive tasks.

the end of each trial (48-s duration). The mathematical problems were displayed on the monitor in front of the subjects. They were asked to verbally recall the four answers at the end of the trial.

Data Analysis The power spectrum of EEG, rectified EMG, and coherence between EEG and EMG were determined for each trial. Power spectra (Eq. 2) and coherence (Eq. 1) were calculated over 2048-point FFT segments with 50% overlap. The total power of the EEG and EMG signals was calculated within the beta band (15-30 Hz) and full band (0-60 Hz). Corticomuscular coherence was computed between C3 and the rectified EMG signal in the right hand. Coherence, $C_{xy}(f)$, is the square of the cross-spectrum of the two signals, normalized by the product of the auto-spectra of each individual signal over frequency, f.

$$\mid C_{xy}(f) \mid^2 = \frac{\mid P_{xy}(f) \mid^2}{P_{xx}(f)P_{yy}(f)} \tag{1}$$

where f is the frequency of interest, $P_{xx}(f)$ (resp. $P_{yy}(f)$) is the power spectrum of the signal $x(t)$ (resp. $y(t)$), and $P_{xy}(f)$ is the cross power spectrum of those two signals. With a continuous time signal, the power spectrum is defined as the square of the modulus of the Fourier transform of the signal, where $P_{xx}(f)$ is the power spectrum and $F(f)$ is the Fourier transform of the time signal.

$$P_{xx}(f) = F_x(f)F_x^*(f) = \mid F_x(f) \mid^2 \tag{2}$$

The amplitude of $P(f)$ is always positive for a real signal, and represents that signal power which exists in the frequency interval f to $f + \mathrm{d}f$. The cross power spectrum, $P_{xy}(f)$, can be calculated between two signals $x(t)$ and $y(t)$ as,

$$P_{xy}(f) = F_x(f)F_y^*(f) \tag{3}$$

Coherence is a real number bound between 0 and 1 that provides a summary measure of the amount of similarity (or correlation) between the surface EMG activity and EEG activity . An arc hyperbolic tangent transform, $Tanh^{-1}\left|C_{xy}(f)\right|$, was taken to stabilize the variance in the distribution of the coherence [45]. To determine significant levels of coherence the confidence interval (cl) of the coherence function was measured [109] at the α quantile for L number of segments. This formula is given for coherence calculations based on the Fourier transform [109] where L is the signal duration minus the overlap, divided by the window length minus the overlap.

$$cl(\alpha = 0.95) = 1 - (1 - \alpha)^{\frac{1}{L-1}} \tag{4}$$

Coherence was considered to be significant if the value in the beta band (15-30 Hz) was above the 95% confidence limit (Figure 7). Significant corticomuscular coherence during the unilateral motor task was observed only for the first 5% and 10% MVC levels; therefore only data from these periods were included for further analysis. The comparison of coherence across tasks was to compare the magnitude of coherence at the same frequency bin that had the highest peak during the right-hand unilateral motor task across tasks. The highest significant peaks of coherence were observed for the contralateral right and left hands with C3 and C4 EEG electrodes, respectively. Reported results are for EEG channels C3 and C4. Peak value of the coherence in the beta band was determined. Cortico-cortico inter-hemispheric coherence (C3-C4) was also calculated.

Variability and accuracy of motor output were used for assessing fine motor skills. Force signals were low-pass filtered at 100 Hz and detrended. The coefficient of variation (CV, standard deviation divided by mean) was determined for variability. To assess the accuracy of motor output, absolute error was calculated as the error

ratio using the following equation. Error ratio

$$Errorratio = \left| \frac{EF - TF}{TF} \right| * 100\% \tag{5}$$

where EF is exerted force and TF is target force. In addition, variability of muscle activity was assessed with the CV of EMG that was full-wave rectified, low-pass filtered at 5 Hz, and detrended.

Cognitive accuracy was calculated as the ratio between the number of correct responses and the number of the math problems, represented by percentages. If a subject answered with the exact value for the problem set it was considered correct, any other response was considered incorrect. For example, if 3 out of 4 responses were correct then the accuracy was 75%.

4.1.1 Statistical Analysis

Statistical analysis was performed to assess the influence of adding a concurrent motor and non-motor task to a unilateral motor task in the right hand. The calculated variables were determined in each trial and averaged across 4 trials in each task. The dependent variables were peak corticomuscular and cortico-cortico coherence, EEG and EMG spectral power, coefficient of variation of force and EMG, standard deviation of force, error ratio of force, and cognitive accuracy. Statistical significance of these dependent variables was tested between unilateral motor (right hand), unilateral motor (left hand), bilateral motor, motor-cognitive, and cognitive tasks for appropriate combinations. To test the variables associated with the right-hand contraction (peak coherence between EEG in the left motor cortex and EMG in the right hand, peak coherence between EEG in the left and right motor cortices, spectral power of those EEG and EMG, coefficient of variation of force and EMG, standard deviation of force, and error ratio of force in the right hand), a two-factor, 3 x 2 analysis of variance (ANOVA) with repeated measures was used for each variable. The factors

were task (unilateral motor (right hand), bilateral motor, motor-cognitive) and contraction intensity (5% and 10% MVC). To test peak coherence between EEG in the right motor cortex and EMG in the left hand during the tasks that involved the left-hand contraction, a two-factor, 2 x 2 ANOVA with repeated measures was used. The factors were task (unilateral motor (left hand) and bilateral motor) and contraction intensity (5% and 10% MVC). Post-hoc analysis was performed using Tukey's test for pair-wise comparison when appropriate. The association between peak coherence and the coefficient of variation of force and EMG was evaluated using a Pearson's correlation coefficient. Cognitive accuracy was measured at the termination of each trial for the individual cognitive task and the motor-cognitive task. The difference in cognitive accuracy between these tasks was assessed with a paired t-test. An alpha level of 0.05 was chosen for all statistical comparisons. $P < 0.05$ or $P < 0.01$ was additionally noted where appropriate. Unless stated otherwise, the data are presented as mean ± SE. Standard error is used to visually view the statistical differences in the figures and is consistent with the text.

4.2 First Study Results: Neural Control of Movement with Simple Task

Coherence. For the unilateral motor task with the right hand, eight of the ten subjects displayed significant coherence between the EMG in the right hand and EEG in the left motor cortex (C3). Strength of C3-right hand coherence was maximal across subjects at 0.22 and the peak frequency ranged from 15.0 to 27.5 Hz (mean frequency: 22.5 Hz, median frequency: 23.0 Hz) across subjects (Table 1). Corticomuscular coherence was not significantly different between the 5% and 10% MVC levels, hence the factor of contraction intensity is not considered in the subsequent analysis of EMG and EEG [61].

Table 1: Summary of coherence results across subjects and tasks

Maximum coherence	***Frequency range***	***Mean frequency***
0.22	15 - 27.5 Hz	22.5 Hz

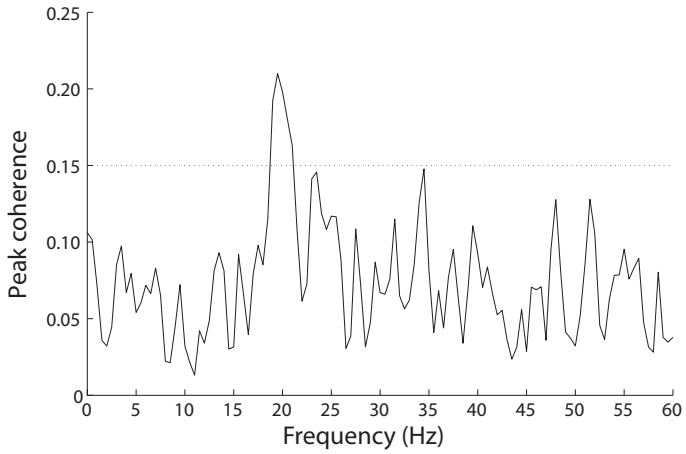

Figure 7: Representative coherence.

Corticomuscular coherence decreased significantly from the unilateral motor task with the right hand to both bilateral motor (P <0.05) and motor-cognitive (P <0.05) tasks (Figure 8) [61]. The decrease in coherence with either of these tasks was observed in 88% of the cases. There was no significant difference in corticomuscular coherence between the bilateral motor and motor-cognitive tasks. Of the eight subjects showing significant corticomuscular coherence during the unilateral motor task with the right hand, there were zero and two subjects who showed significant corticomuscular coherence during the bilateral motor task and the motor-cognitive task, respectively. The data are shown from using the value of coherence that corresponds to the frequency where a peak was observed in the unilateral motor task with the right hand as a control.

For the unilateral motor task with the left hand, significant coherence between the EMG in the left hand and EEG in the right motor cortex (C4) was observed in 5 out of the 8 subjects (Figure 8b). In these 5 subjects, as with the unilateral motor task with the right hand, corticomuscular coherence was not significantly different

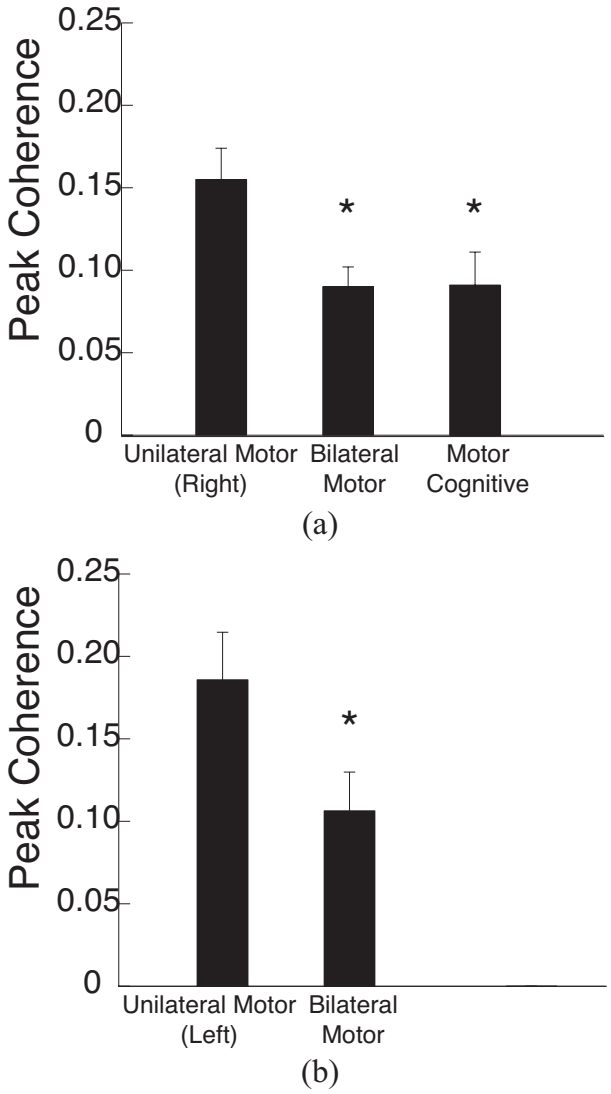

Figure 8: (a) Peak coherence between EEG in the left motor cortex (C3) and EMG in the right hand for the unilateral motor task, bilateral motor task, and concurrent motor cognitive task (N = 8). (b) Peak coherence between EEG in the right motor cortex (C4) and EMG in the left hand for the unilateral motor task with the left hand and bilateral motor task (N = 5). Data were averaged for intensity. *, P <0.05 vs. unilateral motor task.

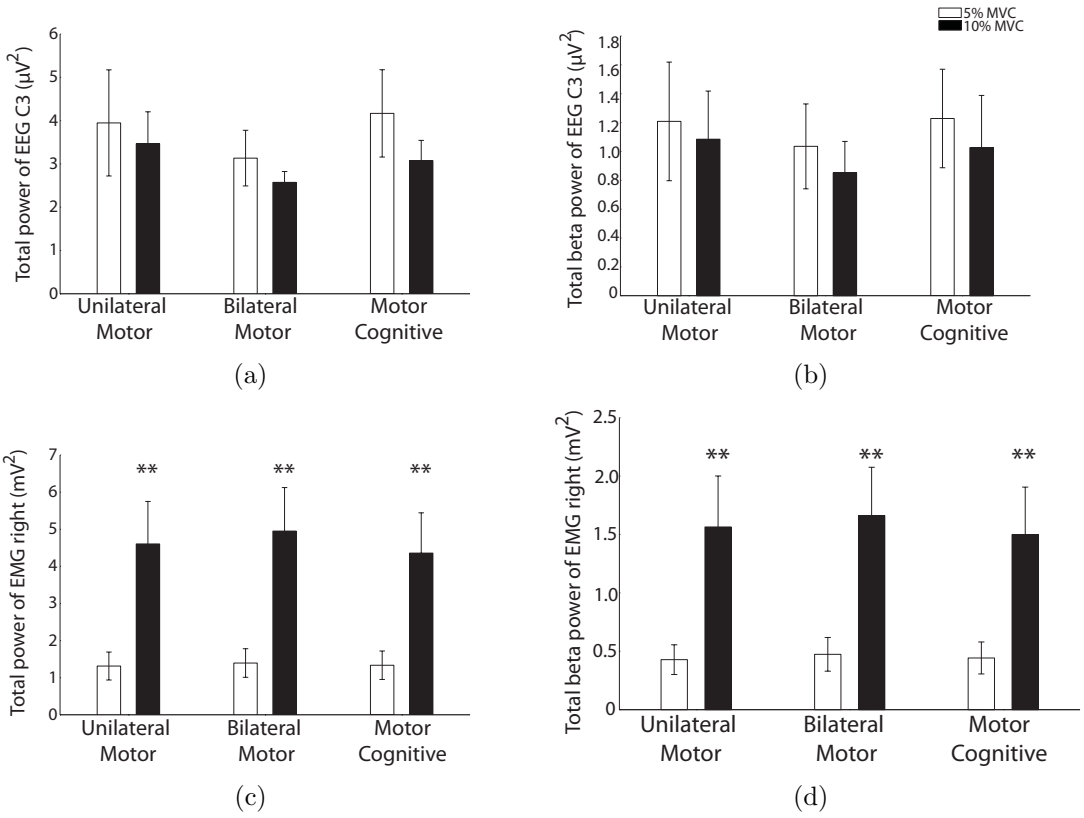

Figure 9: Total and beta-band power of EEG (C3) and EMG during the unilateral motor task, bilateral motor task, and concurrent motor cognitive task at two levels of contraction intensity. (a), total power of EEG in the left motor cortex; (b), beta-band power of EEG in the left motor cortex; (c), total power of EMG in the right hand; (d), beta band power of EMG in the right hand. N = 8. **, P <0.01 vs. 5% MVC

between 5% and 10% MVC. Coherence during the unilateral motor task with the left hand decreased significantly during the bilateral motor task (P <0.05). In addition, the two subjects who did not show significant coherence between the right hand and left motor cortex (C3) for the unilateral right hand motor task also did not show significant corticomuscular coherence for the left hand and right motor cortex in the unilateral left hand task.

Inter-hemispheric coherence between C3 and C4 was observed in 5 out of the 8 subjects indicating significant corticomuscular coherence. As with corticomuscular coherence, cortico-cortico coherence was not significantly different between 5% and 10% MVC. The direction of coherence alteration with task varied across subjects, resulting in the absence of statistical significance across tasks, unilateral motor right (0.29 ± 0.13), bilateral motor (0.30 ± 0.13) and motor-cognitive (0.26 ± 0.09) tasks, respectively [61].

Cortical and Muscular Spectral Power. EEG spectral power was calculated for the left motor cortex (C3) (Figure 9). Total power of the EEG, full band and beta band, were not significantly different across the unilateral motor, bilateral motor and motor-cognitive tasks. This was also true for the total power of the EMG in the right hand across tasks although there was a significant difference between contraction intensities for the total power (full-band and beta band) of the EMG in the right hand (full-band: P <0.01; beta band: P <0.01) [61].

Motor Output Variability and Accuracy. An additional task influenced motor output variability of EMG, but not of force (Table 2). The coefficient of variation of EMG was significantly greater during the bilateral motor task when compared with the unilateral motor task (P <0.05) [61]. The coefficient of variation of force was significantly smaller (P <0.01) at 10% MVC compared with 5% MVC. Also,

Table 2: Fine motor performance during the Unilateral Motor, Bilateral Motor, and Motor-Cognitive tasks. Mean ± SE (N = 8). *, P <0.05 vs. Unilateral Motor, **, P <0.01 vs. Unilateral Motor, †, P <0.01 vs. 5% MVC

	5% MVC	**10 %MVC**
Coefficient of variation of EMG		
Unilateral Motor	0.11 ± 0.00	0.13 ± 0.01
Bilateral Motor	0.14 ± 0.01*	0.14 ± 0.01*
Motor Cognitive	0.13 ± 0.01	0.14 ± 0.01
Coefficient of variation of force		
Unilateral Motor	0.018 ± 0.002	0.009 ± 0.001†
Bilateral Motor	0.020 ± 0.002	0.011 ± 0.001†
Motor Cognitive	0.019 ± 0.001	0.011 ± 0.001†
Standard deviation of force		
Unilateral Motor	0.015 ± 0.003	0.017 ± 0.004
Bilateral Motor	0.018 ± 0.011**	0.020 ± 0.004**
Motor Cognitive	0.018 ± 0.012**	0.021 ± 0.004**
Error ratio of force (%)		
Unilateral Motor	0.88 ± 0.16	0.76 ± 0.12
Bilateral Motor	1.09 ± 0.18	0.91 ± 0.17
Motor Cognitive	1.19 ± 0.28	0.84 ± 0.22

standard deviation of force was significantly greater during the bilateral motor (P <0.01) and motor cognitive (P <0.01) tasks compared with the unilateral motor task. Motor accuracy was calculated in terms of the error ratio of the mean exerted force. There were no significant differences in the error ratio across tasks.

Association of Motor Output Variability and Coherence. There was no significant association between peak coherence and motor output variability including CV of EMG or CV and standard deviation of force (Figure 10). In addition, the relative change in the coefficient of EMG and force from the unilateral motor task with the right hand to the bilateral motor task and motor cognitive task were also not shown to be significantly associated with the relative change in peak coherence [61].

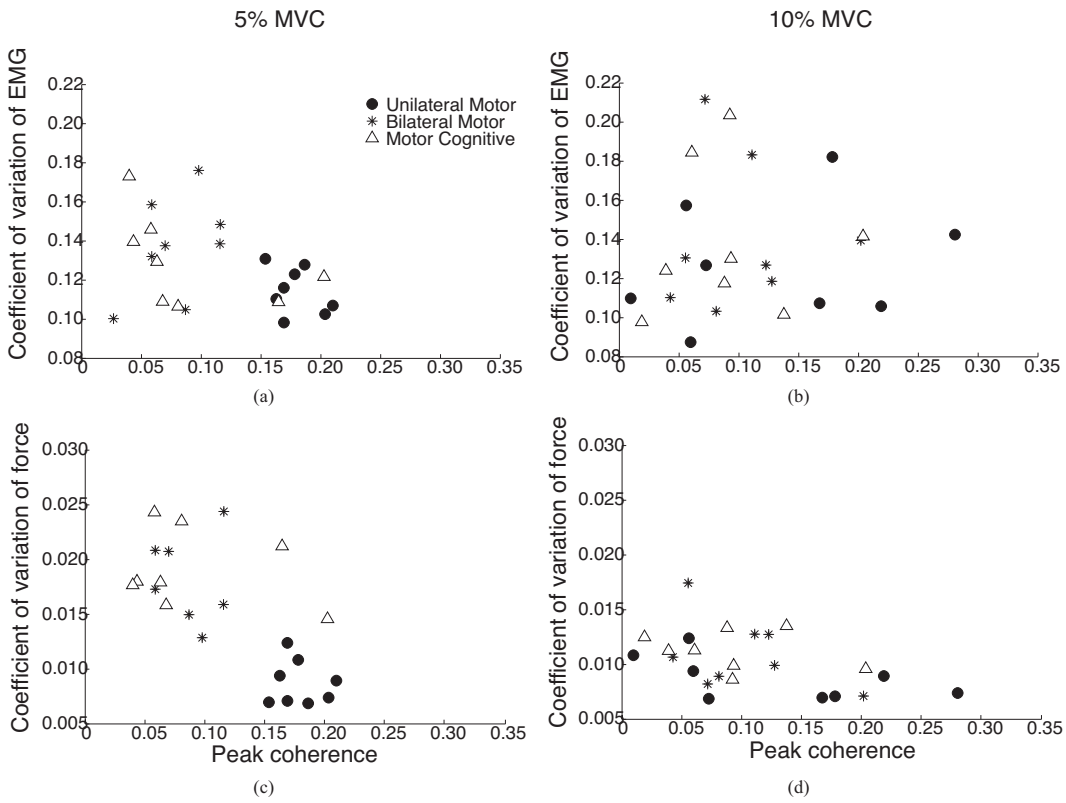

Figure 10: Distribution of corticomuscular coherence (EEG in the left motor cortex - EMG in the right hand) as a function of motor output variability across tasks. Distribution of EMG fluctuations as a function of coherence at 5% MVC (a) and 10% MVC (b). Distribution of force fluctuations as a function of coherence at 5% MVC (c) and 10% MVC (d). N = 8. There was no significant correlation.

Cognitive Performance. Cognitive performance was measured as accuracy or correct responses to cognitive problems. The cognitive accuracy was 95% ± 0.11% during the cognitive task, but it decreased significantly (P <0.01) to 83% ± 0.16% during the motor cognitive task [61].

4.3 Second Study Methodology: Neural Control of Movement Complex Task

The second study in Aim 1 considered the influence of a more complex task than that of the first study on commonly accepted physiological features, focusing on corticomuscular coherence. The incorporation of a more complex task was motivated by the results of the first study to determine if increasing task complexity might further attenuate the reduction in coherence with an additional task. Also, the complex task allowed the investigation into if the lack of an association between the coherence feature and time domain features, to assess motor output variability, was simply because of task simplicity. To increase task difficulty, the bilateral motor task was modified to make the additional motor task more dynamic, and the number of cognitive problems to complete in a designated time period was increased (Figure 11).

Five tasks were performed: unilateral abduction of the right index finger (unilateral motor task); unilateral abduction of the left index finger; cognitive task involving arithmetic and memory (cognitive task); concurrent cognitive-motor task with the right finger (motor cognitive task); and bilateral motor task with the left and right index fingers (bilateral motor task). The performance of the task was similar to the simple task described in Section 4.1. For the unilateral motor task with the right hand, subjects were instructed to abduct the right index finger to exert a force matching 5% of their MVC force. For the unilateral motor task with the left hand, subjects were instructed to abduct the left index finger to exert forces matching 2.5%, 5% and 7.5% of their MVC force. The order of percentages of MVC to match was randomized across subjects. For the bilateral motor task, the motor tasks for the

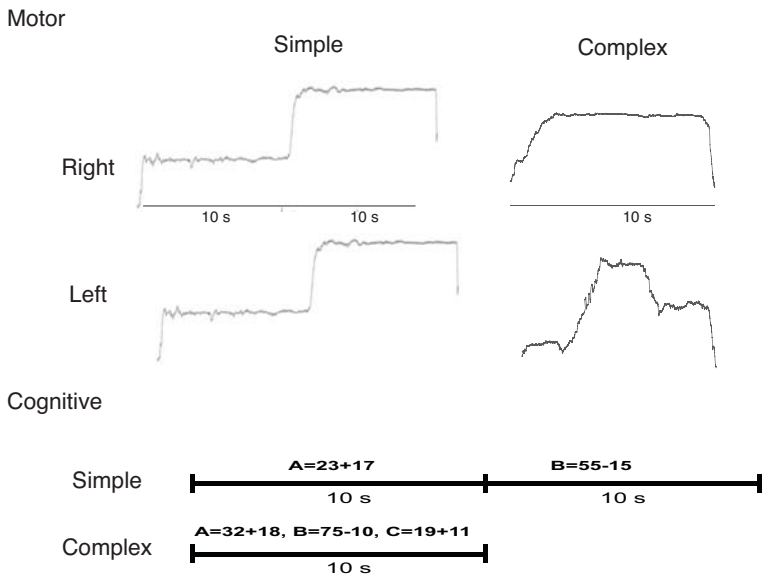

Figure 11: Comparison of the simple task versus the complex task.

right and left hands were performed concurrently. During the cognitive task, subjects were asked to solve three mathematical problems (2-digit addition and subtraction) and remember the answers until the end of each trial (12-s duration). Each trial was 12 s in duration (right hand: 5% MVC matched for 10 s with 2 s for ramping to the level; left hand: each level matched for 2 s with 2 s for ramping to the next level continuously). Just as with the simple task, the cognitive task was performed concurrently with the motor task in the right hand for the motor-cognitive task.

4.4 Second Study Results: Neural Control of Movement Complex Task

Coherence. Corticomuscular coherence decreased significantly from the unilateral motor task with the right hand to both bilateral motor (P <0.05) and motor-cognitive (P <0.05) tasks (Figure 12) just as in the first study with the simple task (Figure 7).

Cortical and Muscular Spectral Power. As with coherence, cortical and muscular power did not change with a more complex task. Total power of the EEG, full

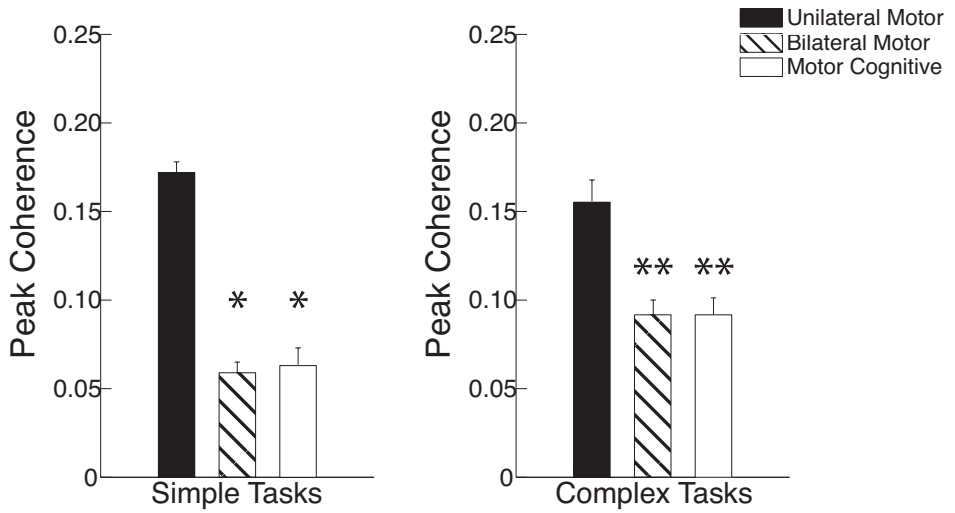

Figure 12: Comparison of the coherence for the simple task versus the complex task.

band and beta band, were not different across the unilateral motor, bilateral motor and motor-cognitive tasks. Total power of the EMG in the right hand was not influenced by task.

Motor Output Variability and Association to Coherence. As opposed to with the simple task, force variability increased with an additional task (P <0.05), but CV of EMG was not influenced. Again, there was no correlation between peak coherence and coefficient of variation of EMG or force.

4.5 Discussion

The main finding of Aim 1 was that beta-band corticomuscular coherence decreased with either an additional motor or non-motor task irrespective of task complexity. In addition, corticomuscular coherence was not associated with motor output variability or accuracy.

Reduction in beta-band coherence with an additional task

Corticomuscular coherence in the beta band is regarded to arise from the oscillatory synchronous discharge of populations of corticospinal cells around 15-30 Hz [2]. The addition of a cognitive or contralateral motor task imposed subjects to divide their attention, and the latter may have induced inter-hemispheric neural interference. Hence, decreases in synchronized oscillatory activity of corticospinal cells due to divided attention or inter-hemispheric interference are possibilities that may explain reduced corticomuscular coherence with an additional task.

Previous reports, although employing different experimental designs than the current one, suggest that oscillatory neural activity or corticomuscular coherence are related to the amount of attention directed toward a task. With regard to oscillatory neural activity, synchronous oscillations of local field potentials and single motor units during fine finger movements (similar to a precision grip task) that would require more attention were more prevalent than during simple wrist flexion and extension in monkeys [90]. In humans, synchronous motor unit activity was greater during tasks that required subjects to focus more attention toward the task (higher visual feedback gain) [114]. These studies showed that greater attention directed toward the task increased synchronous oscillations in local field potentials and motor unit activity.

Similarly, there are reports suggesting greater attention directed toward the motor task may be associated with greater magnitude or incidence of significant corticomuscular coherence. Corticomuscular coherence during a finger flexion/extension movement task was increased when subjects were instructed to put more attention to the task performance [33]. In another study where attention toward the finger precision task was decreased with concurrent mental arithmetic, the incidence of significant corticomuscular coherence was reduced while the amount of decrease was not reported [77]. In the current work, EMG fluctuations increased and cognitive performance decreased, respectively, with the addition of a motor task and non-motor

task. It appears that each task required a substantial amount of divided attention, and the attention placed to the primary task was likely reduced. Although there is no study that reported the potential effect of an additional motor task, all these studies are in line with an interpretation of current findings that corticomuscular coherence decreased with an additional concurrent task due to reduced attention towards the primary motor task.

While attention toward the primary motor task cannot be compared between the motor-cognitive task and the bilateral motor task, the amount of reduction in corticomuscular coherence was similar between the two tasks (Figure 12) for both the simple and complex tasks. It is possible that there is a flooring effect on corticomuscular coherence; once below a certain threshold, there might not be a further reduction of corticomuscular coherence. In other words, there may be a low requirement of divided attention to suppress oscillatory activity in the beta band, so any variability in attention level above this requirement would not suppress the beta-band activity any more or less. This speculation was confirmed with the second study considering a complex task. Even after attempting to divide subject's attention to a greater level, a further reduction in corticomuscular coherence was not observed.

For the potential effect of an additional motor task with the contralateral hand, one might expect inter-hemispheric neural interaction to influence oscillatory neural activity in a hemisphere and corticomuscular coherence because of interactions of neuronal networks including the transfer of excitatory and inhibitory activity via the corpus callosum. However, the literature and current experiments do not support this expectation. A previous study [74] found that while the left hand performed a constant steady contraction and the right hand produced a pair of steady contractions with a ramping phase in between, there was a decrease in the left hand and right motor cortex coherence while the right hand ramped up to another hold phase. This observation suggests inter-hemispheric interaction; however, the absence

of significant coherence between the motor cortices in their study [74] casts doubt on inter-hemispheric interaction for the coherence. A probable reason for the decrease in corticomuscular coherence is the division of attention from maintaining a constant contraction in the left hand to ramping up in the right hand, not inter-hemispheric interaction. In a primate manipulating peanuts, synchronous oscillations of local field potentials were present in both hemispheres for unimanual and bimanual movements at the same rate [91]. For both the simple and complex tasks, direction of inter-hemispheric EEG coherence between C3 and C4 alteration (i.e. an increase or decrease in peak coherence) with task varied across subjects, resulting in the absence of significant differences across tasks. Based on the equal probability of synchronized cortical activity and indifferent inter-hemispheric EEG coherence during both unimanual and bimanual tasks, it is less likely that inter-hemispheric neural interaction has a substantial influence on cortical synchronous oscillations and thus corticomuscular coherence. This is further supported by the current findings that the reduction in corticomuscular coherence during the bimanual task was no more than that during the motor-cognitive task (Figure 12), implying there was no additional effect of inter-hemispheric neural interaction on the presumably attention-induced reduction in corticomuscular coherence.

No association of coherence with fine motor performance

The functional significance of beta-band corticomuscular coherence for motor performance is of interest and importance, especially in light of the potential application of corticomuscular coherence to clinical populations with movement disorders [89, 29]. In the current study on healthy young adults, there was no significant correlation between corticomuscular coherence and motor output steadiness or variability in a hand muscle within or across individuals for both the simple and complex tasks. This finding was against the reported accompanying changes in corticomuscular coherence and

EMG variability in wrist extensor and hand muscles after immobilization [82] and the reported positive correlation between corticomuscular coherence and force accuracy in wrist extension across individuals [76]. The results are in agreement with an absence of association between corticomuscular coherence and position accuracy during ankle dorsi-plantarflexion across individuals [101]. Hence, modulations in beta-band corticomuscular coherence are not necessarily related to alterations in fine motor performance such as steadiness and accuracy. Rather, beta band modulations may be influenced by other factor(s) associated with immobilization and specific tasks, if not attention.

Corticomuscular coherence for different contralateral pairs

Literature on beta-band corticomuscular coherence has mainly focused on unilateral tasks. Although the presence of contralateral corticomuscular coherence has been demonstrated for both hands [74, 14], the potential influence of hand dominance or side of corticomuscular coherence has yet to be directly studied. Incidentally, the experimental design for the simple task allowed us to address this issue. The smaller number of subjects showing coherence for the pair of right motor cortex EEG and left (non-dominant) hand EMG (Figure 8B) indicates that EEG-EMG beta band coherence is less prevalent for the task with the left or non-dominant hand compared with the task with the right or dominant hand. Similar decreases in coherence in the right and left motor cortices with an additional motor task suggested that a reduction in corticomuscular coherence with an additional contralateral motor task was a robust phenomenon independent of hemisphere and hand. While the statistics show a significant difference, the small number of subjects ($n = 5$) showing coherence for the pair with the left hand indicates that further research is necessary to investigate this phenomena in more detail.

Additional Analysis.

As mentioned in Section 3.4, recent studies have questioned the appropriateness of EMG rectification procedure for assessing oscillatory neural activity from interference EMG [93, 94, 126]. For example, using simulated data of central input to the α-motoneuron pool and resultant interference EMG, coherence between central input and rectified EMG was lower compared with unrectified EMG across 1-100 Hz [126]. In another study, when a pair of reconstructed interference EMG signals from contracting muscles were manipulated to have very strong common oscillations in the 12-30 Hz range, an increase in the EMG-EMG coherence in the corresponding frequency range did not manifest with the use of rectified EMG [94]. In the other report cited, when cross-wavelet power spectra between EMGs from a pair of contracting muscles were compared between two contraction intensities, greater power in the 13-30 Hz range at the higher contraction intensity was observed using unrectified EMG, but not rectified EMG [93]. These reports speak against the use of rectified EMG in assessing corticomuscular coherence in the beta band.

While this was not the focus of the dissertation work and the question of rectification is still open, the data was analyzed using unrectified EMG as well. Additionally, the peak corticomuscular coherence within the beta band was independently determined in each task. This approach considered slight shifts in the location of peak coherence across tasks such that essential information on the correlated activity of the EEG and EMG within each task would be captured. The additional analysis took into account recently published literature and technical discussions as the dissertation was in process.

For the simple task, nine out of ten subjects displayed a significant level of corticomuscular coherence. Beta-band corticomuscular coherence was significantly greater in the 10% MVC level in comparison to the 5% MVC level (P <0.01) as a main effect of contraction intensity. Corticomuscular coherence was not significantly influenced

by an additional motor or cognitive task. The results of the complex task with additional analysis are shown in the following chapter with the addition of the elderly population. The lack of a task main effect shows that the approach is sensitive to finding changes with task.

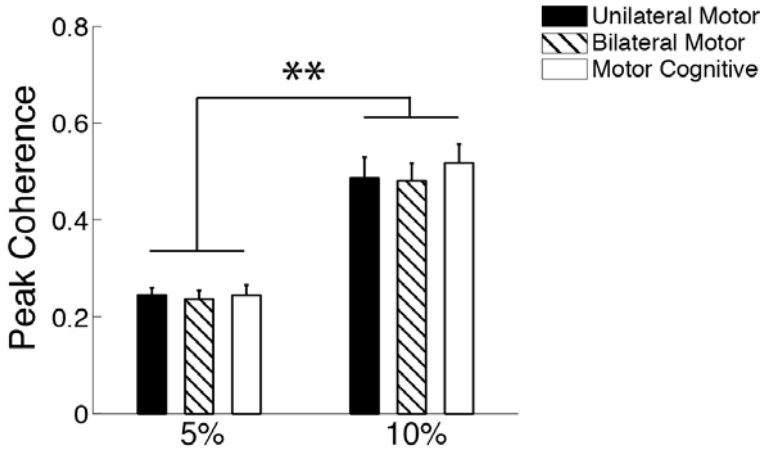

Figure 13: Beta-band corticomuscular coherence with unrectified EMG.

Further research should continue to investigate the process of rectification to determine a consensus for the trade-off between highlighting the timing and discharge pattern of a group of motor units and potentially introducing a non-linearity.

Conclusion.

Aim 1 showed that beta-band corticomuscular coherence decreased with an additional task to the same degree whether the second task was a motor or non-motor task with the inclusion of unrectified EMG. The analysis approach (rectified or unrectified EMG and considering shifts in the peak coherence) is sensitive to detecting effects of task. In addition, beta-band coherence was not associated with fine motor performance such as motor output variability and accuracy. The results suggested that attention toward the primary motor task influenced beta-band corticomuscular coherence.

CHAPTER V

NEURAL CONTROL OF MOVEMENT WITH AGING

Aging and dual tasks often degrade fine motor performance, but the effects of aging on correlated neural activity between motor cortex and contracting muscle during fine motor performance in dual task are unknown. The decline in fine motor performance can be attributed to several factors including age-associated alterations in information processing, motor neuron organization, and neuromotor activity [27, 113, 116, 118, 124]. As one feature of neuromotor activity involved in fine motor performance, correlated oscillatory neural activity between motor cortex and muscle (corticomuscular coherence) has been investigated. As described in Section 1.1, a significant difference in corticomuscular coherence has not been observed into senior age [42]. The purpose of this chapter was to compare the task-dependent change in the corticomuscular coherence feature and fine motor performance between young and elderly adults during the execution of a unilateral fine motor task and concurrent tasks that required substantial divided attention.

Aim 2: Neural Control of Movement with Aging

Approach: Determine the influence of aging on the features in Aim 1, between a unilateral motor task and concurrent motor tasks (additional motor and non-motor). Test the modulation of the neural control of movement between young and elderly adults using the complex task from Aim 1.

Hypothesis: Beta-band corticomuscular coherence in elderly adults will be lower in the beta band and greater in the alpha band when compared to young adults during dual tasks, due to greater influences of divided attention.

Figure 14: Experimental setup for elderly adults.

5.1 Methodology

Twenty-nine healthy right-handed young (n = 16, 23.9 ± 5.8 yrs, ranging 18-38 yrs; 10 women and 6 men) and elderly (n = 13, 69.2 ± 4.7 yrs, ranging 61-75 yrs; 7 women and 6 men) adults participated in the study. Additionally, young adults were recruited for inclusion in Aim 2 to ensure the young and elderly adults were performing the same task under the same conditions.

Tasks. Subjects performed 5 tasks in a similar manner to the complex task described in Aim 1. Each subject performed 8 trials for each task. Instruction to subjects remained consistent, and similar visual feedback was provided. To reiterate the tasks, subjects were instructed to produce finger abduction force as accurate and steady as possible while keeping their finger level and fully extended in the finger splint. For the unilateral motor task with the right hand, subjects were instructed to abduct the right index finger to exert a force matching 5% of their MVC force for 10 s. For the unilateral motor task with the left hand, subjects were instructed to abduct the left index finger to exert forces matching the target varying between

2.5%, 5% and 7.5% of their MVC force within a trial. They matched each level for 2 s with 2 s for ramping to the next level continuously, and the order of target level to match was randomized across subjects. Visual feedback of target and actual force level were displayed on the monitor. The scale for each hand was relative to 10% of MVC for that hand (57.8 pixels/% MVC or 263.5 pixels/N on average). For the bilateral motor task, the motor tasks for the right and left hands were performed concurrently (Figure 15), and there was no instruction with regard to the prioritization to either of the task. Each trial was 12 s in duration. A longer task duration was not implemented for several reasons. First, prolonged task durations decrease the magnitude of significant coherence observed [72]. Second, longer task durations may induce fatigue with multiple trials. Third, subjects may become irritable with longer task durations as observed especially in elderly adults in the pilot experiments.

Cognitive tasks. During the cognitive task, subjects were asked to solve three mathematical problems (2-digit addition and subtraction) and remember the answers until the end of each trial (12-s duration). The mathematical problems were displayed on the monitor in front of the subjects and they were asked to verbally recall the three answers at the end of the trial. The cognitive task was performed concurrently with the unilateral motor task in the right hand for the motor cognitive task.

Data Analysis

Coherence between EEG and EMG, and variability and accuracy of motor output were assessed for young and elderly subjects in the same manner as Section 4.1. The EEG signal was band-pass filtered (5-200 Hz) and detrended. The EMG signal was obtained from the bipolar EMG that was band-pass filtered (10-500 Hz) and detrended (Figure 15). The process of rectifying the EMG signal introduces a non-linearity into the frequency characteristics of the EMG [30, 93, 94, 126] altering the identification

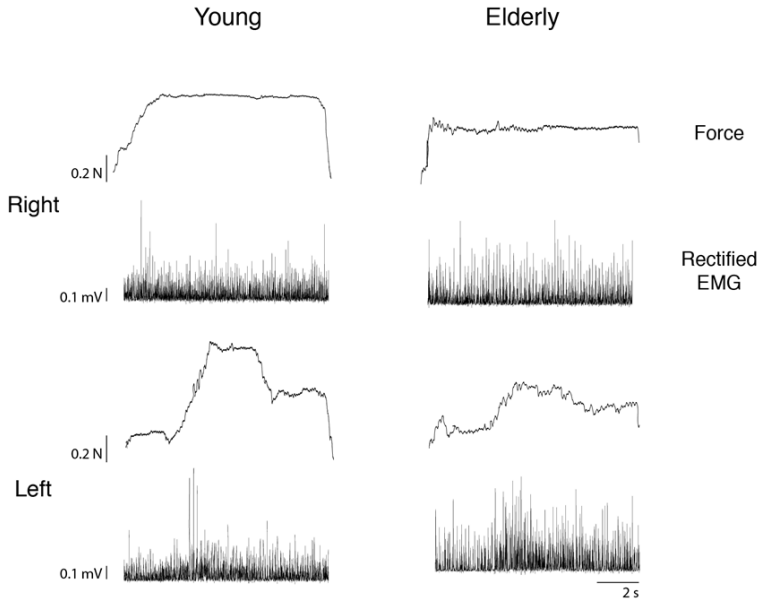

Figure 15: Representative recordings of force and rectified EMG in the first dorsal interosseus muscle in young and elderly adults. The plot indicates the profile of the motor task in the right and left hands. Subjects abducted their right index finger to exert a force matching 5% of their maximal voluntary contraction (MVC) force for the unilateral motor task. For the bilateral motor task, subjects abducted their left index finger to exert forces matching 2.5%, 5% and 7.5% of their MVC force (randomly) while concurrently abducting their right index finger.

of neural oscillations, thus suggesting that unrectified EMG is more appropriate for assessing the frequency content of the EMG signal. Accordingly, current analysis used variables with unrectified EMG as the primary dependent variables for testing the hypothesis. Nonetheless, analysis with rectified EMG was also incorporated for the purpose of comparing the findings with those in the literature that used rectified EMG [42, 53]. The EMG data during all trials were concatenated [65] for each task individually, as were the EEG data. The power spectrum of EEG, power spectrum of EMG, and coherence (Eq. 1) between EEG and EMG were computed. Concatenating the data allows for a more stable measure of coherence because of the additional data points. Concatenating the data was not possible in Aim 1 because of the two different levels of MVC being matched with the right hand. This step was employed to improve the quality of the results. Power spectra and coherence were calculated over 2048-point FFT segments. The peak corticomuscular coherence within the beta band was independently determined in each task. With the inclusion of elderly adults and the potential for shifts in the location and bands of neural activity, this approach considered slight shifts in the location of peak coherence across tasks. Additionaly, pooled corticomuscular coherence, $CC(f)$, [46] was computed to summarize the effects of aging on corticomuscular coherence

$$CC(f) = \left| \frac{\sum_{i=1}^{k} L_i R_{xy}^i(f)}{\sum_{i=1}^{k} L_i} \right|^2 \tag{6}$$

$$cl = 1 - \alpha^{\frac{1}{\sum L_i - 1}} \tag{7}$$

where k is the number of subjects, L is the number of disjoint segments, and α is 0.05. Additionally, inter-hemispheric cortico-cortical coherence (C3-C4) was also calculated in a similar manner.

5.1.1 Statistical Analysis

To test the effect of age and hand on MVC, a two-factor, 2 x 2 analysis of variance (ANOVA) with repeated measures was performed. Statistical significance of laterality quotient and Mini-Mental State Exam (MMSE) score between ages were assessed using a Student's paired t-test. The dependent variables during the unilateral, bilateral, and motor-cognitive tasks were peak corticomuscular and cortico-cortical (C3 and C4) coherence in each band, frequency at which peak value in coherence was observed in each band, normalized EEG (C3) and EMG spectral power in each band, CV of force and EMG, and error ratio of force in the right hand. Statistical significance of these dependent variables was tested between ages (young and elderly) and tasks (unilateral motor, bilateral motor, and motor-cognitive tasks) for appropriate combinations. To test the effects of age and task on variables associated with the right-hand task (peak coherence between EEG in the left motor cortex and EMG in the right hand, normalized spectral power of those EEG and EMG), a two-factor, 2 x 3 ANOVA with repeated measures was used for each variable. Post-hoc analysis was performed using Tukey for pair-wise comparison when appropriate. The association between peak corticomuscular coherence and normalized spectral power of EEG and EMG, the CV of force and EMG, and error ratio was evaluated using a Pearson's correlation coefficient. To test the effects of age and task on root mean square error (RMSE) of force in the left hand, a 2 x 2 ANOVA with repeated measures was performed. The effects of age and task on cognitive accuracy were assessed with a 2 x 2 ANOVA with repeated measures. An alpha level of 0.05 was chosen for all statistical comparisons. $P < 0.05$ or $P < 0.01$ was additionally noted where appropriate. All statistical analyses were performed using Statistica 9.0 software (StatSoft Inc., Tulsa, OK, USA).

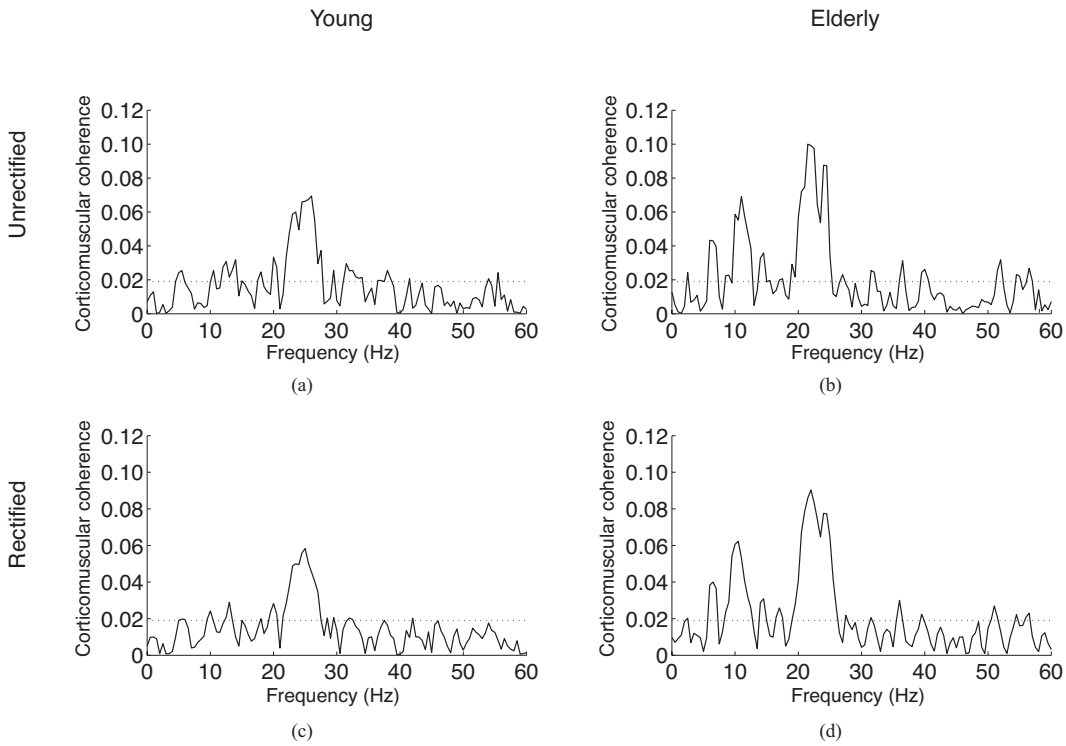

Figure 16: Representative corticomuscular coherence for an individual young (24 years) and individual elderly (71 years) subject between EEG in the left motor cortex (C3) and unrectified EMG (young, (a) and elderly,(b)) and rectified EMG (young, (c) and elderly,(d)) in the right hand during the unilateral motor task with the right hand. The broken horizontal lines indicate the confidence interval.

5.2 Results

The MVC force was comparable between young and elderly adults for both the right (young: 21.7 ± 6.2 N; elderly: 19.6 ± 8.1 N) and left (young: 18.3 ± 4.3 N; elderly: 19.4 ± 8.4 N) hands [58]. The handedness test confirmed that all subjects were right hand dominant, with a slightly higher laterality quotient in elderly adults (0.92 ± 0.10) compared with young adults (0.80 ± 0.17, P <0.05). According to the MMSE, there were no signs of cognitive impairment in the subjects, with all scores ≥ 27 although there was a small difference between young (29.8 ± 0.4) and elderly adults (28.6 ± 1.0; P <0.01).

Coherence. Representative corticomuscular coherence for an individual young (24 years) and individual elderly (71 years) adults are shown in Figure 16. In using unrectified EMG, all subjects had significant corticomuscular coherence between the left motor cortex (C3) and the right hand in the beta band with peak value at similar frequencies of 24.3 ± 5.0 Hz in young subjects and 22.8 ± 5.6 Hz in elderly subjects during the unilateral motor task. Beta-band peak corticomuscular coherence was higher ($F_{1,27} = 10.59$, $P < 0.01$) in elderly adults compared with young adults across tasks (Figure 17d) [58]. Apparent changes in beta-band corticomuscular coherence with additional concurrent tasks were not statistically different compared with the unilateral motor task (Figure 17c). However, when compared with the bilateral motor task, beta-band corticomuscular coherence during the motor cognitive task was greater ($P < 0.05$) across age groups as a main effect of task ($F_{2,54} = 4.26$, $P < 0.05$). There was no significant interaction between age and task. Additionally, subject age was positively correlated with beta-band corticomuscular coherence (pearson correlation coefficient, r=0.374). Relating the results to the additional analysis in the simple task of Aim 1, the results indicate that with an increase in task complexity, a main effect of task is observed. There was a positive association between subject age and beta-band corticomuscular coherence with unrectified EMG (correlation coefficient (r): 0.381, ($P < 0.01$)).

Within the alpha band using unrectified EMG, all but one young subject had significant corticomuscular coherence with the peak value at similar frequencies of 11.6 ± 2.3 Hz in young subjects and 12.3 ± 2.4 Hz in elderly subjects during the unilateral motor task. This alpha-band frequency for peak coherence was not influenced by age or task. Elderly adults also exhibited a higher magnitude of corticomuscular coherence within the alpha band compared with young adults (main effect of age, $F_{1,27} = 6.62$, $P < 0.05$) (Figure 17b) [58]. This difference appears to result mostly from the large increase during the motor-cognitive task in elderly adults. As a main effect of task

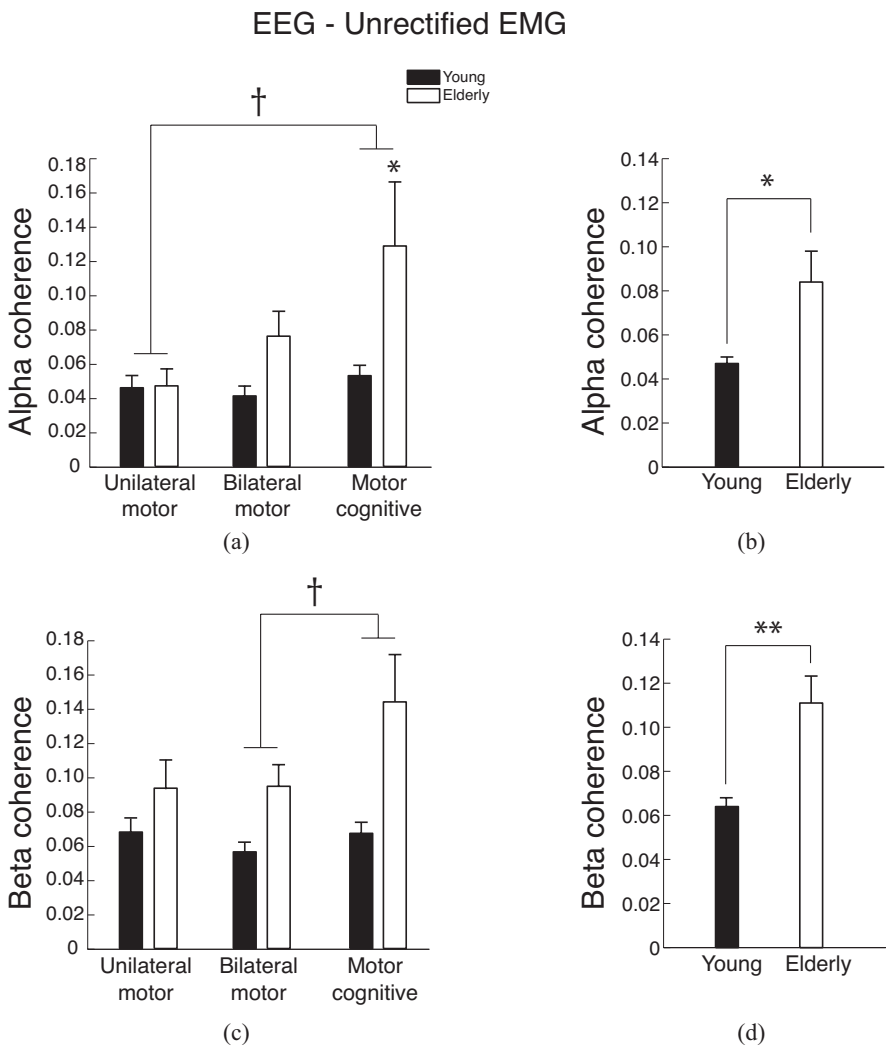

Figure 17: Peak corticomuscular coherence (using unrectified EMG) in the (a) and (b) alpha (8-14 Hz) and (c) and (d) beta (15-32 Hz) bands during the unilateral motor, bilateral motor, and motor-cognitive tasks in young and elderly adults. Data in each task and group are shown in the left column, and the data collapsed across tasks are shown in the right column. *, P <0.05 for the age-related difference across tasks (main effect of age) or at a corresponding task (interaction of age and task). †, P <0.05 due to a main effect of task.

($F_{2,54}$ = 4.83, P <0.05), alpha-band corticomuscular coherence was higher in the motor-cognitive task (0.087 ± 0.097 when collapsed across ages) compared with the unilateral motor task 0.046 ± 0.030) across age groups (Figure 17a). As an interaction of age and task ($F_{2,54}$ = 3.21, P <0.05), alpha-band corticomuscular coherence during

the motor-cognitive task was higher (P <0.05) in elderly than young adults, whereas no significant age-associated difference was observed in other tasks.

For corticomuscular coherence with rectified EMG, elderly adults exhibited higher corticomuscular coherence within the beta band ($F_{1,27} = 10.15$, $P < 0.01$) (Figure 18d) [58]. A significant effect of task was not observed when rectified EMG was used. There was a positive association between subject age and beta-band corticomuscular coherence with rectified EMG ($r = 0.374$, $P < 0.01$). Elderly adults also exhibited higher corticomuscular coherence with rectified EMG in the alpha band ($F_{1,27} = 8.25$, $P < 0.01$) (Figure 18b). This age-associated difference appears to result mostly from the large increase during the motor-cognitive task in elderly adults. As an interaction of age and task ($F_{2,54} = 5.21$, $P < 0.01$), alpha-band corticomuscular coherence with rectified EMG during the motor-cognitive task was higher ($P < 0.01$) in elderly than young adults (Figure 18a).

To summarize the age-associated difference in corticomuscular coherence, pooled coherence was further calculated. For corticomuscular coherence with unrectified EMG, significant pooled coherence was observed between 9 and 32 Hz for young adults and between 10 and 26 Hz for elderly adults (Figure 19a) [58]. Using rectified EMG, significant pooled coherence was observed between 9 and 32 Hz for young adults and between 9 and 26 Hz for elderly adults (Figure 19b). In both cases (using unrectified and rectified EMG), the pooled coherence visually displayed greater corticomuscular coherence in elderly adults compared with young adults.

Inter-hemispheric cortico-cortico coherence between C3 and C4 EEGs tended to be higher in the beta band in elderly adults, on average, but did not have any significant effect of age or task (Table 3).

Cortical and muscular spectral power.

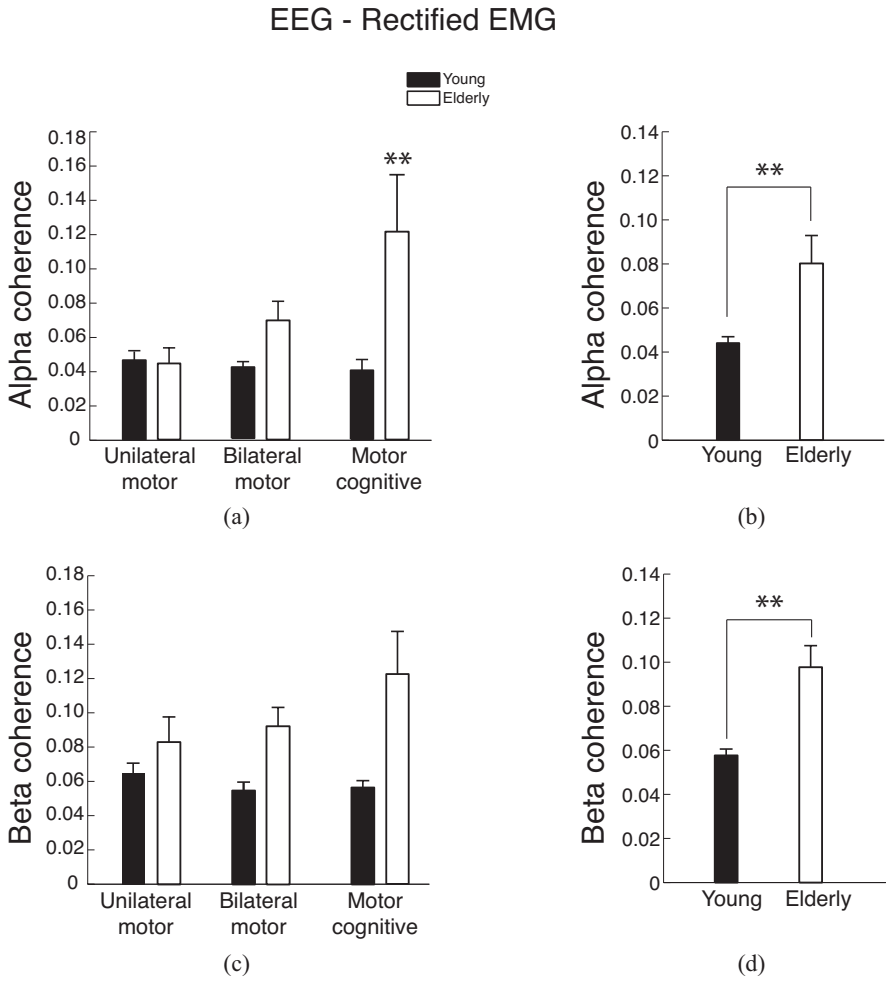

Figure 18: Peak corticomuscular coherence (using rectified EMG) in the (a) and (b) alpha (8-14 Hz) and (c) and (d) beta (15-32 Hz) bands during the unilateral motor, bilateral motor, and motor-cognitive tasks in young and elderly adults. Data in each task and group are shown in the left column, and the data collapsed across tasks are shown in the right column. **, P <0.01 for the age-related difference across tasks (main effect of age) or at a corresponding task (interaction of age and task)

The significant effect of age or task on normalized EEG was observed only in beta-band power in the left motor cortex (C3) [58]. Beta-band EEG (C3) power was greater ($F_{1,27} = 12.18$, P <0.01) in elderly adults (0.454 ± 0.116 when collapsed across tasks) than young adults (0.331 ± 0.081) across tasks (Table 4). Similarly to beta-band corticomuscular coherence, beta-band EEG power during the concurrent

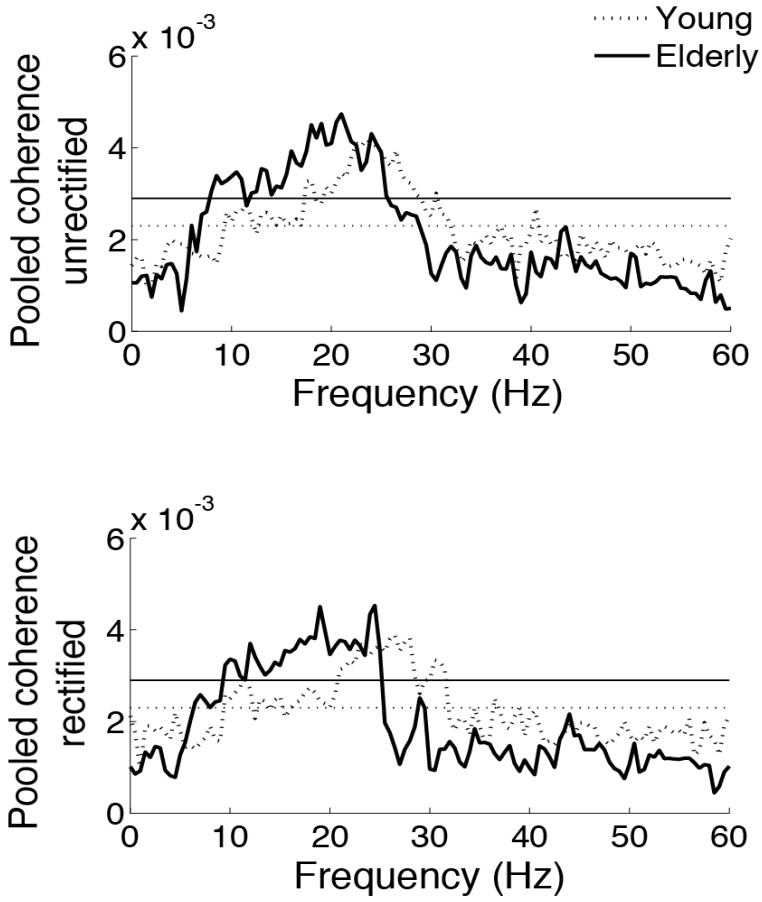

Figure 19: Pooled corticomuscular coherence across young (broken lines, n = 16) and elderly (solid lines, n = 13) adults for unrectified EMG (A) and rectified EMG (B) during the unilateral motor task with the right hand. The broken horizontal lines indicate the confidence interval for young adults and the solid horizontal lines indicate the confidence interval for elderly adults

motor cognitive task was higher (P <0.05) compared with the bilateral motor task across age groups as a main effect of task ($F_{2,54}$ = 3.54, P <0.05). When the data for all age groups and tasks were considered, beta-band EEG power was positively correlated with beta-band corticomuscular coherence with a correlation coefficient (r) of 0.392 (P <0.01). Significant associations were not observed between alpha-band EEG power and alpha-band corticomuscular coherence.

Significant effects of age or task were observed on the normalized EMG in the right hand across frequency bands [58]. Compared with the unilateral task, unrectified

Table 3: Inter-hemispheric cortico-cortico coherence between C3 and C4 EEGs in alpha (8-14 Hz) and beta (15-32 Hz) bands during the unilateral motor, bilateral motor, and motor-cognitive tasks in young and elderly adults. Mean ± SD There was no significant effect of age or task. (Young, n=16; Elderly, n=13)

	Young	**Elderly**
Alpha band		
Unilateral Motor	0.15 ± 0.07	0.14 ± 0.04
Bilateral Motor	0.12 ± 0.10	0.15 ± 0.07
Motor Cognitive	0.16 ± 0.09	0.13 ± 0.07
Beta band		
Unilateral Motor	0.16 ± 0.12	0.20 ± 0.09
Bilateral Motor	0.14 ± 0.08	0.22 ± 0.10
Motor Cognitive	0.15 ± 0.11	0.19 ± 0.10

EMG power during the motor cognitive task was slightly increased in the alpha (P <0.05) and beta (P <0.05) bands across age groups. Beta-band unrectified EMG power was positively correlated with beta-band corticomuscular coherence ($r = 0.360$, P <0.01) when the data from all age groups and tasks were considered. Elderly adults exhibited greater alpha-band unrectified EMG power compared with the young adults across tasks ($F_{1,27} = 5.07$, P <0.05; elderly: 0.030 ± 0.010, young: 0.023 ± 0.008). Elderly adults also exhibited greater alpha-band rectified EMG power compared with young adults (main effect of age, $F_{1,27} = 5.00$, P <0.05; elderly: 0.183 ± 0.028, young: 0.137 ± 0.071).

Coherence and fine motor performance. Motor output variability during steady contraction in the right hand was assessed for the fluctuations in force and EMG. The CV of force was greater (main effect of age, $F_{1,27} = 10.60$, P <0.01) in elderly adults compared with young adults across tasks (Figure 20b) [58]. As a main effect of task ($F_{2,54} = 20.83$, P <0.01), the CV of force during bilateral motor (0.058 ± 0.062 when collapsed across ages, P <0.05) and motor-cognitive (0.061 ± 0.052, P <0.05) tasks were greater compared with the unilateral motor task (0.027 ± 0.021 when collapsed

Table 4: Frequency power of EEG in the left motor cortex (C3) and EMG (unrectified and rectified) in the right hand for the alpha and beta bands during the unilateral motor, bilateral motor, and motor-cognitive tasks in young and elderly adults. Power in each band is normalized to total power. Mean ± SD. *, P <0.05 vs. Young, **, P <0.01 vs. Young; †, P <0.05 vs. Motor cognitive

	Young	**Elderly**
EEG power, C3		
Alpha band		
Unilateral Motor	0.338 ± 0.131	0.298 ± 0.139
Bilateral Motor	0.332 ± 0.126	0.275 ± 0.080
Motor Cognitive	0.342 ± 0.132	0.319 ± 0.108
Beta band		
Unilateral Motor	0.337 ± 0.084	0.436 ± 0.133**
Bilateral Motor	0.318 ± 0.079 †	0.449 ± 0.123**, †
Motor Cognitive	0.340 ± 0.083	0.478 ± 0.096**
Unrectified EMG power		
Alpha band		
Unilateral Motor	0.022 ± 0.006 †	0.029 ± 0.009*, †
Bilateral Motor	0.024 ± 0.008	0.029 ± 0.009*
Motor Cognitive	0.024 ± 0.009	0.033 ± 0.012*
Beta band		
Unilateral Motor	0.288 ± 0.048 †	0.316 ± 0.056 †
Bilateral Motor	0.293 ± 0.043	0.320 ± 0.055
Motor Cognitive	0.304 ± 0.036	0.325 ± 0.047
Rectified EMG power		
Alpha band		
Unilateral Motor	0.138 ± 0.071	0.189 ± 0.026*
Bilateral Motor	0.135 ± 0.067	0.178 ± 0.024*
Motor Cognitive	0.139 ± 0.079	0.184 ± 0.035*
Beta band		
Unilateral Motor	0.366 ± 0.064	0.370 ± 0.044
Bilateral Motor	0.371 ± 0.052	0.376 ± 0.043
Motor Cognitive	0.376 ± 0.052	0.383 ± 0.052

across age groups) across age groups. This task effect appears to be greater in elderly adults based on the age and task interaction ($F_{2,54} = 6.45$, $P < 0.01$), indicating that the CV of force increased by more than a factor of two with an additional motor ($P < 0.01$) and cognitive task ($P < 0.01$) in elderly adults, but not in young adults (Figure 20a). For another measure of motor output variability, the CV of EMG was greater (main effect of age, $F_{1,27} = 8.01$, $P < 0.01$) in elderly than young adults across tasks (Figure 20d).

Motor output error was assessed by the error ratio of the mean exerted force. Error ratio was greater ($F_{1,27} = 11.92$, $P < 0.01$) in elderly than in young adults when averaged across tasks (Figure 20f) [58]. This difference appeared to result mainly from larger values in elderly adults during the bilateral motor task and motor-cognitive tasks, with a greater influence from the latter. As a main effect of task ($F_{2,54} = 12.37$, $P < 0.01$), error ratio during the motor-cognitive task ($9.1 \pm 7.7\%$) was greater when compared with the unilateral motor task ($5.1 \pm 3.3\%$, $P < 0.05$) across age groups (Figure 20E). As an interaction of age and task ($F_{2,54} = 5.03$, $P < 0.05$), error ratio during the bilateral motor ($P < 0.01$) and motor-cognitive ($P < 0.01$) tasks were greater in elderly than young adults, with a greater value in the latter compared with the former ($P < 0.05$). In addition, error ratio during the motor-cognitive task was greater when compared with the unilateral motor task in both young ($P < 0.01$) and elderly ($P < 0.05$) adults, but greater compared with the bilateral motor task only in elderly adults ($P < 0.05$).

Using unrectified EMG, significant correlations between beta-band corticomuscular coherence and fine motor performance were observed only for the motor-cognitive task [58]. There was a negative correlation between error ratio and beta-band corticomuscular coherence using unrectified EMG ($r = -0.629$, $P < 0.01$), but not rectified EMG ($r = -0.417$, $P = 0.11$), across young adults during the motor-cognitive task (Table 5). Thus, young adults that showed a higher coherence showed a lower error

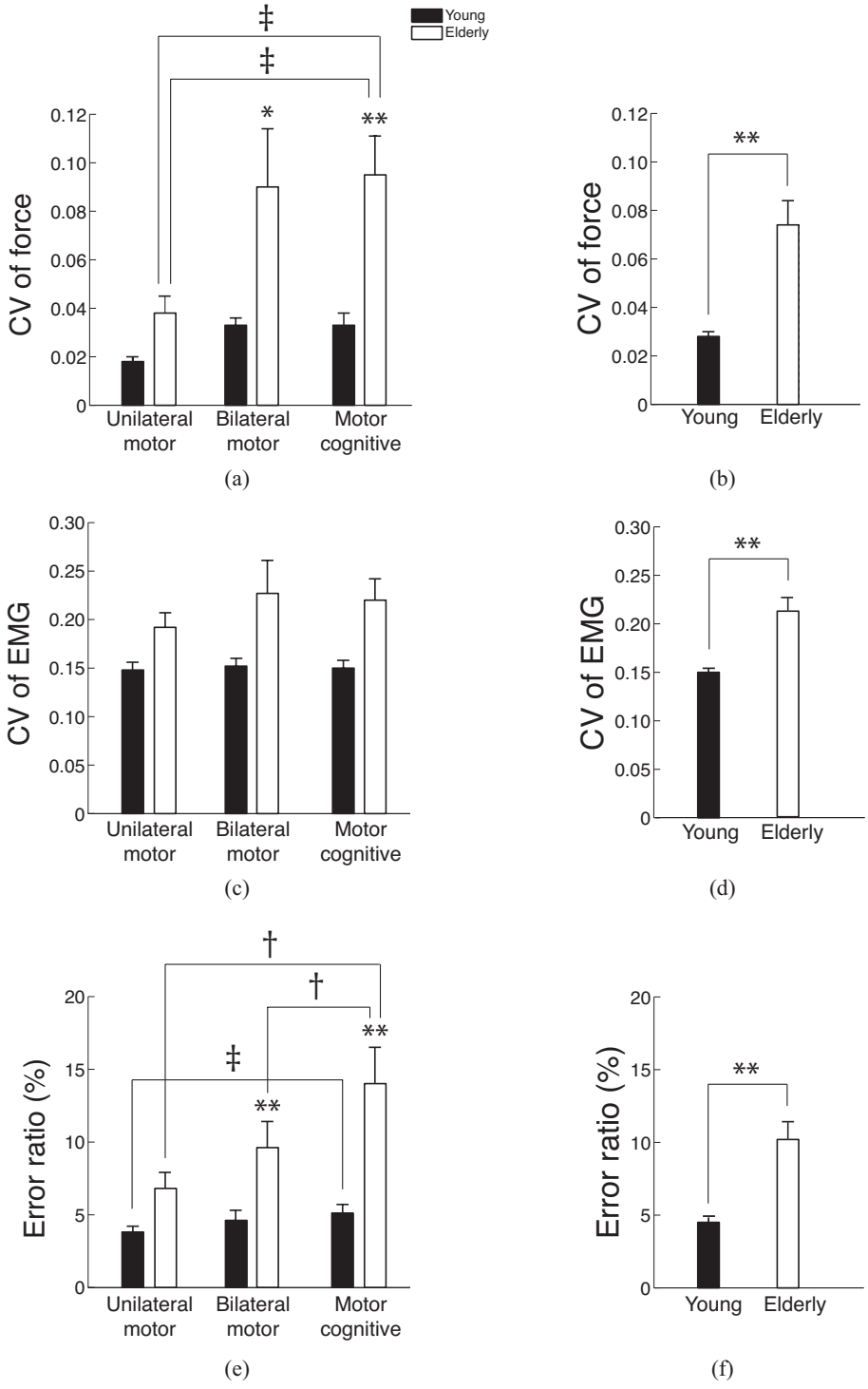

Figure 20: The influences of task and age on fine motor performance. (a) and (b) Coefficient of variation (CV) of force, (c) and (d) CV of EMG, and E and F) error ratio. Data in each task and group are shown in the left column, and the data collapsed across tasks are shown in the right column. †, P <0.05 and ‡, P <0.01 for the task-related difference in the corresponding age groups (interaction of age and task). **, P <0.01 for the age-related difference across tasks (main effect of age) or at a corresponding task (interaction of age and task)

Table 5: Correlations between beta-band corticomuscular coherence and the coefficient of variation (CV) of force, CV of EMG, and error ratio in the motor-cognitive task in young and elderly adults. r, Pearson's coefficient of correlation; *n.s.*, not significant. (young, n=16; elderly, n=13)

	r	***P***
Young		
CV of force	-0.128	*n.s*
CV of EMG	0.152	*n.s.*
Error ratio	-0.629	<0.01
Elderly		
CV of force	0.216	*n.s.*
CV of EMG	0.298	*n.s.*
Error ratio	0.469	*n.s.*

rate during the motor-cognitive task. Using rectified EMG, a significant negative correlation between the CV of force and beta-band corticomuscular coherence appeared across young adults during the unilateral motor task (r = -0.541, P <0.05), which was not significant when unrectified EMG was used (r = -0.328, P = 0.22). Significant associations were not observed for other measures of fine motor performance or in elderly adults whether rectified or unrectified EMG was used for coherence calculation.

Motor performance in the left hand. The RMSE of force was greater (main effect of age, $F_{1,27}$ = 19.58, P <0.01) in elderly adults when compared with young adults across tasks (Table 6) [58]. As a main effect of task ($F_{1,27}$ = 6.77, P <0.05), the RMSE of force in the left hand during bilateral motor (0.361 ± 0.234 N) tasks was greater compared with the unilateral motor task with the left hand (0.276 ± 0.234 N). There was no significant interaction of age and task.

Table 6: Root mean square error (RMSE) during the unilateral motor left and bilateral motor tasks, and average across tasks in young and elderly adults. Mean ± SD. **, P <0.01 vs. Young, ‡, P <0.01 vs. Unilateral motor left

	Young	**Elderly**	**Average**
	(n = 16)	(n = 13)	
Unilateral Motor Left	0.158 ± 0.071 N	0.420 ± 0.295 N	0.276 ± 0.234 N
Bilateral Motor	0.227 ± 0.078 N	0.518 ± 0.249 N	0.361 ± 0.234 N‡
Average	0.192 ± 0.071 N	0.467 ± 0.273 N**	

Table 7: Cognitive accuracy during the cognitive task, motor-cognitive task, and average across tasks in young and elderly adults. Mean ± SD. **, P <0.0 1 vs. Young, ‡, P <0.01 vs. Cognitive

	Young	**Elderly**	**Average**
	(n = 16)	(n = 13)	
Cognitive	88.3% ± 9.8%	72.1% ± 22.5%**	81.0% ± 18.3%
Motor Cognitive	84.1% ± 12.6%	58.0% ± 27.0%**,‡	72.4% ± 23.9%‡
Average	86.2% ± 11.3%	65.1% ± 25.4%**	

Cognitive accuracy. Cognitive accuracy was measured as the percentage of correct responses to cognitive problems. Cognitive accuracy was greater ($F_{1,27}$ = 10.52, P <0.01) for young than elderly subjects when averaged across tasks (Table 7) [58]. As a main effect of task ($F_{1,27}$ = 15.07, P <0.01), cognitive accuracy decreased by approximately 9% during the motor cognitive task compared with the cognitive task across age groups. This difference was more prominent in elderly adults because cognitive accuracy during the motor-cognitive task in elderly adults was significantly less compared with the cognitive task (P <0.01) in young adults as an interaction of age and task ($F_{1,27}$ = 4.46, P <0.01).

5.3 Discussion

The findings with the use of unrectified EMG are highlighted as described in the methodology section. The main findings of Aim 2 include: 1) beta-band corticomuscular coherence was higher in elderly than young adults for both unilateral motor

and dual tasks; 2) alpha-band corticomuscular coherence in the motor-cognitive task was greater in elderly than young adults; and 3) beta-band corticomuscular coherence was negatively correlated with motor output error in the motor-cognitive task across young, but not elderly adults.

Beta band. Age-associated increase in corticomuscular coherence has only been observed up to middle age (59 years) [53] and not to older age [42]. A review of literature has shown that the current work is the first to find a continued increase in beta-band corticomuscular coherence post adulthood into a senior age (62-75 years). Beta-band corticomuscular coherence increased from childhood (4-12 years) to adulthood (21-35 years) in the opponens pollicis muscle during a pinch grip task [42] and from childhood (0 years old) to middle age (59 years old) during a wrist extension or gripping task [53]. However, for advanced age, a significant difference in beta-band corticomuscular coherence was not observed between adulthood (21-35 years) and elderly age (55-80 yrs) in the opponens pollicis muscle during a pinch grip task [42].

The previous studies on aging effects [42, 53] used rectified EMG in the calculation of corticomuscular coherence. The current study found greater corticomuscular coherence in elderly than young adults whether unrectified or rectified EMG was used (Figures 17 and 18). Hence, the different finding from the previous study [42] is not because of the use of EMG rectification. Since the greater beta-band corticomuscular coherence in the first dorsal interosseous muscle was found for elderly adults across unilateral and dual tasks (Figure 17), this difference does not seem to be related to divided attention. Rather, the difference is potentially due to the difference in muscle and other task details that may influence corticomuscular coherence [43, 72, 88, 130].

The potential influence of the tested muscle and task on age-associated changes in common oscillatory activity may also be inferred from studies on EMG-EMG coherence and motor unit coherence. In the developmental ages from adolescence to

adulthood, beta-band EMG-EMG coherence between the abductor pollicis longus and brevis muscles during thumb abduction was smaller in the ages of 7-9 years compared with 12-14 years and adults (22-59 years) [31]. Collectively with the above mentioned increases in corticomusuclar coherence from childhood to adulthood in the opponens pollicis [42] and forearm extensor muscles [53], increases in beta-band common oscillatory activity during motor development appear to be consistent regardless of the tested muscle and task details, at least in the upper limb. In elderly age, the current findings may be indirectly supported by a study on motor unit coherence in the same muscle during a similar task [115]. Compared with young adults (24.1 $\pm$ 4.1 years), coherence in the discharge intervals between pairs of motor units in the first dorsal interosseus muscle tended to be greater within the beta band in elderly adults (70.4 $\pm$ 5.9 years) during steady isometric contraction $\geq$10% MVC with visual feedback of force [115]. In the study that did not observe a difference on beta-band corticomuscular coherence between young and elderly adults on the opponnens pollicis muscle [42], subjects tried to squeeze an object gently and steadily with the thumb and index finger without visual feedback of force, and the steadiness of exerted force was not quantified. Presence or absence of visual feedback may influence muscle activity and force steadiness [5, 140], and potential associations between motor output steadiness and beta-band corticomuscular coherence were suggested [42, 76]. Thus, the absence of visual feedback and/or the variability in the steadiness of motor output may have influenced the comparable beta-band corticomuscular coherence between young and elderly adults in the previous study [42]. Until these possibilities are clarified in future studies, it would be safer to state that beta-band corticomuscular coherence is greater in elderly than young adults during steady contraction with visual feedback.

Corticomuscular coherence originates from oscillatory activity in the cortex, but the influence of aging on cortical spectral power has been unclear at the senior age. Varying changes in beta-band EEG power have been reported with senior age, but it is

proposed here that the inconsistency was probably because of the inclusion of clinical populations. In some reports that showed decreases or no change in beta-band EEG power in elderly adults [52, 110], subjects were not considered to be healthy because of psychogenic disease, mild psychological disorders or physical disability. In other studies that did not mention the inclusion or exclusion of clinical populations, an increase in beta-band EEG power with age was reported [25, 26, 66, 75, 136]. Care was taken in all experiments to control for extraneous factors that might influence neural activity if including unhealthy subjects. Subjects were without evidence of neurological disorders, not medicated, and fully alert. The comparable MVC values between young and elderly subjects support the healthy status of one aspect of their neuromuscular system in their tested muscle. Although Aim 2 did not examine clinical populations, the results are in favor of the contention that beta-band EEG power during motor tasks is increased in healthy elderly adults.

The increase in both EEG power and corticomuscular coherence in the beta band suggests a potential association between the two. A study [76] reported a positive correlation between beta-band cortical power and corticomuscular coherence in the flexor digitorum superficialis muscle during isometric flexion of the index finger. This observation was supported by the current finding of a positive correlation between beta-band cortical power and corticomuscular coherence ($r = 0.392$). Mathematically speaking, a decrease in corticomuscular coherence would result because of an independent increase in EEG power with no change in correlation between EEG and EMG in the beta band (see Eq. 1). Therefore, the positive correlation in the previous [76] and current studies implied that greater beta-band EEG power significantly contributed to producing greater correlated corticomuscular coherence in the beta band in elderly adults. Hence, the results of Aim 2 are interpreted to mean that beta-band corticomuscular coherence in healthy elderly adults is increased due to increased oscillatory synchronous discharges of corticospinal cells.

The greater beta-band corticomuscular coherence in elderly adults across unilateral and dual tasks (Figure 17) was opposite to the hypothesis. Measurement of corticomuscular coherence is regarded as the net result of multiple factors that may independently increase or decrease coherence. Potential factors that were likely involved in the current protocol include attention, stress, and activation of the supplementary motor area. First, the distribution of attention to an additional task would reduce beta-band corticomuscular coherence in the primary motor task [33, 61, 77]. Second, the increased stress due to increased task difficulty with an additional task may increase coherence because various forms of stress appear to increase cortical spectral power. Stress from mental arithmetic increased beta-band cortical activity in humans [144], and post-traumatic stress disorder (PTSD) increased beta-band power in the central (13.5-18 Hz) and frontal (18.5-30 Hz) regions in PTSD subjects in comparison with control subjects [9]. Third, an additional cognitive task may increase cortical activity of the supplementary motor area [67] when a sensorimotor loop may have become engaged contributing to the increase in corticomuscular coherence [3]. Although the apparent net results in beta-band corticomuscular coherence were similar between age groups (Figure 17), it is unknown if neural activity was similarly or differentially influenced by each factor. The present study for Aim 2 originally focused on the potential influence of the first factor (attention) in building the hypothesis, but the effects of the second and third factors above appear to have overridden this assertion.

Considering the reported differences in the responsiveness to the listed factors [86, 136, 137] and in the employed neural strategy for coping with dual tasks between young and elderly adults [36, 38, 48], it would be worthwhile to speculate the possibility that neural activity was differentially influenced by different factors between age groups. Different neural strategies between ages have been observed as increased

activation of sensorimotor and frontal cortex regions in elderly adults during inter-limb dual tasks [48] and bimanual in-phase and anti-phase movements of the wrist [38]. Dual-task paradigms are known to attenuate performance in elderly adults to a greater magnitude compared with young adults [38, 138] (Figure 20 and Table 7). The greater increasing trend in beta-band corticomuscular coherence with additional tasks in elderly adults may imply that they have been influenced more by one or both of the latter two upregulating factors (stress and activation of supplementary motor area) compared with young adults. In line with this speculation, elderly adults demonstrated greater impairment in fine motor (Figure 20) and cognitive performances (Table 7) and verbally expressed frustration and anxiety, especially during the motor-cognitive task. Future studies are warranted to clarify the specific influence of each factor on beta-band corticomuscular coherence and to directly quantify the involvement of each factor in young and elderly adults.

An increase of beta-band corticomuscular coherence in elderly compared with young adults across unilateral and dual tasks was also observed for the inclusion of rectified EMG. However, a significant difference in corticomuscular coherence across task was not observed when rectified EMG was used (Figure 18c and 18d). The frequency range of significant coherence as observed from the pooled coherence was similar between corticomuscular coherence computed with and without rectified EMG (Figure 19). The similar result of increase in corticomuscular coherence with age using unrectified and rectified EMG supports the continued increase in beta-band corticomuscular coherence post adulthood into senior age. According to the most recent examination on coherence calculation with rectified EMG, when a single EEG channel is used, signal interference from other sources in the brain appears to be reflected more in corticomuscular coherence with rectified EMG than unrectified EMG [6]. Differences in the influence of task highlights the potential sensitivity of rectification for detecting changes in specific neural activity across tasks.

Alpha band. Until Aim 2 of the dissertation work was conducted, the only implication about the influence of healthy aging on alpha-band corticomuscular coherence had been a possible increase with healthy aging. The possibility was because alpha-band corticomuscular coherence was observed in elderly adults in more cases than in young adults for the right opponens pollicis muscle during an isometric pinch-grip task [42]. Aim 2 considered the potential influence of attention on this implication because significant alpha-band corticomuscular coherence was observed during tasks requiring divided attention between motor and arithmetic tasks [77] or focused attention to complete a rapid movement of the index finger to the same positions [33]. As a result, the greater alpha-band corticomuscular coherence during the motor-cognitive task in elderly adults (Figure 17) was consistent with the hypothesis. The level of attention required to perform the task was different between Aim 2 and previous studies [42]. In this previous study [42], subjects performed a unilateral task and did not have a specific target on which to focus because feedback of force was not provided. The increase in alpha-band corticomuscular coherence with an addition of a cognitive task in young and elderly adults (Figure 17) was consistent with the presence of significant alpha-band corticomuscular activity during motor tasks involving additional cognitive task [77]. For the bilateral motor task, the amount of divided attention in the protocol for Aim 2 was likely less than the motor-cognitive task according to a smaller increase in motor output error (Figure 20). Hence, divided attention with an addition of a contralateral motor task in the current protocol may not have been large enough to increase alpha-band corticomuscular coherence by an effective amount. The findings indicated that the influence of aging on alpha-band corticomuscular coherence is task dependent, and collectively with the knowledge in the literature, attention-related cognitive components appear to play a role.

As with the beta band, the influence of aging on alpha-band cortical spectral power

had been unclear at the senior age. From adulthood to a senior age, some reports indicated no change in the occipital region [25] and the sensorimotor cortex [42], and others indicated a decrease on average across the prefrontal, temporal, central and occipital regions [75] in alpha-band EEG power. In agreement with the former two studies, no change was observed in alpha-band EEG power between young and elderly adults. The similarity between young and elderly adults may be related to the healthy status of the young adults included and cortical regions observed. The absence of an association between EEG power and corticomuscular coherence suggested that aging and an additional cognitive task can increase alpha-band corticomuscular coherence independent of the relative amount of oscillatory discharges of corticospinal cells in the alpha band.

Corticomuscular coherence and fine motor performance. As a potential functional significance of corticomuscular coherence, the association between beta-band corticomuscular coherence and fine motor performance (motor output error and variability) had been demonstrated across trials or segments within subjects [42, 76, 82], but not across subjects. For motor output error, no correlation across subjects was found between beta-band corticomuscular coherence and position error during unilateral ankle dorsi-plantarflexion [101] or force error during index finger abduction in either single- or dual-task paradigm (as in Aim 1, [61]). The absence of correlation across subjects during the unilateral motor task (Table 5) was consistent with Aim 1 and [101]. With a difficult motor-cognitive task, a negative correlation appeared between beta-band corticomuscular coherence and motor output error across young, but not elderly adults (Table 5). Although the correlation did not reach statistical significance when rectified EMG was used, these new results were in line with the authors expectation. The difficulty of the current motor-cognitive task was evident from the greater motor error for this task than other tasks (Figure 20e). The

results thus indicated that in a difficult dual task that divides attention and requires substantial cognitive processing, young adults with greater beta-band corticomuscular coherence tend to produce less error (i.e. higher motor accuracy). The absence of correlation across elderly adults between beta-band corticomuscular coherence and motor output error was as expected. The age-related discrepancy in this correlation underscored the distinction in neural strategy for accomplishing dual task between young and elderly adults, such as increased activation of additional cortical regions besides the primary motor cortex in elderly adults [84].

For motor output variability, in Aim 1 (simple task) [61], no correlation was found across young adults between beta-band corticomuscular coherence and force variability or EMG variability. The absence of correlation between beta-band corticomuscular coherence, using unrectified EMG, and motor output variability across young or elderly adults (Table 5) followed the previous findings of Aim 1 [61] and was against the expectation for young adults but not for elderly adults. In young adults, neither additional task induced any significant change in motor output variability (Figure 20), indicating that the employed additional task was not influential to motor output variability in young adults. In elderly adults, large changes in the force variability with little change in EMG variability implied an involvement of an antagonist muscle that would counter an association between motor output variability and beta-band corticomuscular coherence in the agonist muscle. When rectified EMG was used, there was an unexpected appearance of a significant negative correlation between beta-band corticomuscular coherence and the CV of force during the unilateral motor task across young subjects. Considering that this correlation has not been observed in the literature [101] (or Aim 1 [61]) and that corticomuscular coherence using a single EEG channel with rectified EMG may involve greater interference from other sources than with unrectified EMG [6], this inconsistent finding may possibly be influenced by neural activity in areas other than C3. Clarification of this matter

would require a study with multi-channel EEG.

Collectively with the findings in the literature, the following possibilities appear to exist for the potential association between beta-band corticomuscular coherence and fine motor performance. Trials or segments with higher beta-band corticomuscular coherence may produce less motor output errors and variability in some tasks or individuals in young [42, 82], but not elderly adults. Individuals with lower beta-band corticomuscular coherence do not show smaller motor output variability as shown in Aim 1 ([61] and the current aim), but may exhibit more accurate motor output ([76] and current aim) in young, but not elderly adults.

Conclusion.

In support of the NIA's aim to "understand the mechanisms involved in normal brain aging; the role of cognition in everyday functioning; protective factors for sensory, motor, emotional, and cognitive function" [98] the results have provided insight into the neural control of fine motor tasks with healthy aging. Aim 2 showed that during steady contraction with visual feedback corticomuscular coherence (a measure of the correlated activity between brain and muscle) was higher in elderly adults compared with young adults in the alpha and beta bands across unilateral and dual tasks. In the alpha band, the increase in corticomuscular coherence was largest with an additional cognitive task in elderly adults. In the beta band, corticomuscular coherence was increased with an additional task in the same manner between young and elderly subjects. In addition, beta-band corticomuscular coherence in the motor-cognitive task was negatively correlated with motor output error across young, but not elderly adults. The results suggest that 1) corticomuscular coherence was increased in senior age with a greater influence of an additional cognitive task in the alpha-band and 2) individuals with lower beta-band corticomuscular coherence may exhibit more accurate motor output in young, but not elderly adults, during steady contraction

with visual feedback.

CHAPTER VI

CLASSIFY NEURAL CONTROL OF MOVEMENT

To begin developing a methodology for investigating the neural control of movement, changes in neuromuscular activity with task and healthy aging were considered in Aims 1 and 2. The results indicated that with the addition of a motor or cognitive task to a unilateral motor task, both time and frequency domain features are statistically changed with respect to healthy aging.

Extending the knowledge acquired in the first two Aims leads to the purpose of the current chapter: to provide a data mining context to classifying the neural control of movement with consideration for unilateral and concurrent motor/cognitive tasks and healthy aging. The extension in this Aim automates the process of distinguishing between young and elderly adults utilizing a data mining approach. Features beyond the classical ones of coherence and power spectral density were also investigated.

Aim 3: Model the Neural Control of Movement

Develop a set of features that best distinguish between age (young and elderly) during unilateral and concurrent motor/cognitive tasks.

Approach:

1. Determine the appropriate parameters for feature extraction.

2. Determine the optimal subset of features from time, frequency and information theory domains. Test automatic speech recognition features (cepstrum) for application to EEG and EMG and signal classification.

3. Classify selected features to provide a proof of concept for a methodology and computational tool for use by physiologists in practice.

6.1 Preliminary: Classify the Neural Control of Movement

Section 6.1 focuses on the efficacy of classifying between young and elderly adults using time and frequency domain features and determines the optimal feature selection algorithm. The section also investigates the efficacy of the real cepstrum for classification of non-speech signals and the use of minimum classification error for Gaussian mixture model classification.

6.1.1 Age (Time/Frequency Features)

To begin developing a methodology for investigating the neural control of movement with aging, time and frequency domain features were selected and classified via a Support Vector Machine classifier to distinguish age differences.

Twelve healthy right-hand dominant young (n = 6; mean age: 26.0 ± 7.3 yrs) and elderly (n = 6; mean age: 67.3 ± 4.8 yrs) adults were considered. Eight of the twelve subjects (young, n=4 and elderly, n=4) were used to test the feature selection approach that yielded the highest classification accuracy with the smallest subset of features. Four subjects (young, n=2 and elderly, n=2) were used to test the applicability of the selected features by classifying the additional subjects and comparing the classification accuracies.

The following features were extracted from the signals: mean absolute value, variance, coefficient of variation, root mean square, energy, kurtosis, power spectral density, and coherence. Mean absolute value is a nonnegative measurement of the signal's amplitude. The variance feature is a measure of how the signal is dispersed with respect to mean value of the signal. Quantitatively, the coefficient of variation is a measure of the spread of the signal's distribution normalized by the signal's mean and provides a measure of the variability of the signal. Root mean square is a measure of the signal's magnitude of variation. The energy feature shows the average energy (signal amplitude squared) of the signal in the time domain. The kurtosis feature

shows the sensitivity of the signal's distribution to outliers. Power spectral density (PSD) provides a measure of a signal's distribution of power with respect to frequency. The maximum PSD considers the peak power in a particular band and relative PSD is a measure of the signal's power within a particular band of frequencies relative to the total power across the complete range of frequencies in question. Coherence as described previously is a measure of the correlated activity between two signals in the frequency domain.

Power spectral density and coherence features were extracted from alpha (8-14.5 Hz), beta (15-30 Hz), and gamma (30.5-55 Hz) bands. Feature extraction involved a moving average window of length L that calculated the feature values. A one second window length was employed with no overlap. Features were calculated over all channels, except coefficient of variation which was only calculated for EMG and coherence specifically calculated for EMGRt-C3, C3-C4, F3-F4, and FC3-FC4. Prior to data analysis, class labels were assigned to young and old data. Features were normalized by subtracting the mean and dividing by the standard deviation, prior to feature selection. Seventy-six features were extracted creating the feature vector, $\mathbf{X}_M = \{x_1, x_2, ..., x_M\}$, where M=76. Feature selection reduced the feature set, $\mathbf{X}_M$, to a subset, $\mathbf{X}_m = \{x_1, x_2, ..., x_m\}, m<M$ such that the objective function for the feature selection algorithm was maximized.

Feature selection algorithms Forward Selection (FS), Backward Selection (BS), and Branch-and-Bound Selection (BB) were executed for varying feature subset sizes ($1 \geq m \geq 29$) for classifying young and elderly subjects within tasks (unilateral motor, bilateral motor and motor-cognitive). Subsets were selected up to 29 features because the aim was to have a minimal number of features in a subset in order to reduce computational cost. Feature selection optimization for the FS, BS, and BB algorithms was obtained using the Mahalanobis distance objective function

$$D = \sqrt{(\mathbf{x} - \boldsymbol{\mu})^T \mathbf{C}^{-1} (\mathbf{x} - \boldsymbol{\mu})} \tag{8}$$

where D is the Mahalanobis distance, $\mathbf{x}$ is the feature vector, $\boldsymbol{\mu}$ is the mean vector, and $\mathbf{C}^{-1}$ is the covariance matrix. The Mahalanobis distance accounts for the covariance among the features in calculating distances. Unlike with the Euclidean distance, the problems of imbalanced feature scale and correlated features are not an issue.

Forward selection (FS) is an iterative algorithm which starts by considering an empty matrix and adds a feature based on optimizing the objective function [15]. If the performance metric increases, then the feature being considered is added to the feature subset. If the number of features in the subset is less than the desired number, then the process continues, otherwise the subset is complete.

Backward selection (BS) aims to exclude one feature at a time from the original extracted feature set, such that the reduced feature set leads to optimizing the objective function (reduce classification error or increase classification accuracy) [15]. Backward selection is similar to forward selection except that backward selection excludes one feature until the subset number is equal to the desired number of features.

Branch and bound selection (BB) reduces the number of features if the objective function, *J(.)*, satisfies the monotonicity property [123]. The objective function satisfies this property whenever two arbitrary subsets F_1 and F_2 of F satisfies $J(F_1) \leq J(F_2)$ for any $F_1 \subseteq F_2$. The algorithm constructs a search tree and starts from the root of the tree traversing through the leaves. At the root of the tree where all features are considered, *J(F)* is computed. *J(F)* is continuously computed at each new leaf (subset of F). When a leaf has an objective function lower than the current bound, that leaf (subset) is removed from the tree, reducing the number of computations. The monotonicity property removes subsets of features where the objective function is not better than the current bound, thus avoiding evaluations where the subset is not the optimal solution.

Support Vector Machine

A Support Vector Machine (SVM) with a Gaussian radial basis function (RBF) kernel was used for classification. Given a set of observations, each of m input features, $x_i \in \mathbf{X}_m$, with corresponding class labels, $y \in \{+1, -1\}$, the SVM attempts to define a hyperplane,

$$y(\mathbf{x}) = \mathbf{w}^T\mathbf{x} + w_0, \tag{9}$$

that discriminates between the two classes. The parameters $\mathbf{w}$ and w_0 are the weight vector and hyperplane bias, respectively, selected to maximize the margin of the hyperplane. To minimize generalization error, the SVM selects the hyperplane with the largest margin, where the margin is the distance between the closest members from the two classes. For linearly separable cases,

$$\mathbf{w}^T x_i + w_0 \geq 0 \text{ for y = 1} \tag{10}$$

$$\mathbf{w}^T x_i + w_0 \leq 0 \text{ for y = -1} \tag{11}$$

for a new point x_i. Generally speaking, most data are not linearly separable, thus in these cases a soft margin SVM is used which allows some data points to be misclassified. The soft margin SVM solves the optimization problem,

$$min \left\{ \frac{1}{2}\mathbf{w}^T\mathbf{w} \right\} + C \sum_i \varsigma_i, \tag{12}$$

for all $\{(\mathbf{x}_i, y_i)\}$, such that $y_i \left(\mathbf{w}^T\mathbf{x}_i + w_0\right) \geq 1 - \varsigma_i$.

The parameter C is a regularization parameter that controls trade off between complexity of the machine and the number of non-separable points. If C becomes too large, the classifier can suffer from over-fitting. If C becomes too small the training error can potentially be large. The parameters ς_i are the slack variables

which correspond to the deviation from the margin borders and they control the allowable error.

The non-linear SVM maps the input vector of features into vectors in a high-dimensional feature space to perform classification in the high dimensional space. The data cast nonlinearly into a high dimensional feature space is more likely to be linearly separable there than in a lower-dimensional space [24]. The Gaussian radial basis function (RBF) kernel function

$$k\left(x, x_i\right) = e^{\frac{-\|x_i - x\|^2}{\sigma^2}} \tag{13}$$

was used to do the mapping. Kernels are able to operate in the input space, where the solution of the classification problem is a weighted sum of kernel functions evaluated at the support vector. Parameters for the SVM were estimated from the combinations $\sigma = [0.1, 0.5, 1, 5, 10]$ and $C = [0.1, 1, 10, 100]$ to minimize the quadtratic programming equation, Equation 12.

For the training set, a balanced proportion of young and old data was used for training the classifier. A balanced proportion of class data during training increases the potential for representative classification during testing [12], preventing bias in the classification process. Cross-validation of the classification accuracy was performed using 10 hold-out cross-validations within a loop with equal probability of each class for testing and training. To validate the optimal subset of features, 4 subjects, young and elderly, were used for classification.

6.1.1.1 Age (Time/Frequency Features) Results

The highest classification accuracies were observed at 93.1% (15 features), 94.1% (13 features), and 88.4% (15 features) for the unilateral, bilateral, and motor cognitive

Table 8: Classification results for forward selection. Time domain features are selected over frequency domain features across EEG and EMG channels.

Task	Test	Validation	# of features
Unilateral Motor	93.1%	87.4%	15
Bilateral Motor	94.1%	92.6%	13
Motor Cognitive	88.4%	81.3%	15

tasks, respectively (Table 8) for the forward selection algorithm. The branch-and-bound algorithm also yielded high accuracies (91.6% (11 features), 90.8% (21 features), and 85.6% (13 features)), although not as high as FS. The subset of features selected (coefficient of variation, variance, mean absolute value, root mean square, and energy) from the FS algorithm were the same across tasks. These features all belonged to the time domain. Frequency domain features were not included in the subsets until at least 17 features were selected. Validation of the selected features was performed using the FS optimal subsets because this algorithm yielded the highest classification accuracies. Classification accuracy decreased by 6.1% (original: 93.1% $\pm$ 1.1%; validation: 87.4% $\pm$ 2.8%) for validation of the unilateral motor subset. Validation of the optimal subset for the bilateral motor task showed a 1.6% decrease in classification accuracy (original: 94.1% $\pm$ 0.8%; validation: 92.6% $\pm$ 1.5%). Lastly, for the motor cognitive task using the optimal subset of features, classification accuracy decreased by 8.0% with validation (original: 88.4% 0.9%; validation: 81.3% $\pm$ 1.7%).

6.1.1.2 Age (Time/Frequency Features) Discussion

In spite of previously observed (Table 4, Figure 17) frequency domain features showing class distinctions, when the time and frequency domain features were used in a data mining context, subsets of time domain features were selected over the frequency domain features with high classification accuracies. This finding was interesting to

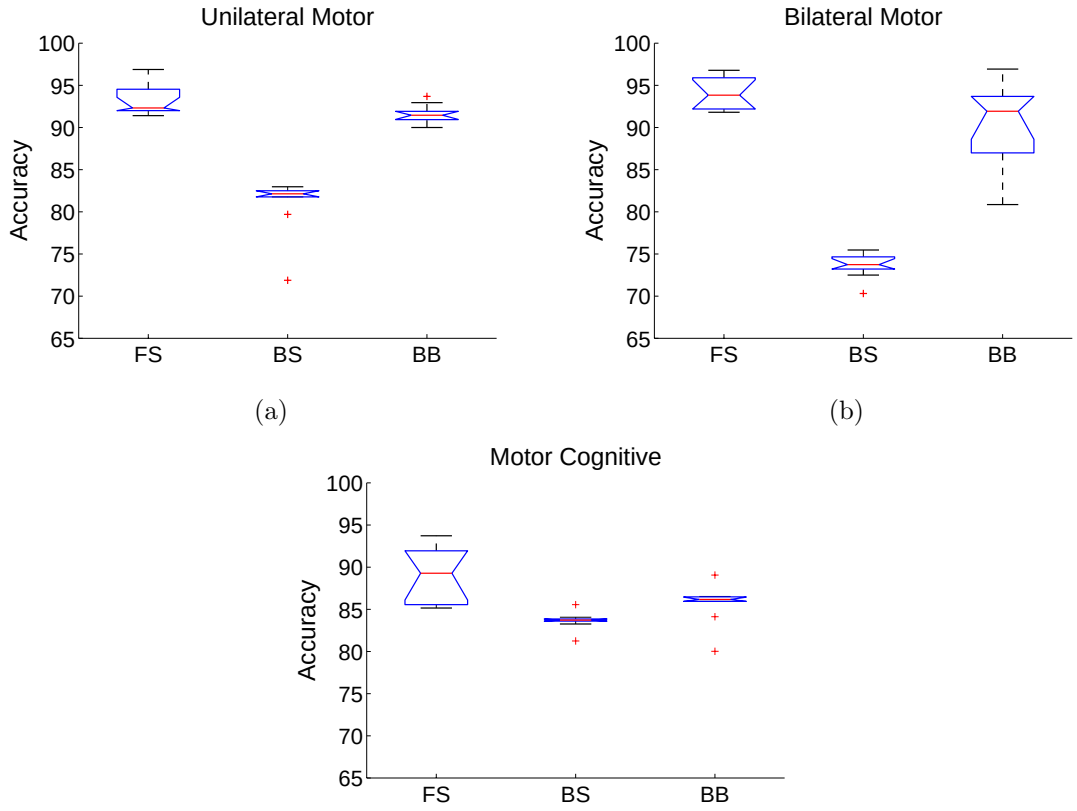

Figure 21: Box plot of feature selection algorithms forward selection (FS), backward selection (BS), and branch-and-bound (BB) selection for the (a) unilateral motor, (b) bilateral motor, and (c) motor cognitive tasks.

note because literature and the previously observed results in Chapter 5 show frequency domain changes [75, 60, 57], in addition to time domain changes, with age. The frequency domain features extracted were all relative, as opposed to the time domain features which were both absolute and relative. This difference in the observation may have played a role in the features that were ultimately selected. The preliminary results encouraged further research into these features and incorporation of additional features (absolute and relative) from other relevant domains to highlight the physiological changes in the signals, including consideration of non-traditional features (cepstrum) for EEG/EMG analysis.

6.1.2 Automatic Speech Recognition Features for Biological Signal Analysis

6.1.2.1 Real Cepstral Analysis

Automatic speech recognition (ASR) features are used in speech processing to cancel out noise contribution in the signal from speech recorded using multiple microphones. Speech recognition considers the frequency content of different sounds; therefore, features that provide spectral information (e.g. FFT) are desired, just as in EEG analysis. For this reason, the cepstrum is often computed to extract the spectral information from the speech signal. The computation of the cepstrum can be related to a deconvolution of the signal. The noise removing deconvolution of the speech signal is applicable to removing the inherent environmental noise associated with recording EEG signals. As in speech recognition, neural changes in EEG as well as EMG are dominant in the frequency domain with age and the control of movement.

Initial consideration of the real cepstrum was evaluated for classification of seizure and non-seizure states within the EEG signal. The real cepstrum is the inverse Fourier transform of the real logarithm of the magnitude of the Fourier transform of a signal. Seizure data was used for preliminary investigations because the signature of seizures in EEG are more distinct than signatures of age. Seizures are sudden abnormal

discharges in the brain often represented by convulsions or loss of consciousness. This brain abnormality is represented in electroencephalogram (EEG) recordings by frequency changes and increased signal amplitudes [41]. The ability to accurately capture the frequency and amplitude changes is key to the detection of seizure and non-seizure states. Several techniques capable of classifying seizure and non-seizure states from EEG signals have been presented in the literature [121, 120, 32, 129, 128]. Si et al. [121] reports on an automated pediatric seizure detector based on fuzzy logic and neural networks with 91% overall recognition. Faul et al. [32] uses Gaussian Process (GP) modeling theory to detect neonatal seizures. The GP EEG measure, Gaussian variance, provided a classification accuracy of 82.8%. Thomas et al. [129] obtained a 79% detection rate using Gaussian mixture models and frequency, time, and information theory domain features for neonatal seizures. Expanding on this work, Temko et al. [128] incorporated automatic speech recognition features to classify neonatal seizures using a support vector machine classifier. Assessing the area under the Receiver Operating Curve (ROC), they obtained 93.1% with spectral-enveloped based features and cepstral coefficients.

While all of these approaches have made contributions towards a real-time system, the challenges of unbalanced data (seizure and non-seizure) and system computational efficiency still remain. The rare occurrence of a seizure over hours of EEG recordings makes training and testing of the model difficult because of the potential class bias towards the non-seizure state, increasing the number of false alarms. The dissertation results add to the body of work with the incorporation of the MCE algorithm applied on Gaussian mixture models to classify seizure and non-seizure states using cepstral analysis. The approach is novel in that it accounted for the challenge of unbalanced datasets (seizure and non-seizure), while also showing a system capable of real-time feature extraction.

This section of Aim 3 tested the efficacy of the application of speech processing

techniques (real cepstrum) to discriminate between seizure and non-seizure states in EEG signals. Additionally, the use of the Minimum Classification Error (MCE) algorithm applied on Gaussian mixture models for improving classification accuracy was tested; showing the comparison of the efficacy of MCE with two classification schemes, including support vector machines and standard Gaussian mixture models. More importantly, the MCE algorithm specifically targeted the constraint of unbalanced data.

6.1.2.2 Methodology

To begin the investigation of the application of ASR features for EEG/EMG signal analysis and classification, the real cepstrum feature was extracted from pediatric seizure data to classify seizure and non-seizure segments [59]. Seizure data was used for preliminary investigations because the signature of seizure in EEG is more distinct than the signature of performing a different task, age or even stroke. A dataset of pediatric EEG recordings was obtained from the PhysioNet on-line database [39] for the preliminary investigation. The database included recordings from 22 subjects (males: n=5, ages 3-22; females: n=17, ages 1.5-19) recorded at the Children's Hospital Boston. Recordings were of 23 surface EEG channels sampled at 256 Hz, from subjects with intractable seizures. The data consisted of 182 seizures with approximately 6 hours of data per subject. Each subject had approximately 8 seizures.

The real cepstrum feature was extracted over 10 second windows of EEG samples. Consecutive moving windows of 3 seconds were used, resulting in a 66% overlap. A cepstral transformation was applied on each of these windows. The cepstral transformation is well known for its ability to preserve the envelope of the spectrum. It provides a compact representation of the spectrum into a small set of features that are well decorrelated. For these initial experiments, the first 12 cepstral coefficients

were retained. Binary labels were assigned to each feature vector of 12 cepstral coefficients, following a simple majority rule. If in the time domain, less than 50% of the EEG samples belonged to a segment of seizure activity, the feature vector takes the label of class C_2 (non-seizure). Otherwise, the feature vector was labeled with class C_1 (seizure).

Support Vector Machine

A SVM classifier with a Gaussian RBF kernel was used for classification as described in Section 6.1. Again, the SVM was programmed to use the best combination of parameters to minimize the quadratic programming problem, Equation (12).

Discriminative training of Gaussian Mixture Models (GMMs)

The generative and discriminative approaches to classification problems are two competing philosophies in machine learning. The generative approach attempts to directly fit a model to training data on a category-per-category basis, typically based on the Maximum Likelihood (ML) criterion or Mean Square Error. Classification is done by comparing the score of each model and choosing the classes whose model yields the optimum score. In contrast, the discriminative approach tries to directly estimate the boundaries between classes.

Gaussian Mixture Models (GMMs)

The GMM classification model will be explained using the seizure detection problem. A model is created for each category (seizure or non-seizure), and detection is based on the optimum score of a category given a sample. Gaussian Mixture Models are a widely used modeling approach, typically applied to clustering or pattern classification, in particular in the context of speaker identification, language identification, or image segmentation. Its attractiveness is because of its ability to approximate the

data distribution of a given class, making it a judicious choice for detection problems that exhibit differences in distribution across categorical data.

Formally, a GMM represents the probability density function (pdf) of a random variable, $\mathbf{x} \in R^d$, as a weighted sum of k Gaussian distributions:

$$p\left(\mathbf{x}|\Theta\right) = \sum_{m=1}^{k} \alpha_m p\left(\mathbf{x}|\theta_m\right), \tag{14}$$

where Θ is the mixture model, α_m corresponds to the weight of component m and the density of each component is given by the normal probability distribution:

$$p\left(\mathbf{x}|\theta_m\right) = \frac{\left|\sum_m\right|^{-1/2}}{\left(2\pi\right)^{d/2}} \exp\left\{-\frac{1}{2}\left(\mathbf{x}-\mu_m\right)^T \sum_m^{-1}\left(\mathbf{x}-\mu_m\right)\right\}. \tag{15}$$

MCE Motivation

The Maximum Likelihood Criteria is the standard estimation approach for GMM in which the parameters α, μ and $\sum$ are iteratively estimated via the Expectation Maximization (EM) algorithm in order to maximize the log-likelihood of the model. Theoretically, a ML-trained GMM can approximate any probability distribution, provided a sufficiently large training set and an optimal choice of the model order (number of mixtures k) are available. However, in practical situations, the training set is usually not sufficiently large, or the optimal model order is unknown. Furthermore, by estimating the model of each category separately, ML only provides an indirect approach to the classification task. To remedy these deficiencies, the Minimum Classification Error (MCE) algorithm was employed to correct and enhance a given ML-trained GMM, based on an optimization criterion that closely reflects the error rate on a training set.

Minimum Classification Error was utilized based on its success in speech and usability across a broad range of classifiers. The choice of the MCE approach is motivated by its straightforward applicability to various types of classifiers and its flexibility in tuning the learning parameters to achieve the targeted performance. In

addition, MCE training has found a range of applications in various areas, including speech recognition and handwriting recognition.

MCE minimizes a smooth approximation of the error rate [63] and unlike ML, MCE does not attempt to fit a distribution, but rather to discriminate against competing models [63]. MCE training is more directly aimed at reducing the recognizer's mistakes. MCE has been found efficient in handwriting recognition [11] and feature extraction [12] and to the author's knowledge has never been applied to seizure detection. This section describes the MCE application to Gaussian Mixtures Models (GMMs).

Minimum Classification Error training of Gaussian Mixture Models

The MCE learning paradigm provides a correction of the ML-estimation techniques by its focus on directly improving the detection capabilities of the GMM. Given a two-class problem in which the goal is to classify data between seizure and non-seizure states (or young and elderly), the two categories C_1 and C_2 are represented by two GMMs of parameters Θ_1 and Θ_2. The parameter $\Theta = \{\Theta_i\}$ for $i = 1, 2$, is defined as the parameter space of the overall model. Given a feature vector X, the MCE training procedure is implemented as follows.

First, the discriminant function (g_i) of category C_i is defined as

$$g_i(X; \Theta_i) = \log p\left(\mathbf{x}|\Theta_i\right) + \log P(C_i) \tag{16}$$

where $P(C_i)$ is the prior probability of the category C_i; this prior probability is estimated from training data. The computation of prior probability is a unique modification to account for potentially unbalanced datasets for each class. The discriminant function is the score generated by the GMM of category C_i, given a sample X; it is an estimation of how likely the given sample belongs to that category (seizure or non-seizure; young or elderly). Decoding is done by choosing the category that has the highest discrimination measure (the highest score). That is,

$$\text{choose} \quad C_i \quad \text{if} \quad i = \arg\max_{1,2} g_j(X;\Theta_j). \tag{17}$$

Second, assuming that X belongs to C_i, we define the misclassification measure (d_i) of C_i as

$$d_i(X;\Theta) = -g_i(X;\Theta_i) + g_{j,j\neq i}(X;\Theta_j). \tag{18}$$

This misclassification measure estimates how well the model of category C_i can discriminate against another category, given a sample dataset. The sign of the misclassification measure reflects the performance of the model. A negative sign indicates a correct detection and a positive sign represents an incorrect detection. Finally, the MCE loss assigned to X is defined as $\ell(X;\theta) = \ell(d_i(X;\theta)$, where $\ell(\cdot)$ is a smooth approximation of the step-wise $0-1$ loss function, typically chosen to be a sigmoid

$$\ell(d) = \frac{1}{1+\exp(-\alpha d)} \tag{19}$$

with a positive α chosen to allow for reasonable degree of smoothness. The MCE loss is a smooth approximation of the 0-1 loss, which reflects a correct versus incorrect decision made by the system.

The method optimizes the classification by minimizing the expected loss $L(\Theta)$, defined as a function of the overall parameter set:

$$L(\Theta) = \sum_{i=1}^{2} \int_{X\in C_i} \ell(X;\Theta) P(X) dX. \tag{20}$$

In practice, MCE training focuses on the minimization of the MCE average loss defined over a body of training data of size N as

$$L_N(\Theta) = \frac{1}{N} \sum_{i=1}^{M} \ell(X;\Theta). \tag{21}$$

Clearly, $L_N(\Theta)$ approximates the empirical error rate, given that a body of training data and its evolution closely reflect the performance of the system on the training

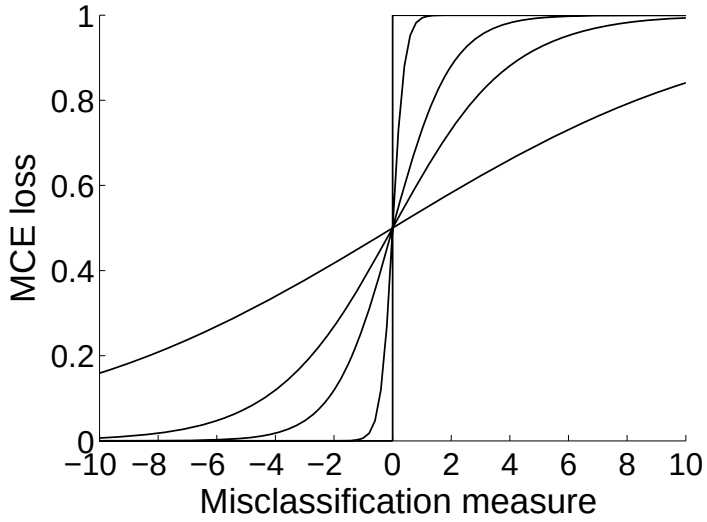

Figure 22: Minimum classification error smooth approximation of the 0-1 loss error function.

set. By minimizing $L_N(\Theta)$, the error in the training is more directly minimized than when done with the standard ML technique.

To minimize $L_N(\Theta)$, a gradient descent approach was used in which the Θ parameters of the system are iteratively updated as follows:

$$\Theta_{\tau+1} = \Theta_\tau - \mu \nabla L(\Theta_\tau) \tag{22}$$

where μ is a learning rate, which specifies the rate of convergence of the algorithm.

Model Implementation

The efficacy of the approach was tested during a summer of 2010 internship with the Exploratory Stream Analytics Group at the T.J. Watson Research Center in Hawthorne, NY. Initial testing was performed using Matlab$^{\text{TM}}$; however, despite the favorable modeling capabilities of the software, it struggled to handle the large data set. Attempts to extract features using windows of several EEG signals were unsuccessful with Matlab due to the computational burden of the modeling step.

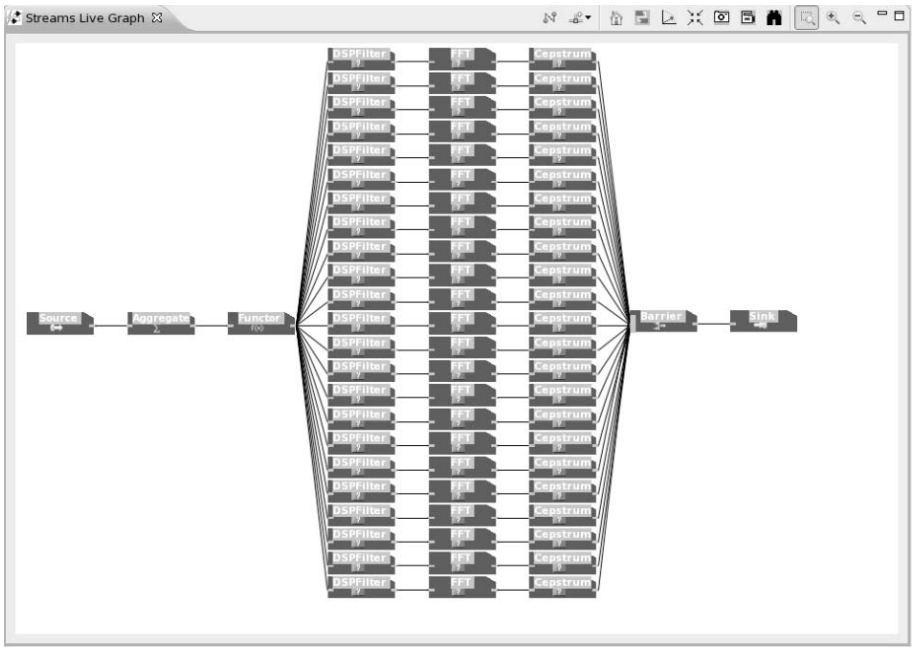

Figure 23: Spade analysis graph for EEG filtering, feature extraction, and labeling.

SPSS^{TM}[125] and Weka^{TM}[139] were also considered; however, these software platforms were also unable to handle processing the large dataset. As a result, IBM's InfoSphere Streams^{TM}(Streams) platform was used to build an experimental test-bed for the EEG analysis (Figure 23). The use of Streams allowed for a forward look into the potential for a real-time application of the model. Other applications are discussed in Section 8.2.

Streams is a highly scalable and programmable stream computing software platform allowing application developers to process structured, as well as unstructured streaming data. It provides several services in addition to its analytical capabilities, including fault tolerance, scheduling and placement optimization, distributed job management, storage services, and security. Streams was designed to scale to a large collection of computational nodes, simultaneously hosting multiple applications.

Streams applications are represented as directed data flow graphs (Figure 23) consisting of a set of processing elements (PEs) connected by data streams. Each data

stream carries a series of stream data elements. A PE implements data stream analytics and is the basic execution container that is distributed over computational hosts. At the operating system level, PEs are within in their own processes and communicate with each other via their input and output ports, using the TCP/IP network stack. Input and output ports are connected by streams to form these directed data flow graphs. More detailed information on the use of Streams can be in found in [59].

6.1.2.3 Seizure Results

Preliminary results from the use of cepstral analysis and GMM

Feature vectors were classified using standard Gaussian Mixture Models (GMM) using ML and MCE applied to these standard GMMs. The GMM modeling was performed by optimally growing the number of Gaussians up to 32. MCE training starts from the ML-estimated GMM model and adjusts the parameters of that model to generate a better performing model on the training set. A 10-fold cross validation approach was used.

Application of the real cepstrum and GMM showed comparable accuracy results (overall 91.7% recognition with standard GMM) in comparison to the use of the same dataset for seizure/non-seizure classification, but with time and frequency domain features (overall 95.0% recognition) [120]. The recognition rates with the standard GMM were 92.2% for non-seizure windows and only 64.2% for the rare seizure events (Table 9) [59]. The low frequency of seizure events in the data set makes it hard for the classifier to have good detection accuracy for seizure events. However, the application of MCE to better discriminate (account for the unbalanced seizure/non-seizure states) between these two classes significantly boosted the seizure detection accuracy. With MCE applied to the GMM model described above, the recognition accuracy of non-seizure events was slightly decreased, while significantly boosting the recognition accuracy of seizure events by 42.4% in comparison to the standard GMM

Table 9: Seizure classification results.

	Non-Seizure	Seizure
SVM	90.0%	81.0%
standard GMM	92.2%	64.2%
GMM + MCE	84.9%	91.4%

(Table 9) [59]. The SVM classifier using RBF achieved a comparable recognition rate for the non-seizure class in comparison to the standard GMM, but the result for the seizure class was inferior to the accuracy reached with MCE on the seizure class.

6.2 Extension: Classify the Neural Control of Movement

This section uses EEG and EMG data to classify between healthy young and elderly adults expanding the nature of features used for classification. Time, frequency, information theory, and automatic speech recognition features are incorporated and selected from using the forward selection algorithm as tested and described in Section 6.1. The automatic speech recognition features are optimized and the GMM using MCE classifier is tested against the SVM and GMM using ML for classification between young and elderly adults.

6.2.1 Features

The feature subset from Section 6.1 has been expanded (Table 10, Appendix C) to include additional time and frequency domain features, as well as the cepstral features noted in the previous section. Additionally, nonlinear features, katz fractal dimension and nonlinear energy, were included for analysis. The following explains the new features added for extraction. The nonlinear features were included due to their ability to better characterize nonlinear aspects of the EMG and EEG signals. Katz Fractal dimension is a measure of the long-range dependence of the signal. It provides a measure of the signal's self-similarity and complexity. Shannon entropy

provides a measure of the randomness of the amplitude values of the signal. Thus, the higher the entropy, the more disorder is expected within the signal. Quantitatively, complexity is a measure of the slope of the mobility of the signal, where mobility is the average slope of the signal. Complexity provides a measure of the randomness of the signal. Mutual information is a measure of the amount information one random variable contains with respect to another. The random variable can be used as a general description of the EEG and EMG signals [96]. The mutual information feature provides a measure of the interdependence of either the EEG and EMG, or EEG and EEG for intracortical interactions. Wavelet coherence is similar to the coherence previously described; however, wavelet coherence provides a measure of the time and frequency domain characteristics simultaneously. Zero crossing is a measure of the number times the signal crosses the zero value "line".

Features were extracted from all channels: EMGRt, C3, C4, F3, F4, FC3, and FC4, for three window lengths (0.5s, 1s, 2s). Class labels were assigned to young and old data segments. Features were normalized by subtracting the mean and dividing by the standard deviation, prior to feature selection. Based on the preliminary results, features were selected using forward selection with the objective function being the sum of estimated Mahalanobis distance for classifying young and elderly subjects within tasks (unilateral motor, bilateral motor, and motor-cognitive). Feature subset sizes ($1 \geq m \geq 75$) were considered. Subsets were selected up to 75 features because the aim was to have a minimal number of features that reduce computational cost for distinguishing between young and elderly adults.

Table 10: Feature Table.

Feature Number	Feature Name
1	Mutual Information
2	Coherence: Delta
3	Coherence: Theta
4	Coherence: Alpha
5	Coherence: Beta
6	Coherence: Gamma
7	Mean
8	Standard Deviation
9	Kurtosis
10	Zero Crossing
11	Sample Entropy
12	Shannon Entropy
13	Max PSD: Delta
14	Max PSD: Theta
15	Max PSD: Alpha
16	Max PSD: Beta
17	Max PSD: Gamma
18	Relative PSD: Delta
19	Relative PSD: Theta
20	Relative PSD: Alpha
21	Relative PSD: Beta
22	Relative PSD: Gamma
23	Complexity
24	Nonlinear Energy
25	Katz Fractal Dimension
26	Modified Real Cepstrum
27	Modified MFCC
28	Wavelet Coherence

6.2.1.1 Cepstral Analysis Optimization

The preliminary results of the application of the real cepstrum for classification of seizure and non-seizure states was expanded to also include the mel-frequency cepstrum coefficient for classification between young and elderly adults. As noted, the real cepstrum is the inverse Fourier transform of the real logarithm of the magnitude of the Fourier transform of a signal. Mel-Frequency Cepstral Coefficients (MFCC) are

short-term frequency based features computed by taking the discrete Fourier transform of a window, the log of the amplitude spectrum ignoring the phase component, converting to a Mel spectrum, then taking the Discrete Cosine Transform. The mel scale is linear up to 1000 Hz and then logarithmic afterwards. The equation for the mel scale is

$$m = 2595 \log(1 + \frac{f}{700}). \tag{23}$$

Despite both speech and EEG/EMG signals having significant spectral characteristics, the application of ASR features for biological data (EEG and EMG) is only recently being investigated. The inclusion of cepstral analysis for EEG and EMG signals required investigation of the number of coefficients for both the real cepstrum and MFCC and the filterbank spacing for the mel-frequency cepstrum. The MFCC feature was modified for application to EEG and EMG by modifying the Mel-Frequency Warping to equally spaced filterbanks. The Mel-frequency cepstrum originally used a linear-spaced filter up to approximately 1 kHz followed by a log-spaced filterbank. The filterbank spacing for application to non-speech signals was adjusted to include a linear-spaced filterbank between 0.5 and 55 Hz. The MFCC feature was extracted using a linear-spaced Hamming window.

The determination of the number of coefficients to maintain for speech has been determined empirically and used throughout the speech community. In a similar manner to [105], the number of coefficients to maintain for EEG and EMG analysis was determined using principle component analysis (PCA). The main purpose of PCA is to derive a relatively small number of uncorrelated linear combinations (principle components) of a set of random zero-mean variables while retaining as much of the information from the original variable as possible [24]. The PCA transform is derived from the eigenvalues and eigenvectors of the covariance of the training data. Dimensionality is reduced by removing principle components corresponding to relatively low

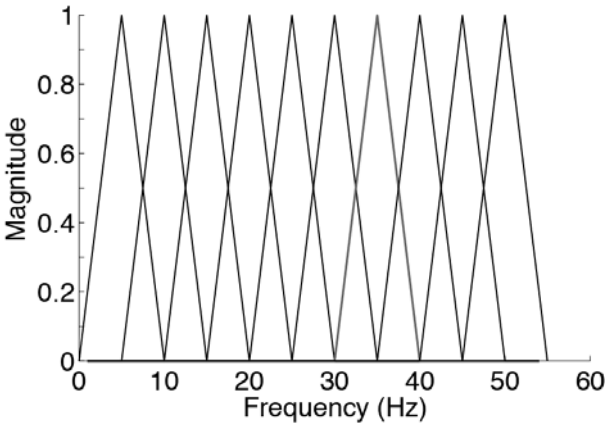

Figure 24: Modified linear filterbank spacing for the mel-frequency cepstrum.

eigenvalues. The desired amount of variance accounted for depends on the number of components retained.

The number of cepstral coefficients for both the real cepstrum and MFCC were determined using PCA on each of the EMG and EEG signals (n = 7), maintaining only the components accounting for 90 percent of the variance. This was performed for each task (unilateral motor, bilateral motor, and motor-cognitive) and window length (0.5 s, 1 s, 2 s) to account for the influence of these parameters. Figure 25 depicts the number of coefficients that were determined from each of the seven channels for the real cepstrum and the MFCC. EEG channels ranged from 7-9 coefficients for the real cepstrum and 2 coefficients for each of the channels for the MFCC. The EMG channel ranged from 4-5 coefficients for the real cepstrum and 2 for the MFCC. This included the coefficients that accounted for 90% of the variance across young and elderly subjects. For the cases where a channel had a different number of components, the maximum number of components across all test sets was used for that channel. Thus, in the end for the real cepstrum, 9 coefficients were maintained for each EEG channel and 5 coefficients for the EMG channel. For the MFCC, 2 coefficients were maintained for each of the EEG and EMG channels.

To assess the potential improvement of classification accuracy with optimization

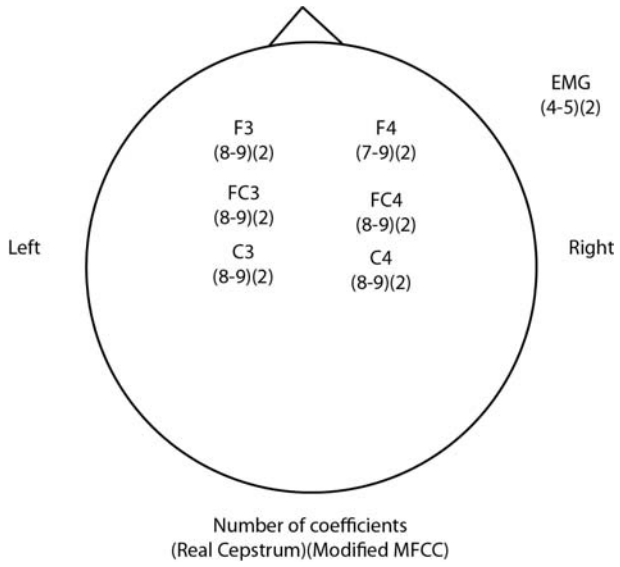

Figure 25: Optimal number of real cepstrum and mel-frequency cepstrum coefficients.

of the real cepstrum and MFCC, classification was performed with and without the optimization.

6.2.2 Classification

Classification of features was performed using the SVM classifier, the GMM classifier with Maximum Likelihood, and Minimum Classification Error as described in Section 6.1. A SVM with a Gaussian RBF kernel was used, and the parameters were estimated using cross-validation. Classification was also performed with a GMM classifier using both Maximum Likelihood and Minimum Classification Error.

The features were analyzed in groups to highlight individual differences and then analyzed all together to observe the overall influence from each feature. Classifier performance was defined as

$$ClassificationAccuracy = \left(\frac{\sum(P_{algorithm} = P_{expected})}{P_{total}} \right) * 100 \qquad (24)$$

where $P_{algorithm}$ is the classifier's output for the window, $P_{expected}$ is the expert labeling for the window, and P_{total} is the total number of windows.

6.2.2.1 Support Vector Machine

The results of feature classification using SVM are shown in Figures 26 - 32. Classification results across window lengths and tasks are summarized in Tables 11 - 16, showing the maximum classification accuracy and corresponding number of features in bold. For the SVM, the 1 and 2 second windows resulted in the highest classification accuracies across tasks, with the 2 second window providing significantly higher classification accuracies over the 0.5 second window.

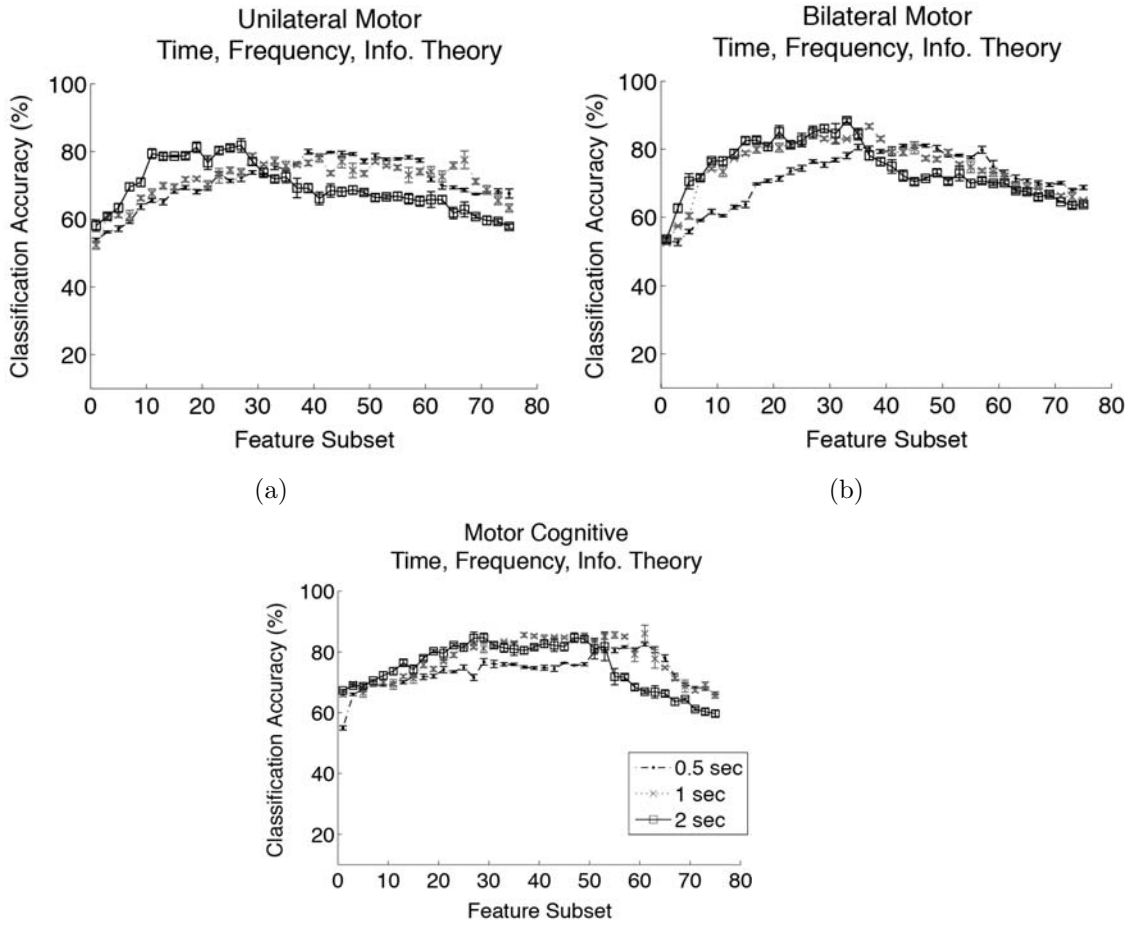

Figure 26: Time, Frequency, and Information Theory features (Support Vector Machine) for the (a) unilateral motor, (b) bilateral motor, and (c) motor cognitive tasks.

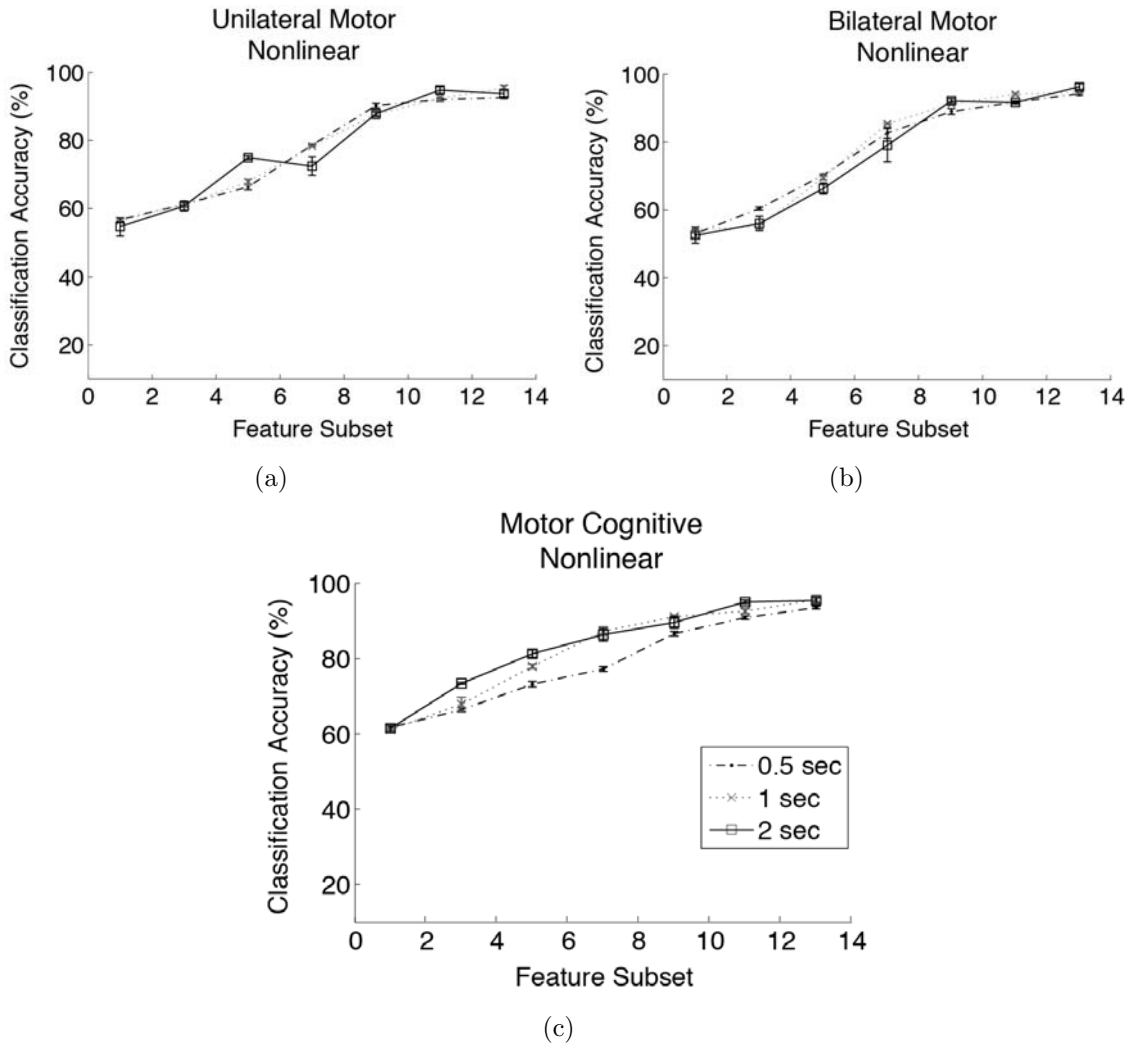

Figure 27: Nonlinear features (Support Vector Machine) for the (a) unilateral motor, (b) bilateral motor, and (c) motor cognitive tasks.

Table 11: Time, frequency, and information theory features SVM classification results (maximum classification accuracy, number of features).

	0.5 second	1 second	2 second
Unilateral Motor	81.0%, 43	78.9%, 41	**83.5%, 25**
Bilateral Motor	82.3%, 43	**84.9%, 37**	88.3%, 33
Motor Cognitive	82.2%, 51	**86.6%, 39**	85.4%, 41

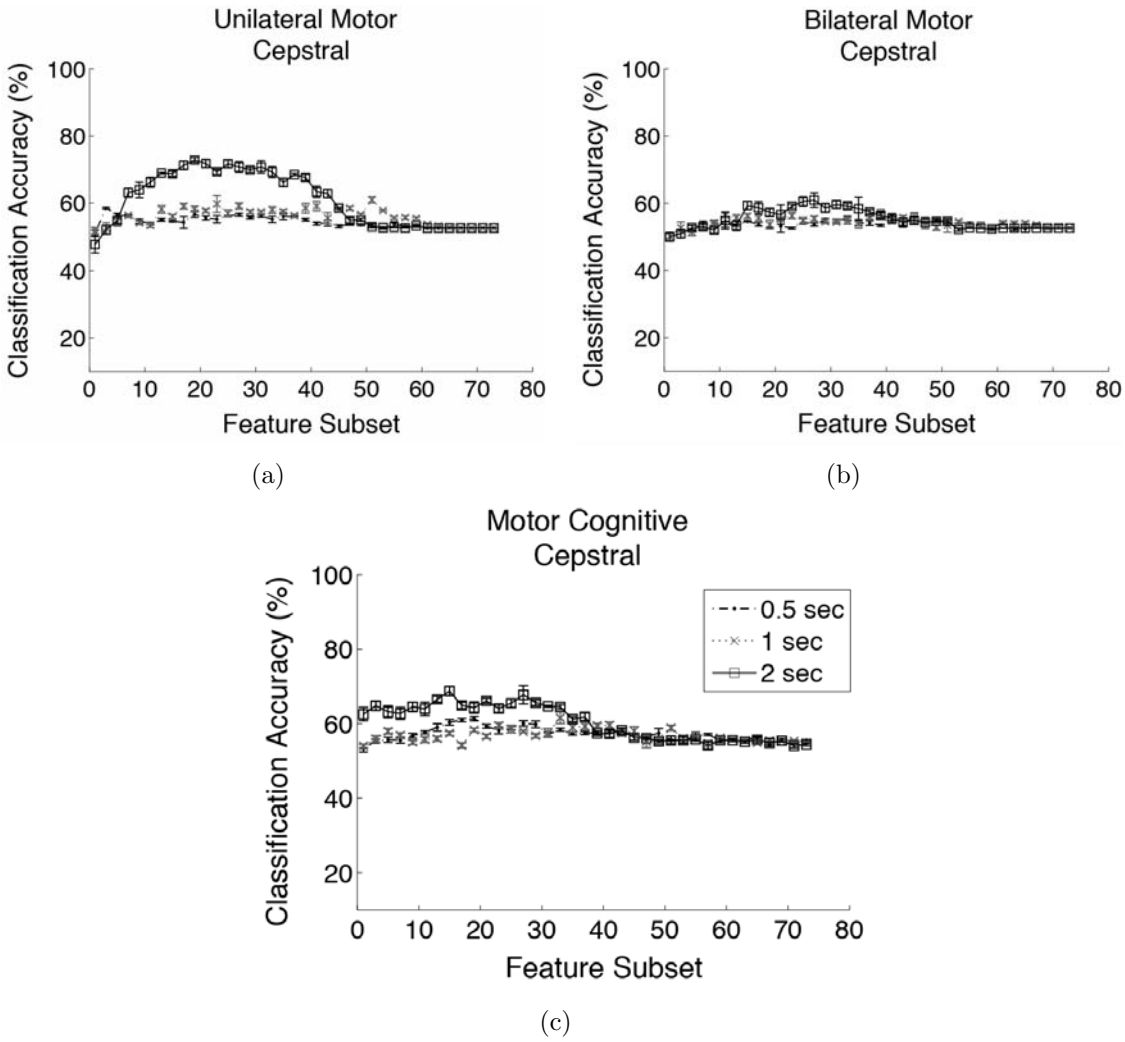

Figure 28: Cepstral features (Support Vector Machine) for the (a) unilateral motor, (b) bilateral motor, and (c) motor cognitive tasks.

Table 12: Nonlinear features SVM classification results (maximum classification accuracy, number of features).

	0.5 second	1 second	2 second
Unilateral Motor	92.7%, 13	95.3%, 13	**95.4%, 13**
Bilateral Motor	94.0%, 13	93.8%, 13	**95.6%, 13**
Motor Cognitive	93.8%, 13	97.0%, 13	**96.2%, 13**

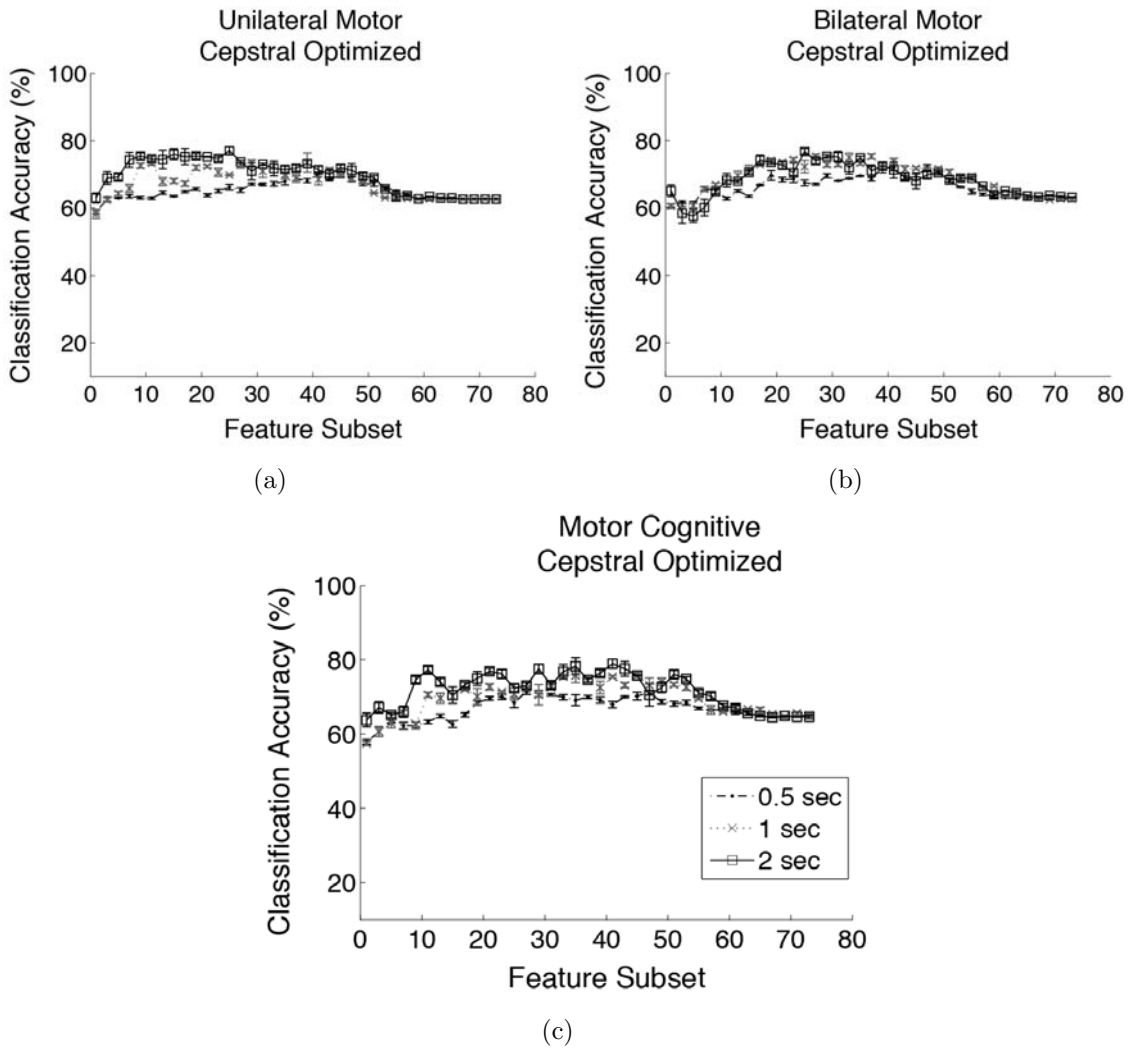

Figure 29: Cepstral Optimized features (Support Vector Machine) for the (a) unilateral motor, (b) bilateral motor, and (c) motor cognitive tasks.

Table 13: Cepstral features SVM classification results (maximum classification accuracy, number of features).

	0.5 second	1 second	2 second
Unilateral Motor	58.0%, 3	59.7%, 23	**72.9%, 19**
Bilateral Motor	56.5%, 41	57.0%, 39	**60.9%, 27**
Motor Cognitive	61.4%, 19	61.6%, 33	**68.8%, 15**

Overall, the results indicate that the nonlinear features, katz fractal dimension and nonlinear energy, produce the highest classification accuracies (unilateral motor: 95.44%, bilateral motor: 95.5%, motor cognitive: 97%) (Table 12) when comparing

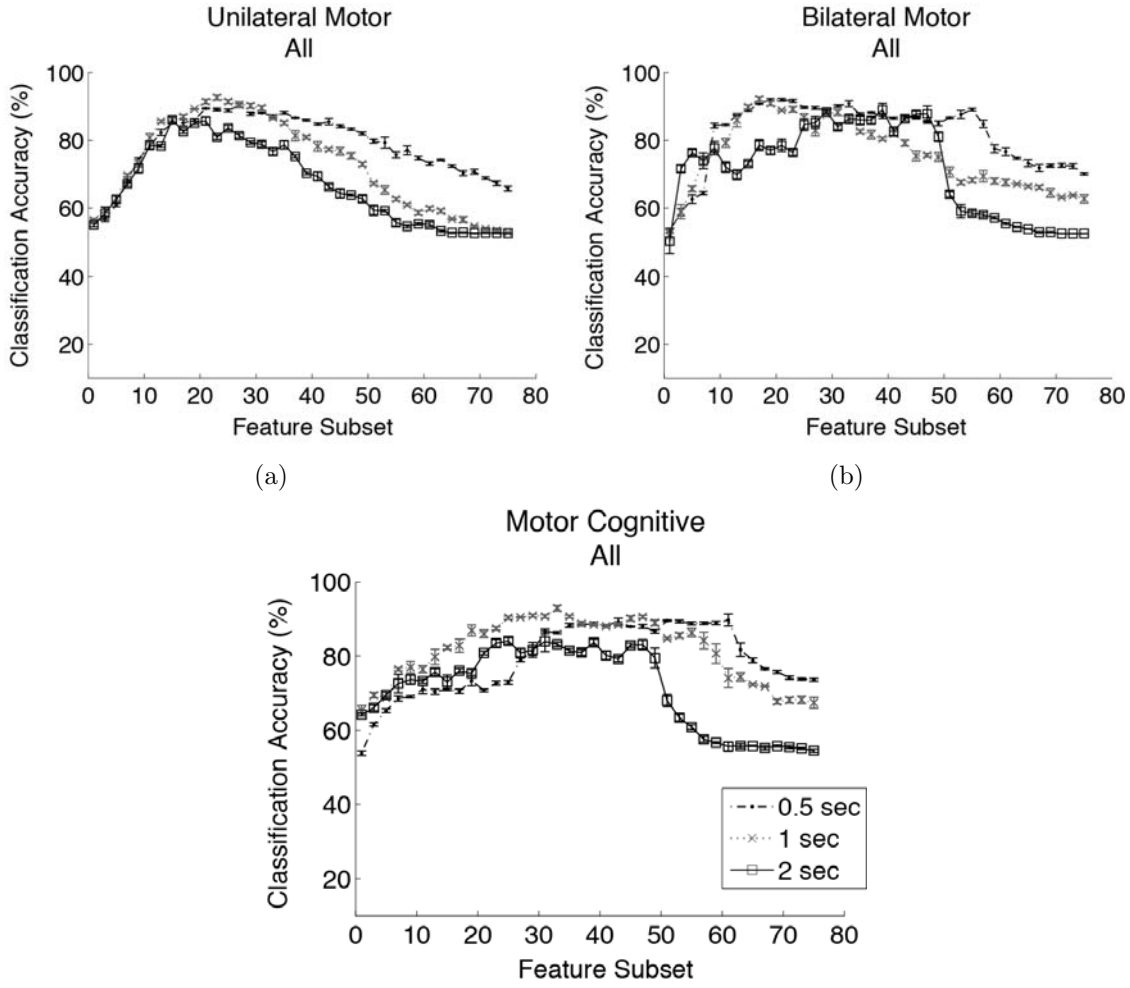

Figure 30: All features (Support Vector Machine) for the (a) unilateral motor, (b) bilateral motor, and (c) motor cognitive tasks.

Table 14: Cepstral features (optimized) SVM classification results (maximum classification accuracy, number of features).

	0.5 second	1 second	2 second
Unilateral Motor	60.0%, 41	63.0%, 39	**77.0%, 25**
Bilateral Motor	62.2%, 47	65.0%, 37	**76.8%, 25**
Motor Cognitive	61.0%, 27	65.8%, 45	**78.9%, 41**

against the time, frequency, information theory, and cepstral features. As noted, the cepstral features were classified before and after making the modifications for application to EEG and EMG signal analysis. After modifying the filterbank spacing and

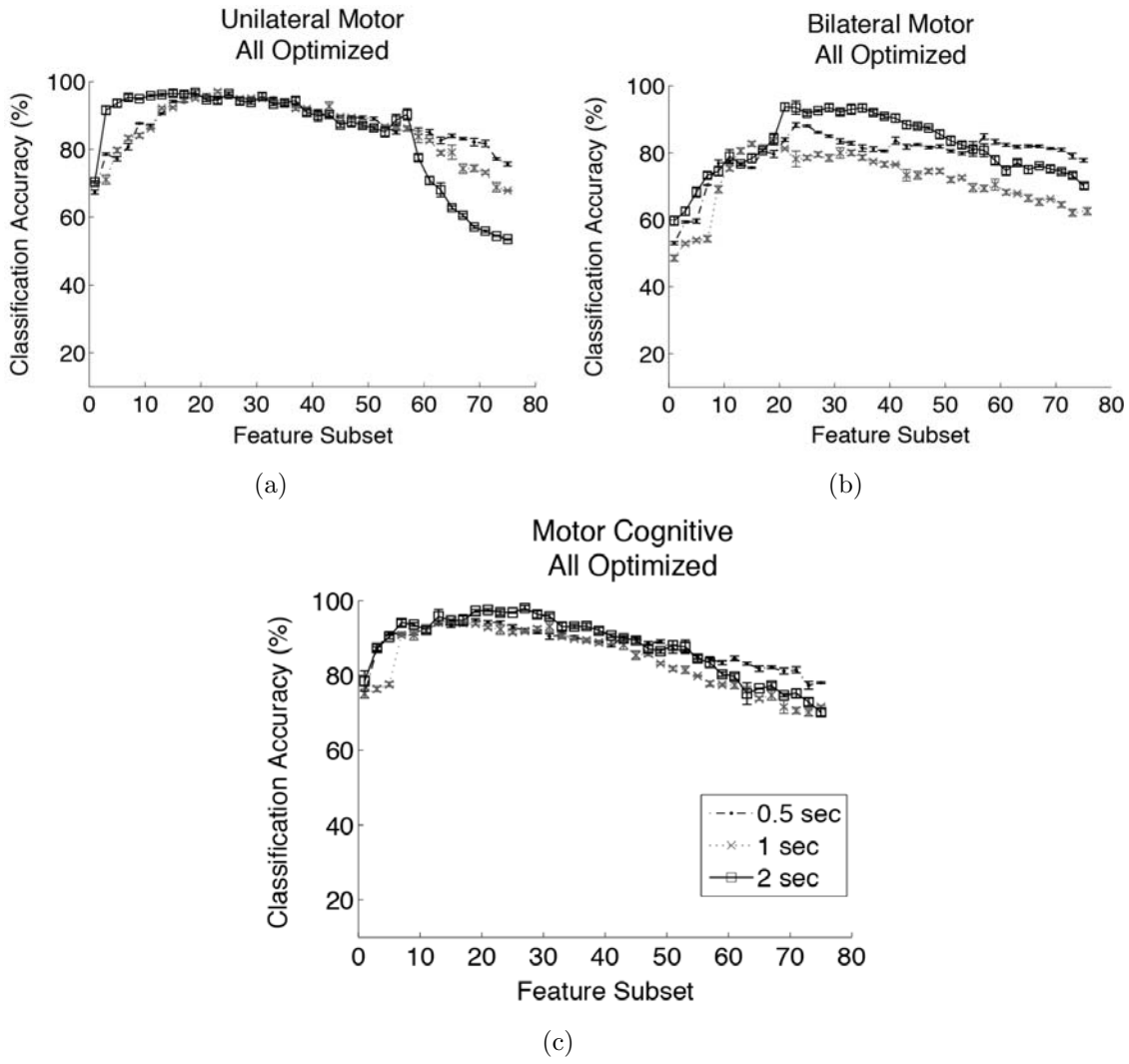

Figure 31: All Optimized features (Support Vector Machine) for the (a) unilateral motor, (b) bilateral motor, and (c) motor cognitive tasks.

Table 15: All features SVM classification results (maximum classification accuracy, number of features).

	0.5 second	1 second	2 second
Unilateral Motor	89.1%, 27	**92.5%, 27**	86.9%, 15
Bilateral Motor	91.6%, 19	**92.6%, 17**	90.3%, 43
Motor Cognitive	89.3%, 33	**92.3%, 33**	85.7%, 23

number of coefficients for the cepstral features, the classification accuracy increased by 5.6% for the unilateral task, 26.1% for the bilateral task, and 14.7% for the motor cognitive task (Tables 13 and 14).

Table 16: All features (optimized) SVM classification results (maximum classification accuracy, number of features).

	0.5 second	1 second	2 second
Unilateral Motor	96.0%, 21	**96.5%, 23**	96.1%, 19
Bilateral Motor	88.0%, 23	83.0%, 19	**93.7%, 21**
Motor Cognitive	94.1%, 19	94.0%, 15	**98.0%, 27**

The inclusion of all features from Table 10 was also compared before and after the cepstral features were optimized. The incorporation of modified cepstral features improved classification accuracy when using all features (Figure 32). Classification accuracy significantly increased from using all features to using all features after the optimization of the cepstral features (unilateral motor: $P < 0.01$; bilateral motor: $P < 0.01$; motor cognitive: $P < 0.01$) (Figure 32). For the bilateral motor task, the cepstral features were not included in the subsets where the classification line for "All features"' was greater than for "All features Optimized"' (Figure 32b). For the optimal subsets, classification accuracy increased by 4.3% for the unilateral task, 1.2% for the bilateral task, and 6.2% for the motor cognitive task (Tables 15 and 16, respectively).

The maximum classification accuracy of 96.5% obtained for the unilateral motor task corresponded to 92.5% accuracy for the young class and 99.0% accuracy for the elderly class. For the bilateral motor task, a maximum classification accuracy of 93.7% was obtained, corresponding to 96.4% accuracy for the young class and 90.7% accuracy for the elderly class. The maximum classification accuracy of 98.0% obtained for the motor cognitive task corresponded to 98.5% accuracy for the young class and 97.4% accuracy for the elderly class.

6.2.2.2 Gaussian Mixture Model: ML and MCE

Statistically significant increases in classification accuracy using the GMM with MCE were observed across all feature subsets in comparison to the GMM with Maximum

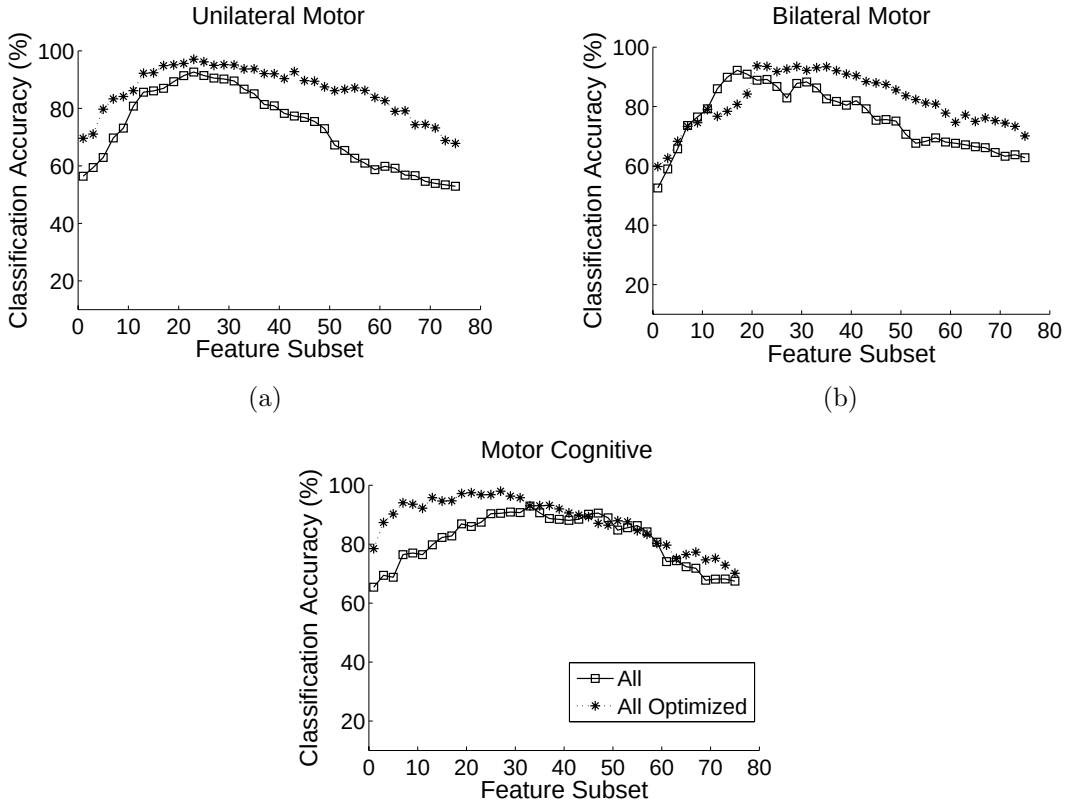

Figure 32: Comparison of All features versus All features optimized for Support Vector Machine Classification for the (a) unilateral motor, (b) bilateral motor, and (c) motor cognitive tasks.

Likelihood and SVM (unilateral motor: $P < 0.01$; bilateral motor: $P < 0.05$; motor cognitive: $P < 0.01$). At the optimal feature subset, increased accuracy was observed between MCE and ML; however, a smaller increase was observed in MCE over the SVM (Figure 33). Figure 33 provides a graphical representation of the statistical differences between the three classifiers using the optimal subset of features. The box plot shows the 75th percentile, median, and 25th percentile. As noted statistically when compared, the median classification accuracy of the GMM with MCE is greater than the other two classifiers. The description of the results will primarily focus on the GMM with MCE because this classifier produced the highest overall accuracies for the model.

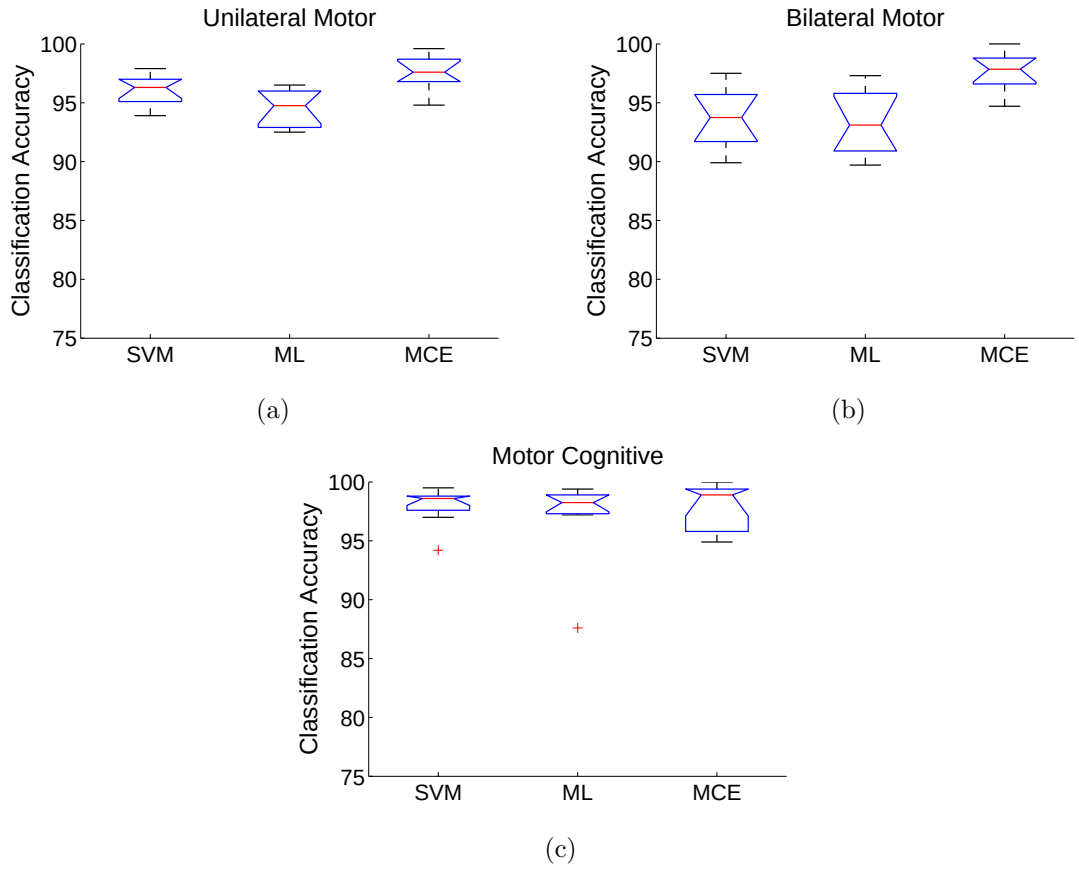

Figure 33: Box plot comparison of classification accuracies across the Support Vector Machine (SVM), Gaussian Mixture Model with Maximum Likelihood (ML) and Gaussian Mixture Model with Minimum Classification Error (MCE) classifiers for the (a) unilateral motor, (b) bilateral motor, and (c) motor cognitive tasks.

The 2-second window yielded higher classification accuracies for the GMM for both ML and MCE, with significantly higher accuracies for the 2-second window in comparison to the 0.5-second window (Figures 34 - 45). As with the SVM classifier, classification accuracy was the highest with the use of the nonlinear features in comparison to the other feature domain groups (Table 18). Additionally, classification accuracy increased with the optimization of the cepstral features. The classification accuracy increased by 9.3% for the unilateral task, 11.2% for the bilateral task, and 10.6% for the motor cognitive task (Table 19 and 20).

Optimizing the cepstral features increased classification accuracy from using All

features to using "'All features after the optimization of the cepstral features by 9.0% for the unilateral task, 7.6% for the bilateral task, and 7.1% for the motor cognitive task (Tables 21 and 22, respectively). The maximum classification accuracy of 97.7% obtained for the unilateral motor task corresponded to 97.0% accuracy for the young class and 98.1% accuracy for the elderly class. For the bilateral motor task, a maximum classification accuracy of 97.7% was obtained corresponding to 96.8% accuracy for the young class and 98.0% accuracy for the elderly class. The maximum classification accuracy of 98.0% obtained for the motor cognitive task corresponded to 98.3% accuracy for the young class and 98.0% accuracy for the elderly class.

Table 17: Time, Frequency, and Information Theory features Gaussian Mixture Model classification results (maximum classification accuracy, number of features).

	0.5 second	1 second	2 second
Maximum Likelihood			
Unilateral Motor	83.8%, 59	84.8%, 59	**86.5%, 33**
Bilateral Motor	83.2%, 57	90.0%, 51	**90.7%, 35**
Motor Cognitive	81.7%, 51	86.5%, 57	**88.8%, 31**
Minimum Classification Error			
Unilateral Motor	87.1%, 57	89.8%, 59	**92.1%, 35**
Bilateral Motor	87.6%, 47	93.8%, 51	**95.4%, 45**
Motor Cognitive	86.2%, 57	89.1%, 39	**91.8%, 41**

Table 18: Nonlinear features Gaussian Mixture Model classification results (maximum classification accuracy, number of features).

	0.5 second	1 second	2 second
Maximum Likelihood			
Unilateral Motor	88.9%, 11	**92.1%, 13**	84.9%, 13
Bilateral Motor	88.3%, 13	**90.1%, 9**	84.8%, 11
Motor Cognitive	72.5%, 13	84.5%, 7	**86.8%, 13**
Minimum Classification Error			
Unilateral Motor	**95.2%, 13**	93.7%, 13	91.5%, 13
Bilateral Motor	93.6%, 11	**94.7%, 11**	90.7%, 7
Motor Cognitive	**94.2%, 13**	91.1%, 13	91.5%, 13

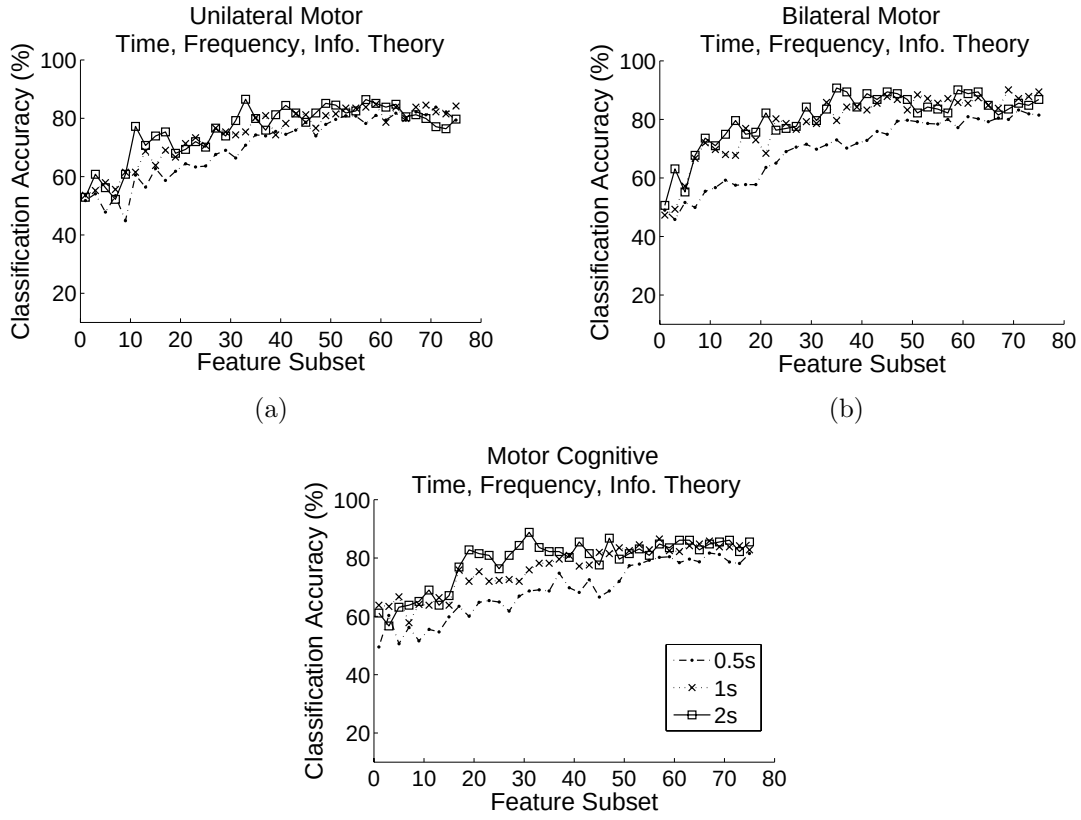

Figure 34: Time, Frequency, Information Theory features (GMM Maximum Likelihood) for the (a) unilateral motor, (b) bilateral motor, and (c) motor cognitive tasks.

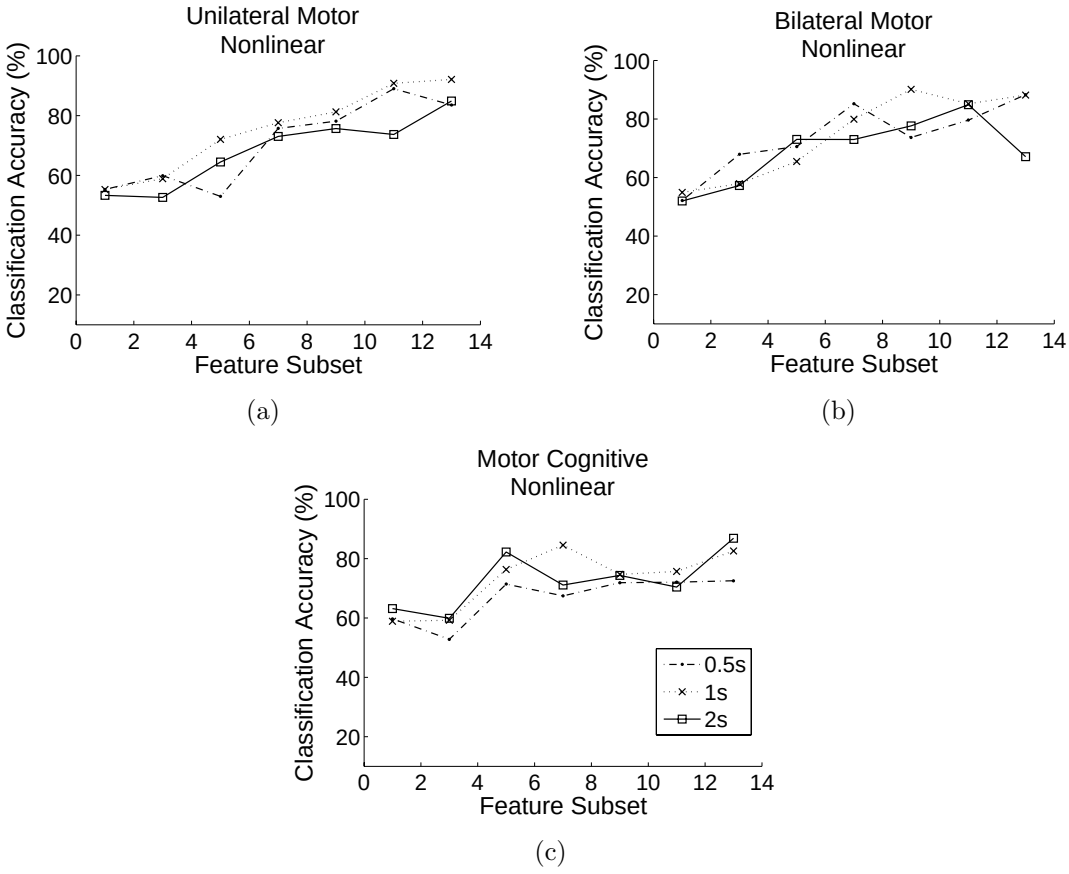

Figure 35: Nonlinear features (GMM Maximum Likelihood) for the (a) unilateral motor, (b) bilateral motor, and (c) motor cognitive tasks.

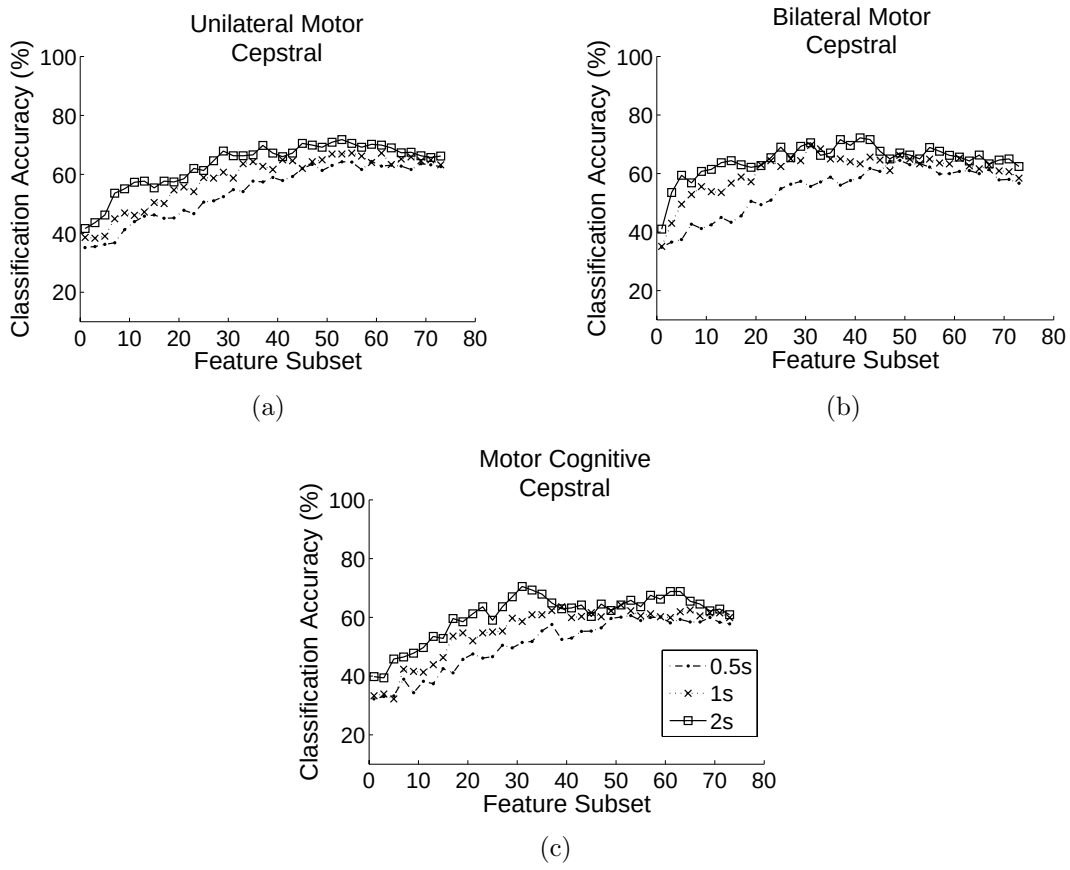

Figure 36: Cepstral features (GMM Maximum Likelihood) for the (a) unilateral motor, (b) bilateral motor, and (c) motor cognitive tasks.

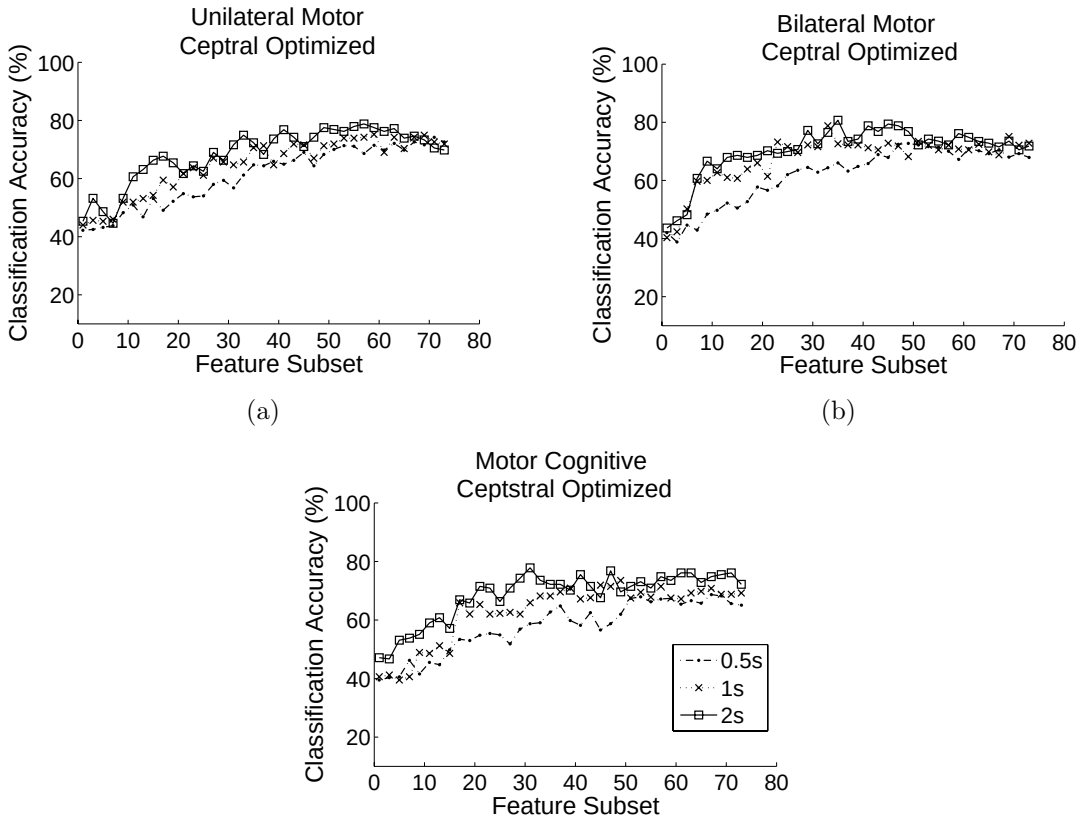

Figure 37: Cepstral Optimized features (GMM Maximum Likelihood) for the (a) unilateral motor, (b) bilateral motor, and (c) motor cognitive tasks.

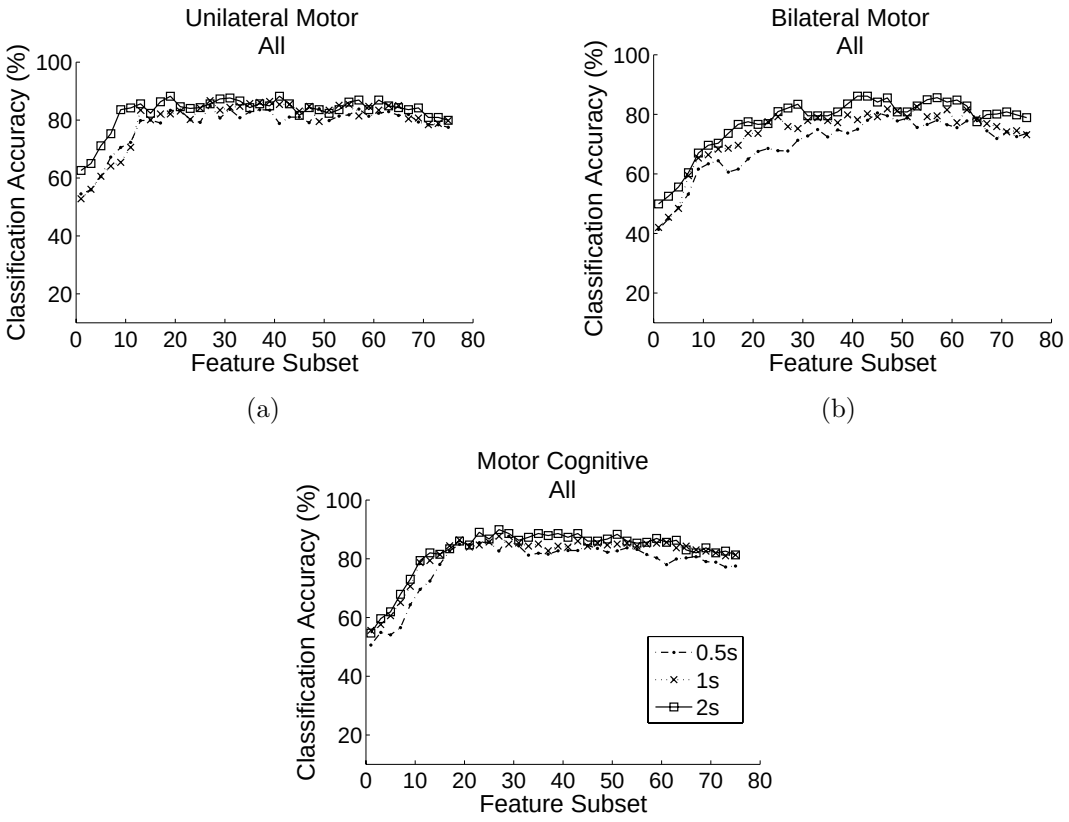

Figure 38: All features (GMM Maximum Likelihood) for the (a) unilateral motor, (b) bilateral motor, and (c) motor cognitive tasks.

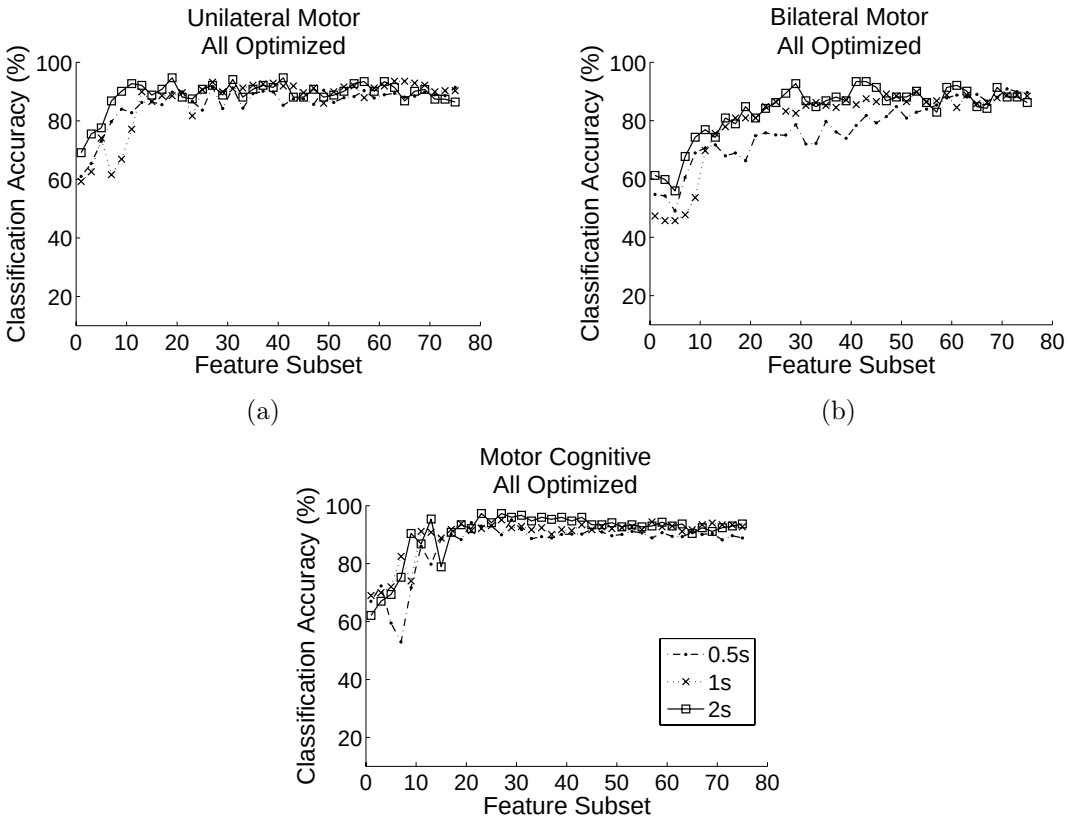

Figure 39: All Optimized features (GMM Maximum Likelihood) for the (a) unilateral motor, (b) bilateral motor, and (c) motor cognitive tasks.

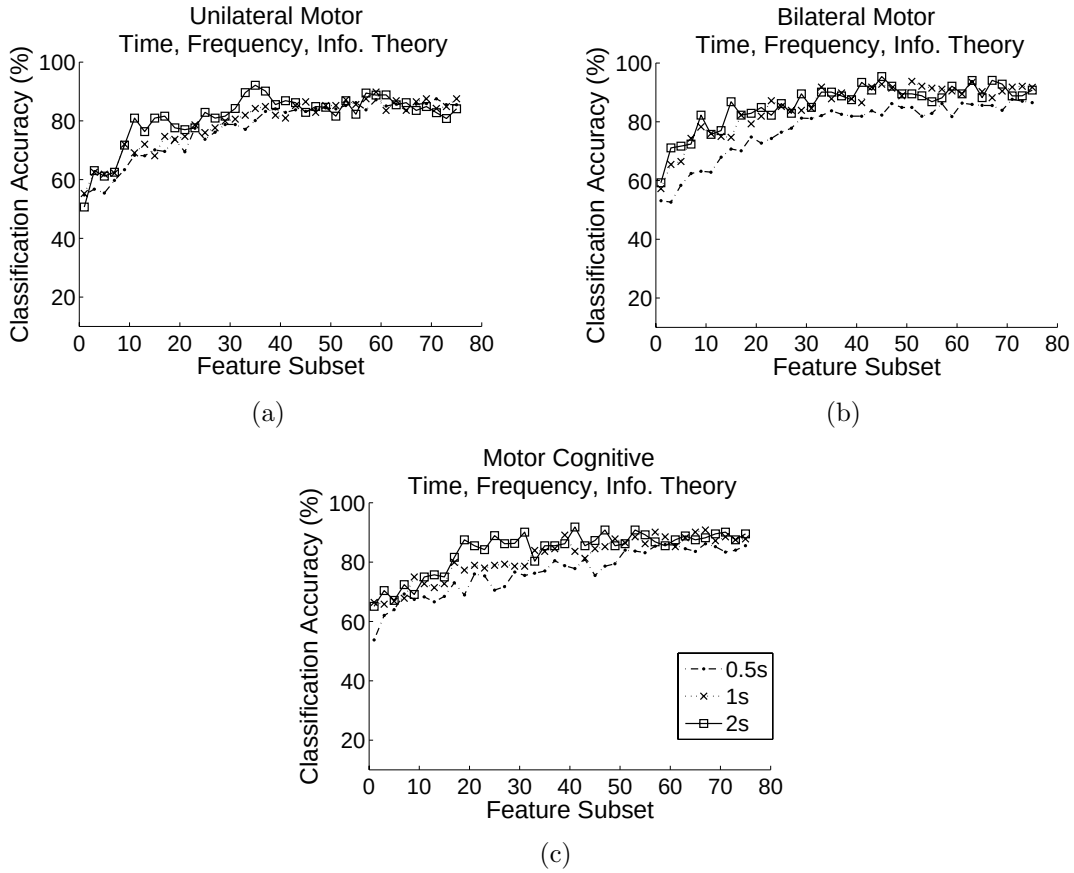

Figure 40: Time, Frequency, Information Theory features (GMM Minimum Classification Error) for the (a) unilateral motor, (b) bilateral motor, and (c) motor cognitive tasks.

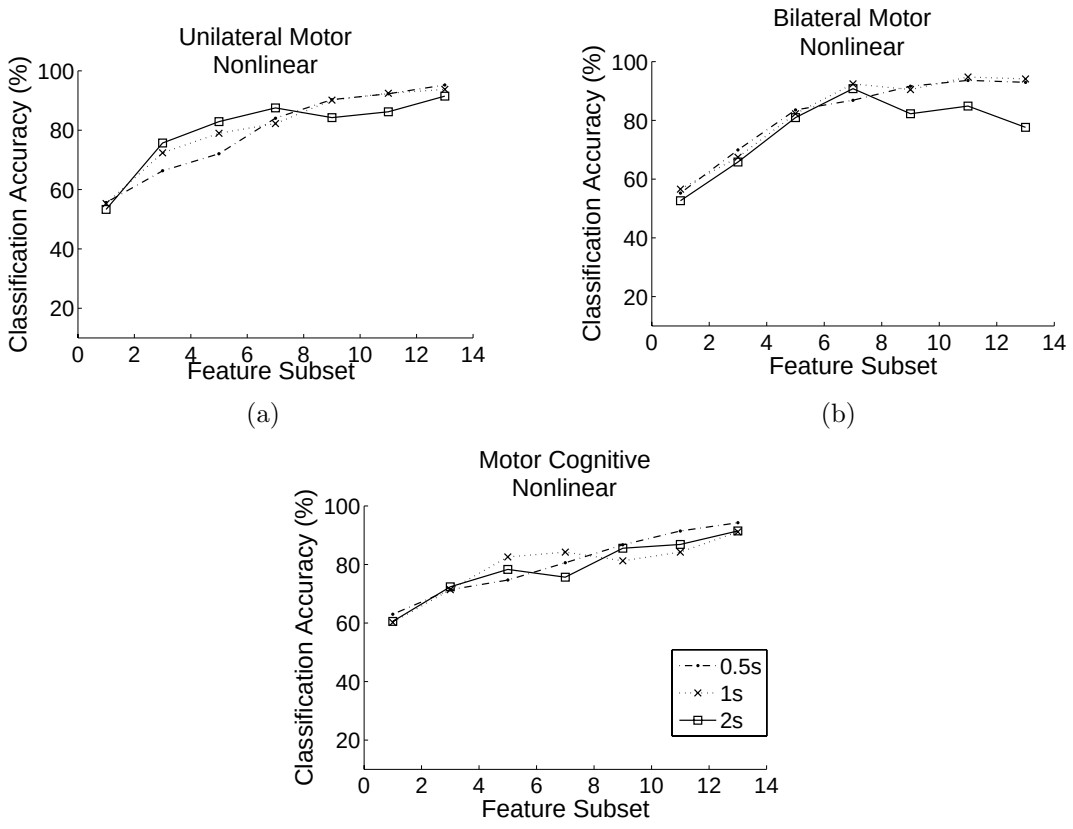

Figure 41: Nonlinear features (GMM Minimum Classification Error) for the (a) unilateral motor, (b) bilateral motor, and (c) motor cognitive tasks.

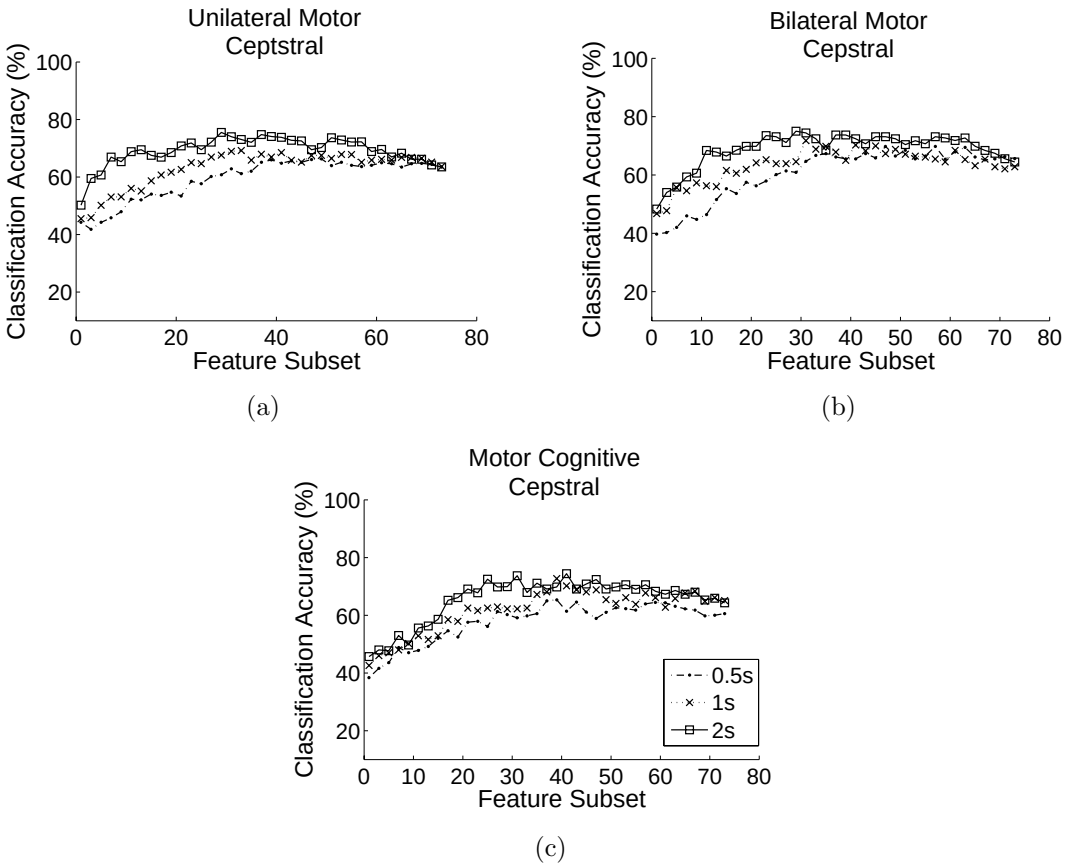

Figure 42: Cepstral features (GMM Minimum Classification Error) for the (a) unilateral motor, (b) bilateral motor, and (c) motor cognitive tasks.

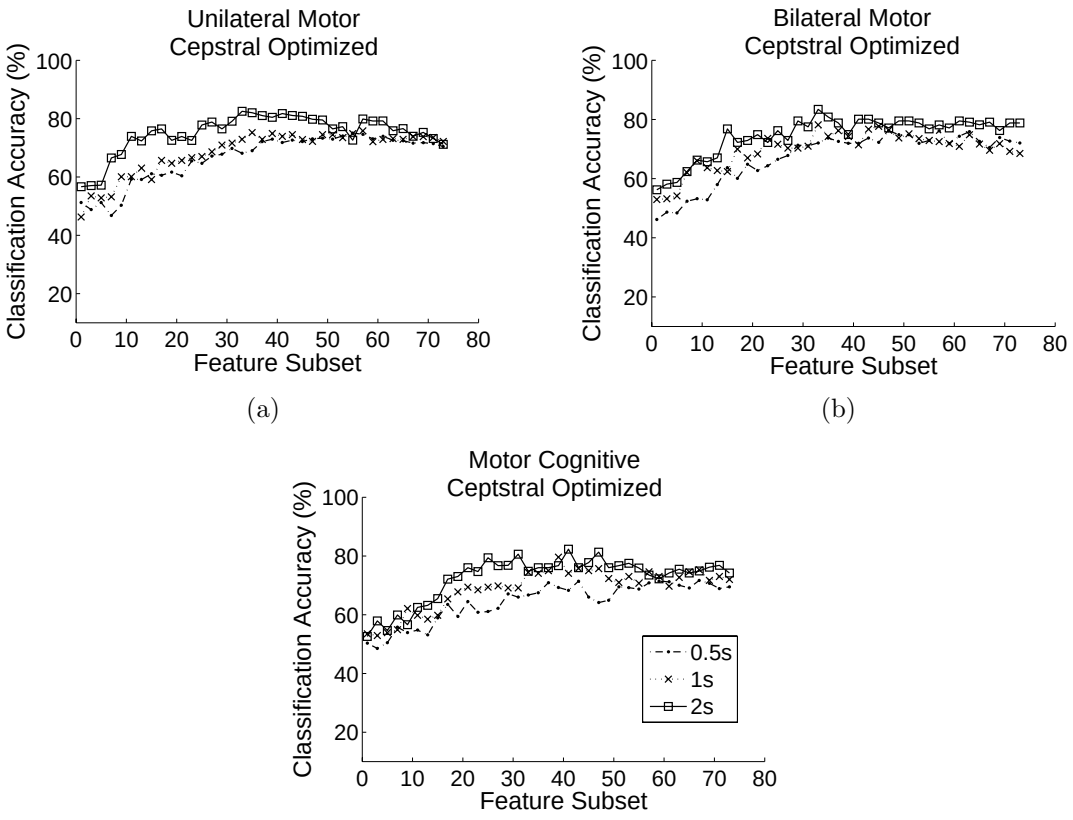

Figure 43: Cepstral Optimized features (GMM Minimum Classification Error) for the (a) unilateral motor, (b) bilateral motor, and (c) motor cognitive tasks.

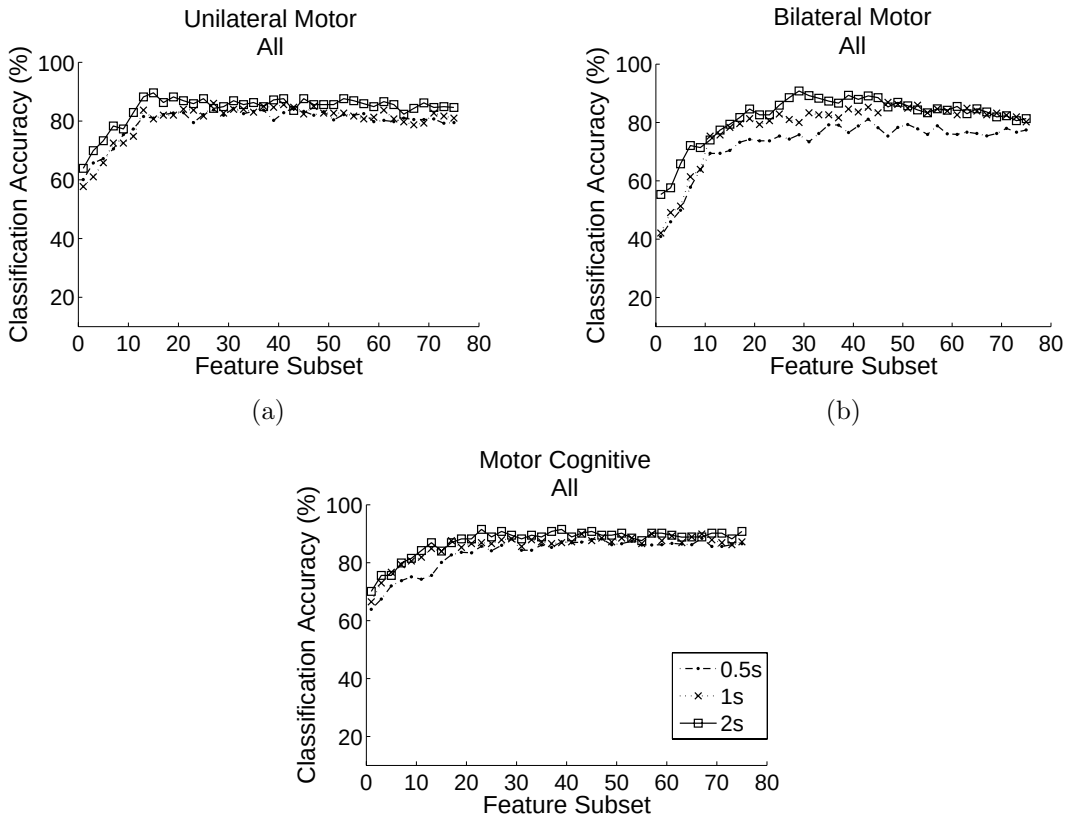

Figure 44: All features (GMM Minimum Classification Error) for the (a) unilateral motor, (b) bilateral motor, and (c) motor cognitive tasks.

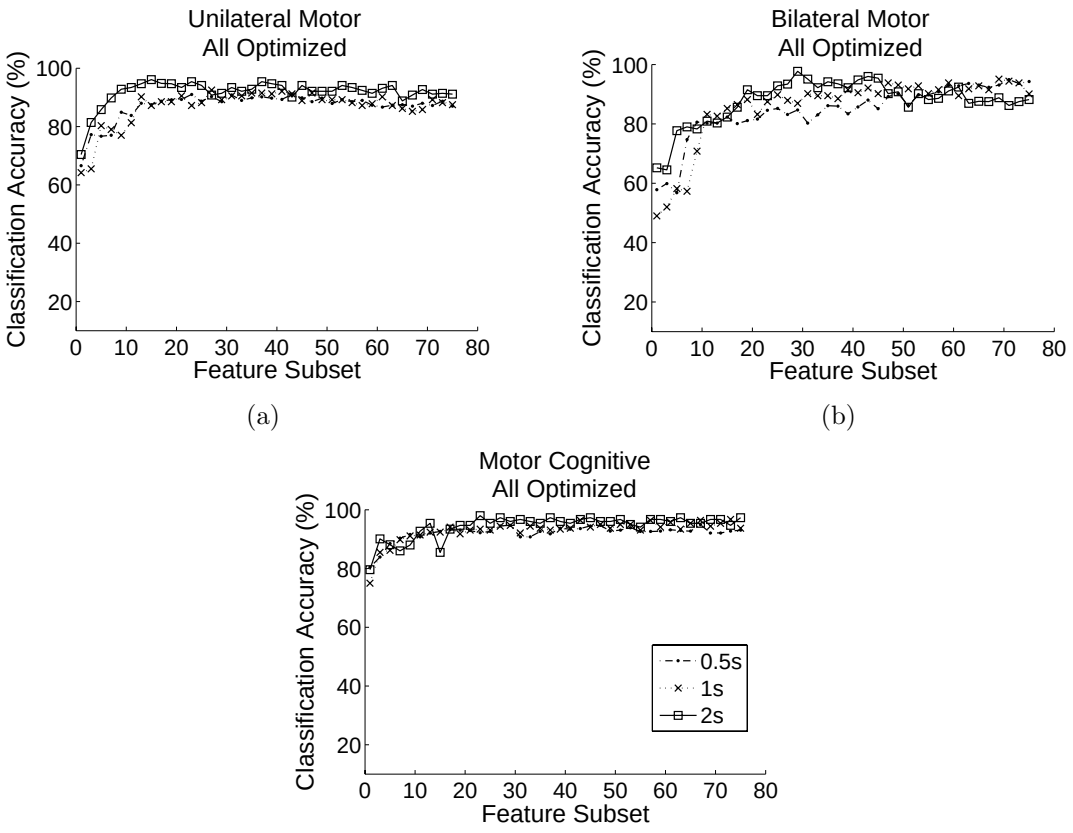

Figure 45: All Optimized features (GMM Minimum Classification Error) for the (a) unilateral motor, (b) bilateral motor, and (c) motor cognitive tasks.

Table 19: Cepstral features Gaussian Mixture Model classification results (maximum classification accuracy, number of features).

	0.5 second	1 second	2 second
Maximum Likelihood			
Unilateral Motor	64.4%, 59	67.2%, 55	**71.8%, 53**
Bilateral Motor	64.5%, 49	69.6%, 31	**72.2%, 41**
Motor Cognitive	60.6%, 53	64.2%, 51	**70.5%, 31**
Minimum Classification Error			
Unilateral Motor	66.3%, 49	69.2%, 33	**75.5%, 29**
Bilateral Motor	69.8%, 47	71.2%, 31	**75%, 29**
Motor Cognitive	65.4%, 39	72.7%, 39	**74.4%, 31**

Table 20: Cepstral features (optimized) Gaussian Mixture Model classification results (maximum classification accuracy, number of features).

	0.5 second	1 second	2 second
Maximum Likelihood			
Unilateral Motor	74.2%, 55	75.2%, 59	**78.8%, 57**
Bilateral Motor	72.7%, 49	75.1%, 51	**80.7%, 35**
Motor Cognitive	68.7%, 51	73.5%, 49	**77.8%, 31**
Minimum Classification Error			
Unilateral Motor	75.1%, 55	75.2%, 35	**82.5%, 33**
Bilateral Motor	76.2%, 47	78.2%, 33	**83.4%, 33**
Motor Cognitive	71.4%, 43	79.6%, 39	**82.3%, 41**

Feature Trends

Investigation of the nature of the features selected indicates that nonlinear features (nonlinear energy and katz fractal dimension) were primarily selected when all

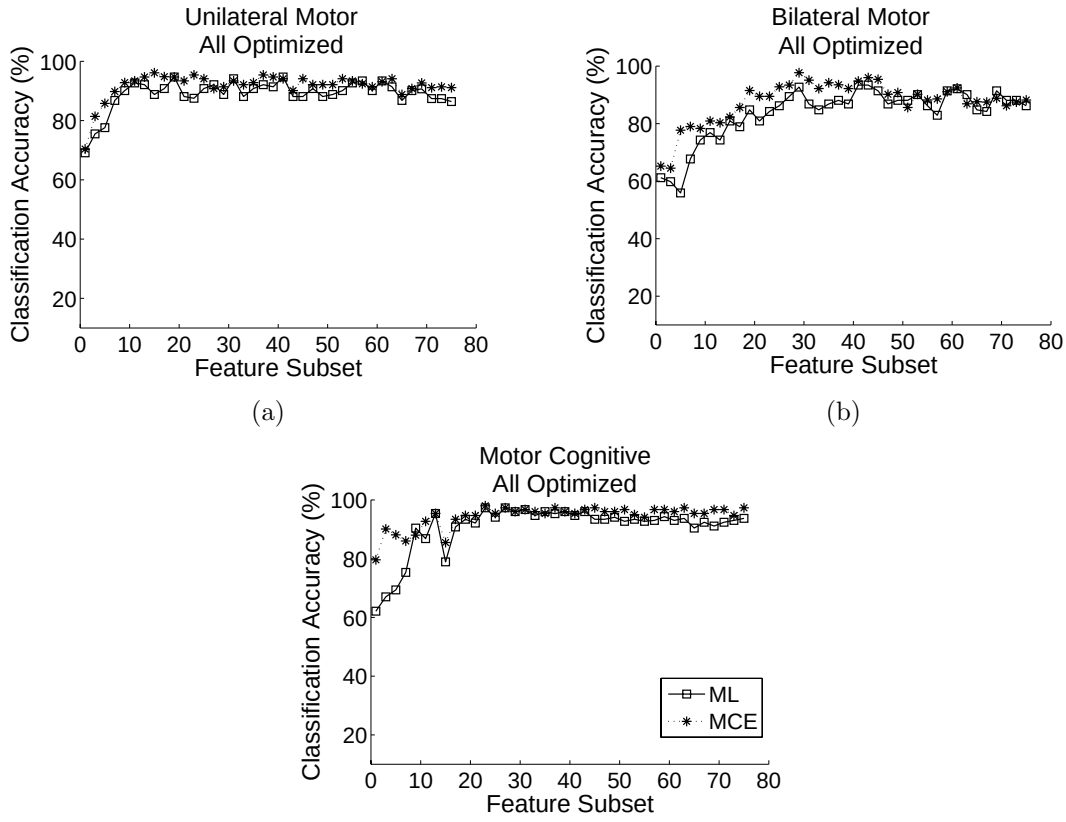

Figure 46: Gaussian Mixture Model Minimum Classification Error versus Maximum Likelihood for All Optimized features for the (a) unilateral motor, (b) bilateral motor, and (c) motor cognitive tasks.

Table 21: All features Gaussian Mixture Model classification results (maximum classification accuracy, number of features).

	0.5 second	1 second	2 second
Maximum Likelihood			
Unilateral Motor	85.1%, 27	86.7%, 27	**88.2%, 19**
Bilateral Motor	80.5%, 45	82.5%, 53	**86.1%, 41**
Motor Cognitive	87.7%, 29	87.7%, 27	**89.9%, 27**
Minimum Classification Error			
Unilateral Motor	84.5%, 43	86.0%, 27	**89.6%, 15**
Bilateral Motor	81.1%, 43	86.9%, 47	**90.8%, 29**
Motor Cognitive	88.4%, 29	89.9%, 43	**91.5%, 23**

Table 22: All features (optimized) Gaussian Mixture Model classification results (maximum classification accuracy, number of features).

	0.5 second	1 second	2 second
Maximum Likelihood			
Unilateral Motor	91.2%, 45	92.5%, 27	**94.7%, 19**
Bilateral Motor	90.1%, 47	89.1%, 47	**93.4%, 41**
Motor Cognitive	94.9%, 27	95.1%, 27	**97.3%, 23**
Minimum Classification Error			
Unilateral Motor	91.0%, 43	93.5%, 27	**97.7%, 15**
Bilateral Motor	94.9%, 49	95.1%, 49	**97.7%, 29**
Motor Cognitive	95.1%, 29	96.4%, 43	**98.0%, 23**

features were considered. Figure 47 shows the overall frequency of the selected features across tasks. The location of the selected features varied according to the task being considered. For the unilateral motor task, features were primarily selected from the left hemisphere (C3 and FC3) (Figure 48a). The nonlinear energy feature was selected from 5 out of the 7 channels recorded (C3, F3, C4, F4, FC4). For the bilateral motor task, features were equally selected within the left and right hemispheres (Figure 48b). Additionally, 9 features were selected from the EMG channel in comparison to 2 EMG features for the unilateral motor task and 3 EMG features for the motor cognitive task. For the motor cognitive task, features were primarily selected from the more frontal electrodes (F3, F4, FC3, and FC4) (Figure 48c). The frequency of features selected was the greatest for nonlinear energy (5 features) and Katz fractal

dimension (3 features) for the unilateral motor task, nonlinear energy (3 features) and Katz fractal dimension (3 features) for the bilateral motor task, and nonlinear energy (4 features), real cepstrum (4 features), and sample entropy (5 features) for the motor cognitive task.

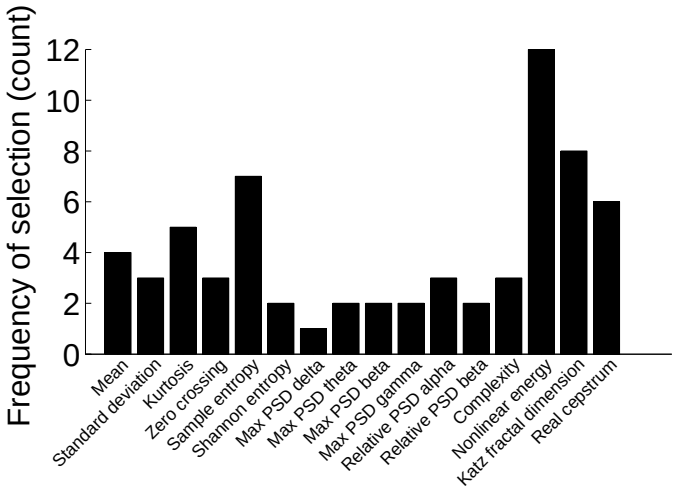

Figure 47: Frequency of selected features across all tasks.

Comparing the location of features selected for the unilateral motor task with the two dual tasks, indicates an increase in the number of features within the right hemisphere for the two dual tasks. Five features were selected in the right hemisphere for the unilateral motor task, 10 features for the bilateral motor task, and 11 features for the motor cognitive task. The real cepstrum features were selected for the two dual tasks (bilateral motor and motor cognitive), but not the unilateral motor task. It is also observed that few frequency domain features are selected across tasks in support of the previous finding from the preliminary investigations [62]. Frequency domain features were selected 1 out of 15 for the unilateral motor task, 8 out of 29 for the bilateral motor task, and 1 out of 23 for the motor cognitive task (Figure 48).

Statistical Validation of Approach

Statistical analysis was performed per task-type for only feature-values computed

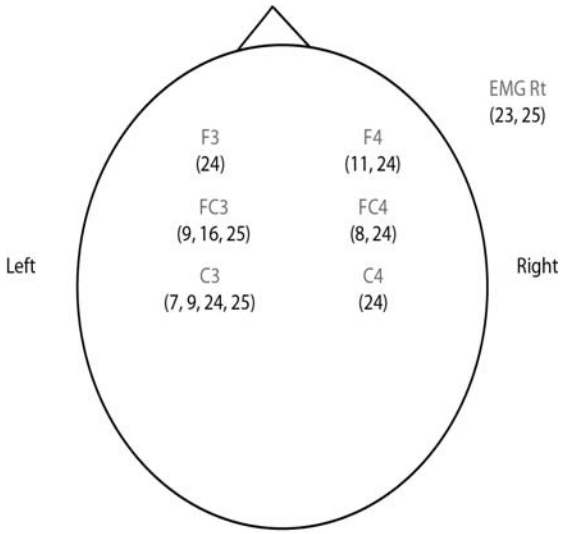

(a)

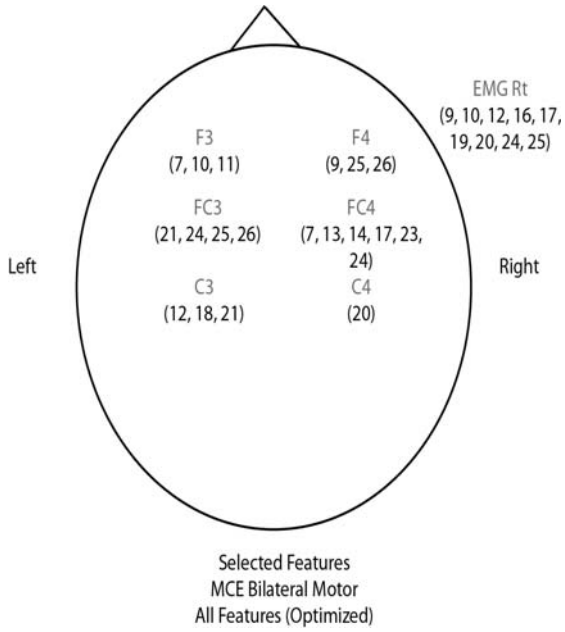

(b)

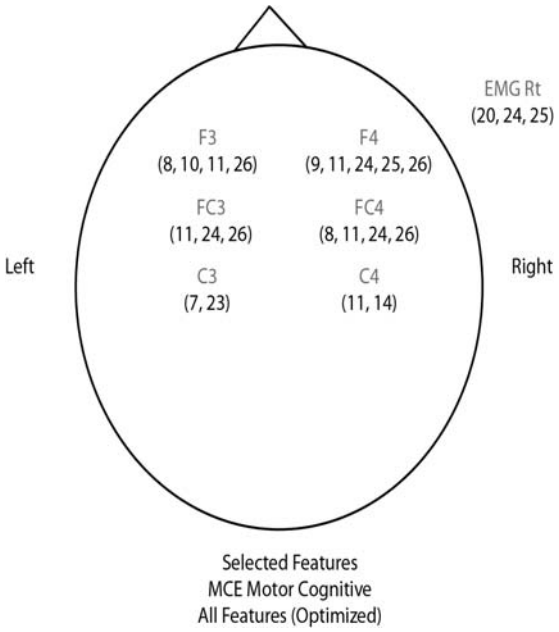

(c)

Figure 48: Selected Features from Gaussian Mixture Model Minimum Classification Error for the (a) unilateral motor, (b) bilateral motor, and (c) motor cognitive tasks.

using the 2-second window-size, which provided the best performance (Section 6.2.2.2). Dependent variables were values of the forward-selected features and the class label (young or elderly) was the independent variable. The data was analyzed using a one-way multivariate analysis of variance (MANOVA) as an omnibus test (p-values less than 0.05 indicated statistically significant differences) and a one-way ANOVA with Bonferroni correction for each feature as a post-hoc test ($p < 0.05/\text{N}$ indicated statistically significant differences, where N was the number of selected features).

The MANOVA determined statistically significant difference between young and old subjects on the features for each task, supporting the use of the selected features for the model. Subsequent ANOVAs further revealed which features most contributed to the differences between subjects. For the unilateral task, 14 out of 15 selected features lead to statistically significant differences (Pillai's Trace = 0.663, F(15,784) = 102.717, p_{MANOVA} <0.001, $\eta^2 = 0.663$, $p_{ANOVA} \leq 0.0033$). For the bilateral task, 11 out of 29 selected features lead to statistically significant differences (Pillai's Trace = 0.677, F(20,770) = 55.676, $p_{MANOVA} < 0.001$, $\eta^2 = 0.677$, $p_{ANOVA} \leq$0.0017). For the motor-cognitive task, 15 out of 23 selected features lead to statistically significant differences (Pillai's Trace = 0.721, F(23,776) = 87.320, $p_{MANOVA} < 0.001$, $\eta^2 = 0.721$, $p_{ANOVA} \leq 0.0022$)

6.3 Discussion

GMM MCE Seizure. The work described an application of cepstral analysis and the Minimum Classification Error (MCE) training scheme to the problem of EEG seizure classification. The MCE criterion was used to estimate the Gaussian Mixture Model (GMM) parameters for the task of classifying seizure episodes in EEG data. Results showed that the MCE algorithm accounted for the unbalanced data and improved the performance of the classifier over the SVM and GMM with Maximum Likelihood (ML). Additionally, the stream computing paradigm accounted for the

computational efficiency required for a future real-time system.

The results with the MCE criterion confirm prior comparative results of the two techniques [10, 85]. The MCE efficiency is due to its ability to formulate a lightweight classifier of maximum efficiency. The presented results are in line with the MCE philosophy which emphasizes all classes equally, weighting them for minimum error purposes.

The efficacy of the real cepstrum and MCE training for seizure classification provided the groundwork and motivation for applying these algorithms to classify aging datasets. The specific applications were considered in more detail and extended to test the efficacy for both EEG and EMG data for classification of young and elderly healthy adults.

Aging. Classification of young and elderly subjects was originally performed using only time and frequency domain features. The results of this analysis suggested that time domain features provided a better indicator of age-related differences. It was hypothesized that the selection of time domain features over frequency domain features may have been related to the incorporation of both absolute and relative features for the time domain and relative features only for the frequency domain. The work was further extended by incorporating additional features from the previously named domains, as well as features from information theory and features from automatic speech recognition (cepstrum).

Similar to the observation in Section 6.1.2.3 with classification of seizure states, classification with GMM using MCE improved classification accuracy over the SVM and GMM with ML. This increase in classification accuracy can be attributed to the ability of the classifier to account for the prior probability of each class before training and testing (Eq. 16). MCE explicitly incorporates classification performance into the training criterion (Eq. 18) and does not attempt to fit a distribution like

Maximum Likelihood, but instead aims to discriminate against competing models and minimize the average loss (Eq. 21). The increase in classification accuracy using MCE in comparison to ML also resulted in fewer features necessary for the classification, potentially decreasing computation time.

The inclusion and optimization of the real cepstrum and mel-frequency cepstrum improved classification accuracy across tasks (9.3% - 11.2%). While the optimized cepstral features provided improvements for distinguishing between young and elderly adults, the absolute value of the classification accuracy was 82.3% to 83.4% across tasks (Table 20). The modest increase in the absolute value of the classification accuracy may reflect the sensitivity of the measure to small changes in the EEG and EMG with healthy aging. The use of cepstral analysis might be more appropriate for applications with more prominent changes as in the case of seizure detection, where higher classification accuracies were obtained (Table 9). Additionally, the real cepstrum features were only selected for the two dual tasks (bilateral motor and motor cognitive). These features were selected in the fronto-central and frontal electrodes. Selection of the real cepstrum features for only the two dual task could suggest a unique characteristic of the EEG signal in regions of higher order processing that is highlighted by the real cepstrum.

Selected Feature Trends. The inclusion of absolute frequency domain features resulted in some being selected, although not to a high degree as with features from other domains. Findings in the literature for changes in power with aging, and the low rate of selection for relative [62] and absolute frequency domain features, suggests that frequency domain measures are not necessarily predictive of age-related changes. Or, the neural aspects of the signals are maintained more than the time domain measures.

Nonlinear features, nonlinear energy and Katz fractal dimension were the most robust in that they were selected more frequently in comparison to the other features.

The nonlinear features are potentially highlighting the characteristic changes with advanced aging. Nonlinear energy has been used as an index to detect the onset of surface EMG activity during isometric contractions in healthy adults [122] and in elderly adults walking [50]. By calculating the energy of the signal while taking into account both the amplitude and frequency changes, the signal to noise ratio is lower [78]. The computation of nonlinear energy differs from the computation of linear feature energy in that it also takes into account frequency information. To the author's knowledge, nonlinear energy methods applied to EEG to assess influences of aging have yet to be published for an automated system. Fractal dimensions have been used for seizure detection in the EEG [28], assessing heart rate variability [40], as well as detection of dementia in the elderly [47]. Katz fractal dimension is derived directly from the waveform and is suggested to be relatively insensitive to noise [28], making it a suitable feature.

Features were primarily selected from the frontal electrodes and the right hemisphere across tasks (Figure 48). The frontal electrodes represent a portion of the cortex that is attributed to higher order processing (executive processing). The selection of more electrodes from the frontal region, as opposed to the central electrodes over the motor cortex could suggest that the differences observed between young and elderly subjects are not their specific task or performance differences, but their neural strategy for accomplishing the tasks. The activation within the motor cortex (C3 and C4 electrodes) would be related more to the subject's ability to perform the task.

The observation/selection of features in the right hemisphere during the unilateral motor and motor cognitive tasks suggest a level of bilateral activation and/or intercortical interactions between the hemispheres which highlights the differences between the two subject groups. Features selected from the right hemisphere during the right hand task which activate the left hemisphere supports the potential difference in hemispheric activation captured in the model. These findings suggest

that motor control in healthy aging is not only isolated to the hemisphere controlling the motor activity of the dominant side (left hemisphere). The results support the finding of bilateral activation with advanced aging. Cabeza et al. [16] reported that high-performing elderly adults attempt to counteract age-related neural changes via neural plasticity. The neural plasticity changes were represented by bilateral activation. While the dissertation did not classify subjects into categories of high or low performance, the recruited elderly adults were all active for daily living purposes, performed comparable to young adults on the MMSE, and self-reported some level of physical activity. This could suggest the included elderly adults to some degree were using a compensatory mechanism resulting in bilateral activation as represented by the features selected from the right hemisphere during the motor task with the right hand.

Literature has suggested that with advanced age, neural networks within the human brain become less "complex" due to neurodegeneration [80]. While it has been reported that with advanced aging and disease, decreased complexity is observed [80, 103], contrasting reports have shown that the potential increase or decrease in complexity is dependent upon the conditions for assessing the dynamical system and the factors that may have been acting upon the dynamical system [132]. The time scale with which the features are measured can influence the potential change, as well as deterministic and stochastic stimuli, and external forces can influence the interpretation of the EEG and EMG. Assessment of complexity changes in the EEG and EMG with age can be made using some of the features in the presented approach. Nonlinear measures (nonlinear energy and Katz fractal dimension), entropy, complexity, and kurtosis are all features that are suggested to provide measures of complexity [80].

One of the points of Aim 3 was to determine an optimal subset of features for classifying young and elderly adults. Additionally, the optimally selected features

from the model were used to determine the statistical significance between young and elderly adults across channels.

The MANOVA statistical test was run as a means to support the results of feature selection and classification. In a similar manner to the data mining methodology presented, the MANOVA considers the collective contribution of the selected subset of features to statistically determine if there is a significant difference between the young and elderly classes. The presented methodology provides an accuracy value and the MANOVA test provides a level of significance. The MANOVA suggested that an even smaller subset of features than the subsets determined by forward selection might sufficiently predict the difference between young and elderly electrographical signals during behavioral tasks. The smaller subsets were based on P-values and effect-size. A potential difference in results between the MANOVA and forward selection was with the bilateral task (11 out of 29 selected features led to statistically significant differences). The use of the Mahalanobis distance objective-function for feature selection versus the partial eta-squared statistic (or a p-value) for the MANOVA highlights a potential difference in the percentage of features showing significant differences. It is conjectured that forward selection may have tolerated some over-fitting for the bilateral and motor cognitive tasks resulting in an increase of the number of features selected. Additionally, the greater physical and mental complexity of each the bilateral and motor cognitive task contrasted against the unilateral task necessitated more measures to characterize the electrographic responses due to each task. As suggested in the literature, specific increases or decreases are highly dependent on the testing conditions. Additionally, trends for increases and decreases varied across cortical regions. The results provide an automated approach for classifying between young and elderly adults, supporting the need for an automated process to detect changes in the EEG [47].

Conclusion.

Chapter 6 determined the appropriate parameters for feature extraction and a subset of the optimal features for distinguishing between young and elderly adults. Nonlinear features were highlighted as being the most robust measures. The efficacy of cepstral features were shown with the optimization of the filterbank spacing and number of coefficients; however, they did not outperform the other features incorporated. Additionally, classification using Gaussian Mixture Models with Minimum Classification Error was shown to increase accuracy and overall to be a useful tool for physiologists in practice. The results support the use of feature selection and data mining tools to determine appropriate measures for assessing the influence of age on the neural control of movement.

CHAPTER VII

NEURAL CONTROL OF MOVEMENT POST-STROKE

Aim 4: Model applications to clinical populations

Approach: Apply the methodology of data preparation, feature selection, and classification to motor stroke data to validate the proposed methodology and suggest how it may be applied to future clinical applications.

Hypothesis: Stroke subjects will exhibit beta-band corticomuscular coherence during the unilateral motor task (however less than the control group) and a decrease in coherence with an additional motor or cognitive task. Additionally, despite recovery, frequency, automatic speech recognition and time domain features will be attenuated due to neural plasticity in the stroke population.

7.1 Methodology

Three right-hemispheric stroke subjects (age: 51.7 ± 9.1 yrs) were recruited and included in the experiment with the approval of the Georgia Tech IRB. Inclusion and exclusion criteria for stroke subjects are detailed in Section 3.2 of the Experimental Design Chapter. Stroke subjects performed the same tasks as young and elderly subjects explained in Aim 2 (Section 5.1). Subjects were allowed additional practice in comparison to the other subject groups to account for the difficulty in performing the tasks due to their motor deficits. Additional practice consisted of practicing the task one additional time prior to each task set.

After considering how the neural control of movement was influenced in terms of the common oscillatory activity (corticomuscular coherence) in the EEG and EMG,

Figure 49: Experimental setup for stroke subjects.

Table 23: Stroke subject demographics

Subject Number	Age	Gender	Date of Stroke
1	53	Male	12/20/2006
2	60	Female	3/14/2009
3	42	Male	07/2008

the optimal subset of features from Chapter 6 were used to distinguish between elderly and stroke subjects to show the application of the methodology to a clinical population.

The limited number of stroke subjects (n=3) did not allow for statistical analysis to be performed, thus trends are described in the results section.

7.2 Results

Stroke subject's MVC force for the right hand was 24.4 $\pm$ 2.6 N and the left hand was 10.8 $\pm$ 7.4 N. The Edinburgh Handedness Inventory confirmed that all stroke subjects were right hand dominant (1.0 $\pm$ 0.0). According to the MMSE, there were no signs of cognitive impairment in the stroke subjects, with all scores $\geq$ 27. While the number of subjects was not large enough to perform statistical comparisons, Table

24 provides a comparison of average values for elderly and stroke subjects.

Table 24: Comparison of behavioral measures

	Elderly	**Stroke**
MVC Right	19.6 N	24.4 N
MVC Left	19.4 N	10.8 N
MMSE	28.6	29.0
Laterality Quotient	0.92	1.00

Significant corticomuscular coherence between unrectified EMG and EEG was observed in all three stroke subjects. Unlike young and elderly adults, peak values of coherence were not centered in the beta band during the unilateral motor task (Figure 50). Peaks in coherence were observed across frequency bands. The magnitude of coherence across task was less in the stroke subjects in comparison to the young and elderly adults (Figure 17) across all bands. Corticomuscular coherence showed a trend for an increase in the alpha band during the bilateral motor task (Figure 51a). The beta band showed a trend for a decrease in coherence during the two dual tasks (bilateral motor and motor cognitive) in support of the hypothesis. Gamma-band coherence did not show task trends.

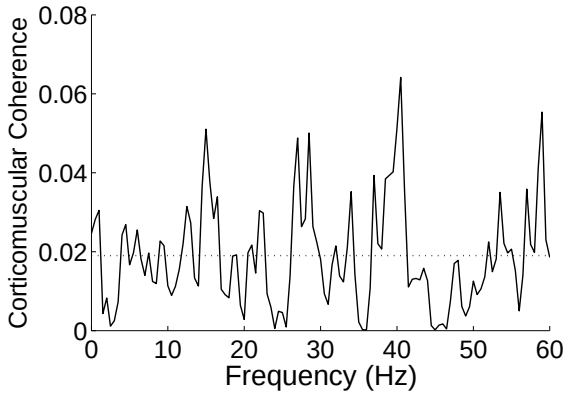

Figure 50: Representative coherence.

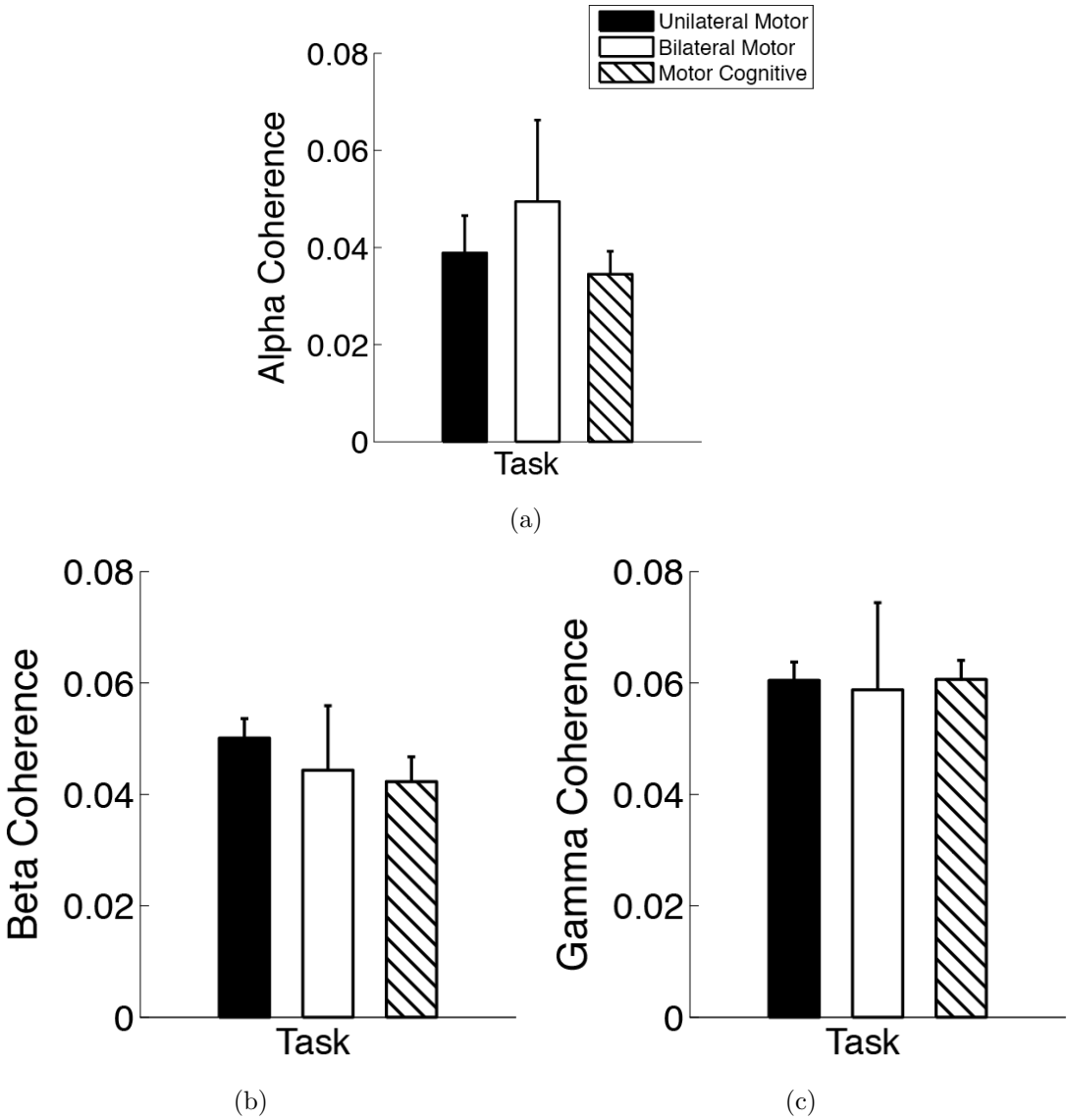

Figure 51: Peak corticomuscular coherence in the (a) alpha (8-14 Hz), (b) beta (15-32 Hz) and (c) gamma (33-55 Hz) bands during the unilateral motor, bilateral motor, and motor-cognitive tasks in stroke subjects (n=3)

EEG and EMG power were both primarily concentrated in the gamma band. Normalized gamma-band power in the EMG was more than double the power in the alpha and beta bands (Table 25).

Motor output variability tended to increase with the motor cognitive task in both the force and EMG signals (Figure 52). Cognitive accuracy was lower in both the cognitive (43.1% $\pm$ 37.6%) and the motor cognitive (44.4% $\pm$ 34.7%) tasks for stroke

Table 25: Frequency power of EEG in the left motor cortex (C3) and EMG in the right hand in alpha, beta and gamma bands during the unilateral motor, bilateral motor, and motor-cognitive tasks in stroke subjects. Power in each band is normalized to total power. Mean ± SD.

	Alpha	**Beta**	**Gamma**
EEG power, C3			
Unilateral Motor	0.231 ± 0.229	0.258 ± 0.058	0.429 ± 0.266
Bilateral Motor	0.202 ± 0.239	0.270 ± 0.032	0.452 ± 0.307
Motor Cognitive	0.207 ± 0.188	0.290 ± 0.027	0.429 ± 0.272
EMG power			
Unilateral Motor	0.021 ± 0.008	0.258 ± 0.020	0.720 ± 0.028
Bilateral Motor	0.019 ± 0.008	0.298 ± 0.042	0.683 ± 0.040
Motor Cognitive	0.023 ± 0.010	0.266 ± 0.019	0.711 ± 0.028

subjects in comparison to young and elderly subjects (Table 7).

Cepstral Analysis. Real cepstrum and mel-frequency coefficients were determined in the same manner as Section 6.2. The maximum number of coefficients from each channel were maintained for further analysis (Figure 53). Nine coefficients for each EEG channel and six coefficients for the EMG channel were maintained for the real cepstrum. Three coefficients were maintained for each channel for the MFCC. Similarly, nine real cepstrum coefficients were maintained for the EEG channels in Section 6.2.1.1 and five were maintained in the EMG channel. Two coefficients were maintained across channels for the MFCC in Section 6.2.1.1. The optimized cepstral features were used for feature selection and classification along with the other features from Table 10.

Classification

The NINDS's goal to 'translate basic and clinical discoveries into better ways to prevent and treat neurological disorders" was applied for the classification of elderly and stroke subjects. The optimal parameters and subsets of features from Aim 3 were applied in Aim 4. Optimal feature subsets from Figure 48 were used with the GMM

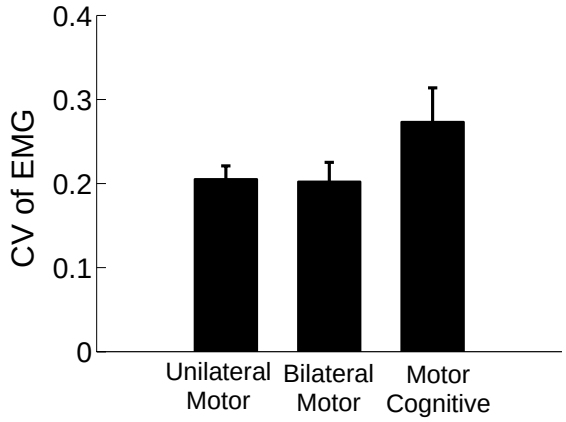

(a)

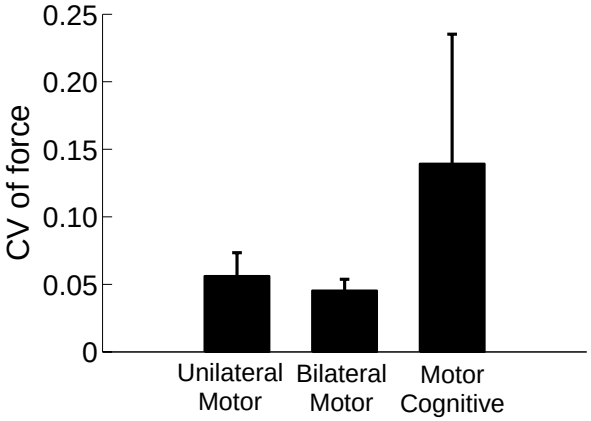

(b)

Figure 52: Motor output variability of stroke subjects (n=3) during unilateral motor, bilateral motor and motor cognitive tasks. (a) CV of force and (b) CV of EMG

with MCE to classify elderly and stroke subjects within each task. A classification accuracy of 99.0% was obtained for the unilateral motor task corresponding to 98.8% accuracy for the elderly class and 99.2% accuracy for the stroke class (Table 26). For the bilateral motor task, a classification accuracy of 80.8% was obtained corresponding to 42.4% accuracy for the elderly class and 95.9% accuracy for the stroke class. A classification accuracy of 97.8% was obtained for the motor cognitive task corresponding to 93.3% accuracy for the elderly class and 99.8% accuracy for the stroke class.

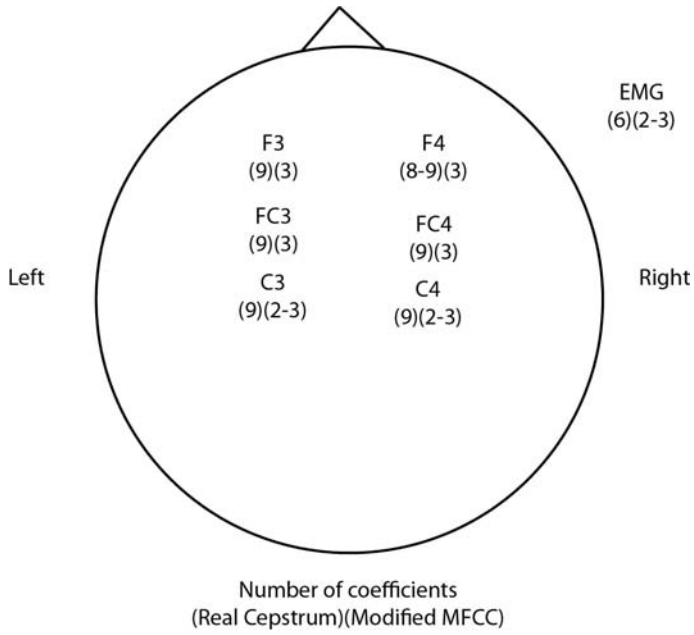

Figure 53: Optimal number of real cepstrum and mel-frequency cepstrum coefficients.

Table 26: Summary of classification results.

	Overall	**Elderly**	**Stroke**
Unilateral Motor	99.0%	98.8%	99.2%
Bilateral Motor	80.8%	95.9%	42.4%
Motor Cognitive	97.8%	93.3%	99.8%

As noted in Figure 47, the nonlinear energy and Katz fractal dimension features were selected the most frequently. Classification considers all of the features within the optimal subset, so to see the influence of an individual feature for distinguishing between age groups, the nonlinear energy and Katz fractal dimension features were plotted. The trend for an increase or decrease depends upon the location of the electrode and the task condition.

7.3 Discussion

The results show that a methodology proven successful for healthy adults can be extrapolated to investigate the stroke population. The approach also confirms application of the selected features for classification of elderly and stroke EEG and EMG data.

Behavioral measures suggest that stroke subjects have compensated for the motor deficits in their left hand by increasing the usefulness of their right hand. The MVC force of stroke subjects was greater than elderly adults, and while only right hand dominant individuals were included, right hand dominance was greater in the stroke subjects (Table 24).

Corticomuscular coherence has been suggested as a useful tool for assessing the functional influences on the neural control of movement post-stroke [89]. Findings from Aims 1 and 2 (Chapters 4 and 5) may potentially contribute to clinical applications of corticomuscular coherence analyses to assess and treat neurological patients including stroke [89, 29]. For example, a smaller beta band corticomuscular coherence was observed on the affected side compared to the unaffected side in well-recovered patients with a subcortical infarction [89]. A significant reduction in corticomuscular coherence was also observed in poorly recovered stroke subjects with varying types of strokes and lesions in different regions of the brain [29]. In addition, bimanual tasks

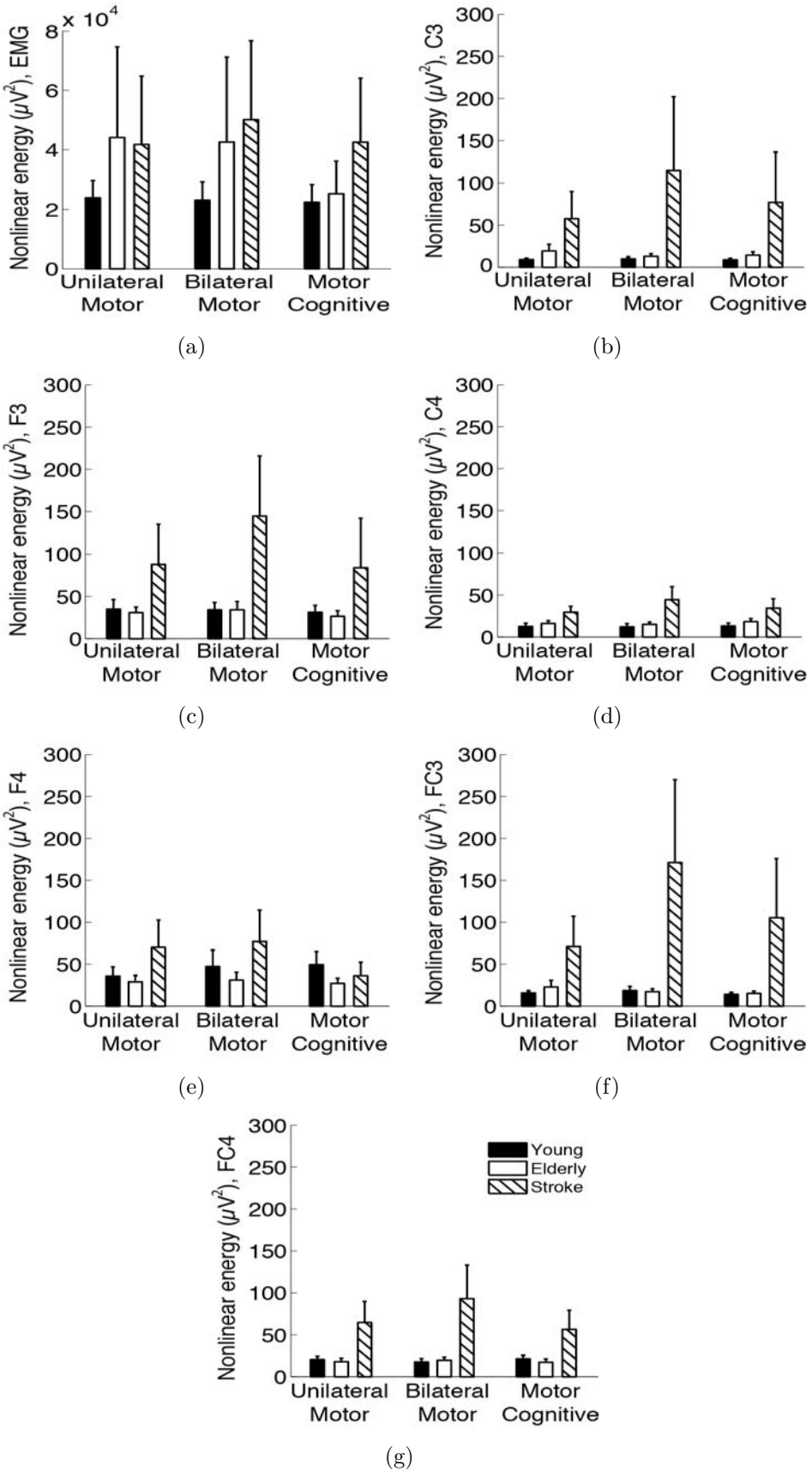

Figure 54: Nonlinear energy across groups and tasks.

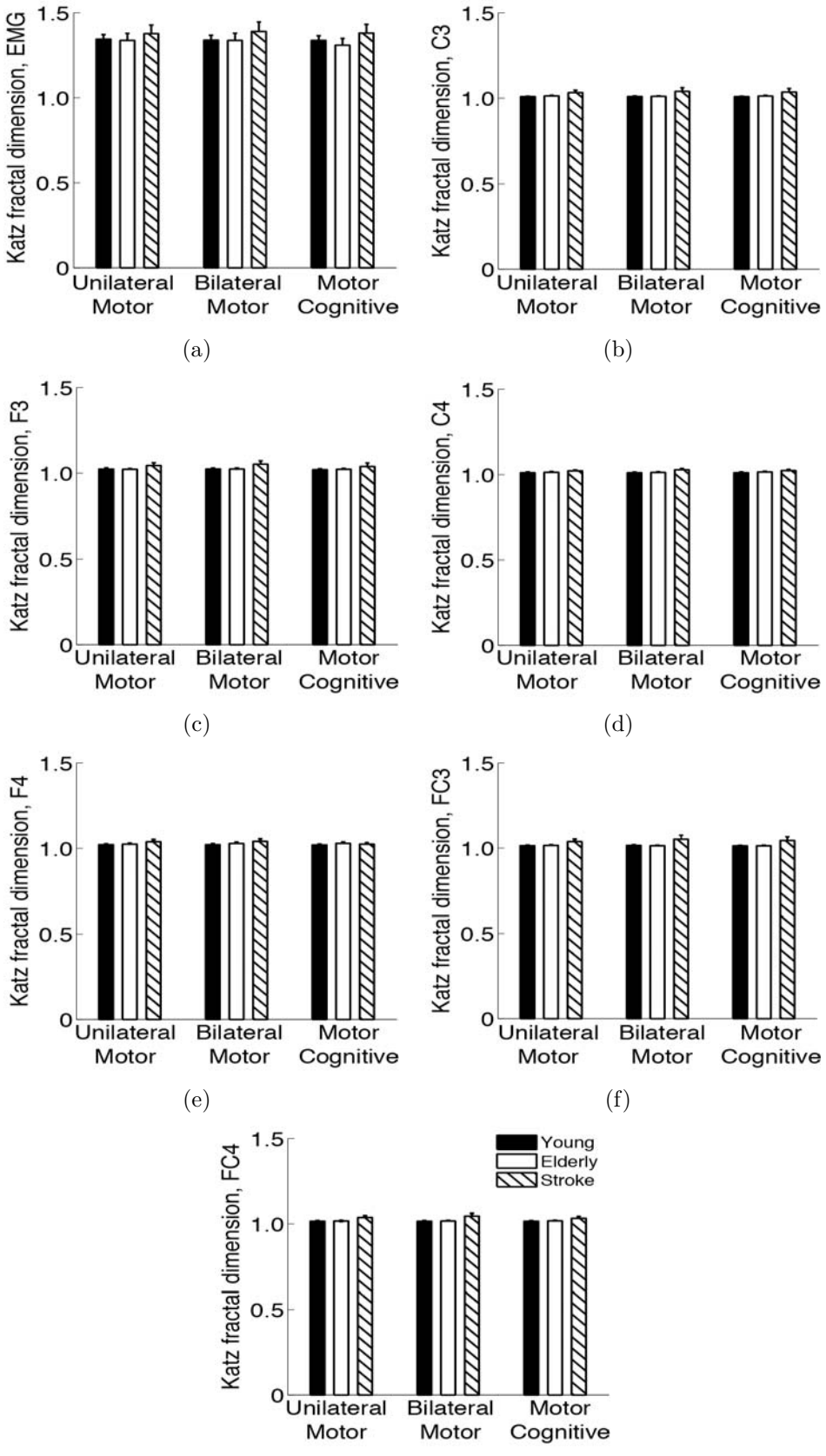

Figure 55: Katz fractal dimension across groups and tasks.

are difficult to perform for individuals with stroke, Parkinson's disease, and even healthy elderly adults [61, 127, 37, 142]. Aim 4 considered the influence of stroke on corticomuscular coherence during unilateral and dual tasks. A decrease in the magnitude of coherence was observed in stroke subjects (Figure 51) in comparison to healthy adults (Figure 17). The trend for task increases and decreases differed between the stroke subjects and their healthy counterparts. It is suggested that corticomuscular coherence decreases with stroke recovery potentially due to neural plasticity changes.

The results support the NINDS's goal to "understand how the normal brain work[s]" to "translate basic and clinical discoveries into better ways to prevent and treat neurological disorders." The optimal subset of features from Chapter 6 provided clear discriminatory information for the classification between elderly and stroke subjects with high accuracy (Table 26). The large number of features from the right hemisphere (same location of the infarction) could account for the classifier's ability to perform well. Increased bilateral activation occurs post-stroke [23, 83], highlighting the greater distinction in the right hemisphere from the healthy subjects because this region of the brain was primarily impacted from the stroke.

Overall classification accuracy for discriminating between elderly and stroke subjects suggests the methodology from Aim 3 is appropriate for the application to the stroke population (Table 26). The overall and individual class accuracies for the unilateral motor and motor cognitive tasks are much higher than the accuracies for the bilateral motor task. Stroke subjects had a very difficult time performing the bilateral motor task because of the complexity of the task and the involvement of their impaired hand. The degree to which the bilateral task was perceived by the author to be difficult for stroke subjects varied across the three subjects. The level of difficulty was potentially due to the stage and type of rehabilitation each subject was undergoing; however, details on rehabilitation interventions were not available to further speculate the influence of recovery on the observed results.

Conclusion.

The results support the goal of the NINDS to take knowledge from healthy individuals and extrapolate them to provide tools for treating patient populations. Stroke subjects compensated for the motor deficits in their left hand by increasing the usefulness of their right hand. Despite the increased useful of the right hand, corticomuscular coherence was variable across stroke subjects. The results validate the application of the approach using the optimal subset of features from Chapter 6 to the stroke population, but with limitations for classification during the bilateral motor task.

CHAPTER VIII

CONCLUSIONS AND FUTURE WORK

8.1 Integration of Findings

The NIA has stated that one of the challenges for the 21st Century is to better understand the aging process "to make these added years as healthy and productive as possible" [98]. The aim of the NIA is critical because the majority of everyday motor tasks necessitate the use of bimanual movements or concurrent cognitive processing. Compared with a simple unimanual movement, the involvement of additional tasks, such as additional contralateral movement or cognitive processing, accompanies divided attention and decreases the quality of motor performance in healthy individuals and often more so in elderly adults and patients with movement disorders (stroke) [79, 7, 37, 146, 138, 49].

One approach to make the aging process as "healthy and productive as possible" is to support the development of methodologies capable of understanding the performance of daily living tasks and how the neural control of movement is influenced by advanced aging. There is a need for an automated process capable for use by general practitioners to detect changes in biological signals [47]. This dissertation considered how the normal brain controls motor activity in a muscle by investigating the correlated activity with age under different task conditions with a focus on the corticomuscular coherence feature. The approach was used to develop a process to automatically classify between young and elderly adults. That information was then extrapolated for the stroke population to further address the aim of the NINDS.

The dissertation showed that beta-band (the frequency band attributed to motor activity) corticomuscular coherence decreased with an additional task to the same

degree whether the second task was a motor or non-motor task. The complexity of the task did not influence this reduction because beta band coherence was not associated with fine motor performance such as motor output variability and accuracy. The same response was observed with increased task complexity. The decrease in beta-band corticomuscular coherence with an additional task is believed to be the result of divided attention toward the primary motor task. Although, it was out of the scope of the dissertation, the influence of the visual feedback provided on attention may have influenced the measurement of coherence. Consideration of visual feedback and measurement from the visual cortex are suggested in Section 8.2 on Future Work.

Attention was shown to have a significant influence on coherence; however, detection of the task difference was also shown to be dependent upon the analysis approach. When unrectified EMG was used for analysis and the peak of coherence was independently determined, the observation of a significant task effect was only observed for the complex task as seen in Aim 2 with young and elderly adults. In spite of the differing trends for a main effect of task with analysis approach, it is still believed that corticomuscular coherence is influenced by the amount of attention directed towards a primary motor task.

The improved analysis approach of unrectified EMG and independently determining the peak of coherence were incorporated to test the influence of aging on correlated activity between muscle and brain. The dissertation work extended previous literature that only considered up to middle age, as well as work that considered into elderly age; however, without a significant difference in coherence. Results of the present work showed a significant increase in corticomuscular coherence with and without rectification of the EMG signal in both the alpha and beta bands across unilateral and dual tasks. In the alpha band, the increase in corticomuscular coherence was largest with an additional cognitive task in elderly adults. Again, this supports the notion of attention because alpha activity is attributed to cognitive processing

which can cause an increase in the necessary level of attention for the task. In the beta band, corticomuscular coherence was increased with an additional task in the same manner between young and elderly subjects. In addition, beta-band corticomuscular coherence in the motor-cognitive task was negatively correlated with motor output error across young, but not elderly adults. The results suggested that 1) corticomuscular coherence was increased in senior age with a greater influence of an additional cognitive task in the alpha-band and 2) individuals with lower beta-band corticomuscular coherence may exhibit more accurate motor output in young, but not elderly adults.

After the neural control of movement was considered for the correlated activity between muscle and brain, the features showing specific age differences were incorporated for developing a methodology to automate the process of determining the optimal features and classifying between young and elderly adults. Despite the corticomuscular coherence feature providing significant discriminatory information using a purely statistical approach, the coherence feature was not selected within any of the optimal subsets for classification. This suggests that while corticomuscular coherence has long been used as a measure for assessing the potential changes in the neural control of movement, there are other features, that together can provide more discriminatory information. Additionally, frequency domain features were not selected as frequently as initially anticipated. This suggests that some aspects of neural strategy might be maintained into senior age and not change to a large degree.

The observation of features (e.g. corticomuscular coherence, power spectral density) showing a significant difference between young and elderly adults using a statistical approach, but not selecting the feature for classification suggests that the features may highlight different aspects of aging using the different approaches. The statistical approach highlights trends for increases or decreases in the observed features, while the data mining approach provides a tool for general classification between the

two groups for potential diagnostic applications. MANOVA, a statistical approach, supported the findings of the data mining approach by indicating significant differences between young and elderly adults for each task. The scientific approach of only focusing on features that have previously been reported to show a significant difference limits the depth of investigation and potentially overlooks features that could improve the physiological understanding of the aging process.

At times value can be added through features that do not show statistical differences individually. Nonlinear energy and Katz fractal dimension were shown to be the most robust features due to the high frequency of their selection and the independent ability of these features to produce high classification accuracies. In Aim 3 these features showed significant differences in cases, but not all between young and elderly adults. The lack of a significant difference in some cases could be attributed to subject variability. Further investigations by increasing the subject number would highlight additional differences between the two populations.

The dissertation also presented a novel approach to classification of young and elderly biological signals with application of cepstral analysis and Gaussian Mixture Models with the Minimum Classification Error training scheme. Results from the dissertation expanded aging research on the classification of young and elderly adults that was previously limited to gait and balance analysis using support vector machines. Aim 3 optimized the real cepstrum and mel-frequency cepstrum for application to the biological signals, EEG and EMG. The inclusion and optimization of the real cepstrum and mel-frequency cepstrum significantly improved classification accuracy across tasks, however the modest increase in the absolute value of the classification accuracy is a reflection of the sensitivity of the measure to small changes in the EEG and EMG with healthy aging. The use of cepstral analysis is believed to be more appropriate for applications with more prominent changes, as seen in the validation with seizure data in the first portion of Aim 3. The MCE criterion was used

to estimate the GMM parameters for the task of classifying young and elderly adults using EEG and EMG data. Experimental results showed that the MCE algorithm improved classification accuracy over the SVM and GMM with ML classifiers. This increase in classification accuracy can be attributed to the classifiers ability to account for the prior probability of each class before training and testing, and discriminating against competing models to minimize the average loss of the classifier.

The findings in this dissertation not only have scientific significance, but also contain clinical importance toward the treatment of individuals with impaired movement. Classification between elderly and stroke subjects with 80.8% to 99.0% accuracy validates the application of the methodology for healthy adults to a clinical population. Validation of the approach is limited for the bilateral motor task because while the overall classification accuracy was 80.8%, the accuracy for the stroke class was 42.4%. This finding highlights the difficulty of the stroke subjects to perform the bilateral motor task, which was the only task to use the impaired left hand. The set of features included is not exhaustive in that there are additional features that could potentially be considered. Potential features could include fluctuations in mu (8-12 Hz) sensorimotor activity of the EEG that occur during movement. Mu activity is a narrow band that often times is masked within the beta band [102]. Additionally, genetically fused features could be considered if the nature of feature is no longer of interests, but mainly the increase in classification accuracy. Additionally, classification for the bilateral motor task could improve with the inclusion of the force signal to capture the variations in motor output variability.

Additional clinical applications for the work are possible for monitoring the rehabilitation from a stroke or traumatic brain injury patients by evaluating the retention of neural strategy via classification throughout the rehabilitation process. Other clinical applications are the developmental steps towards a methodology for real-time

seizure classification and detection. These findings would lead to a better understanding of the functional significance of the neural control of movement with aging and applications to clinical populations.

8.2 Suggested Future Work

The following section lists suggestions for future work to expand the dissertation work.

- Subject inclusion and exclusion criteria should be considered in different context. Inclusion of "non-healthy" elderly adults that represent the progression of aging. For example, the inclusion of elderly adults with hypertension and/or arthritis. Additionally, the small variations in some parameters comparing young and elderly adults may have been due to the definition of elderly adults as >60 years. A future work should include subjects over the age of 75 years, closer to range of oldest old (>85yrs).

- The research primarily focused on the connection of movement to the brain from motor cortex to the muscle, and then considering the proprioceptive feedback. Future work should expand the regions of interests to include the influence of visual feedback, tactile feedback, and cognitive processing to assessing the neural control of movement. Each of those factors are influenced by aging and their potential impact on the system. Figure 56 displays a block diagram of the interaction of each region for performing the task.

- Expansion of the work to the stroke community, to further address the NINDS aims, would benefit from working with physicians more closely to understand the recovery stage of stroke subjects and their rehabilitation regimen might influence the ability to classify between healthy and stroke subjects.

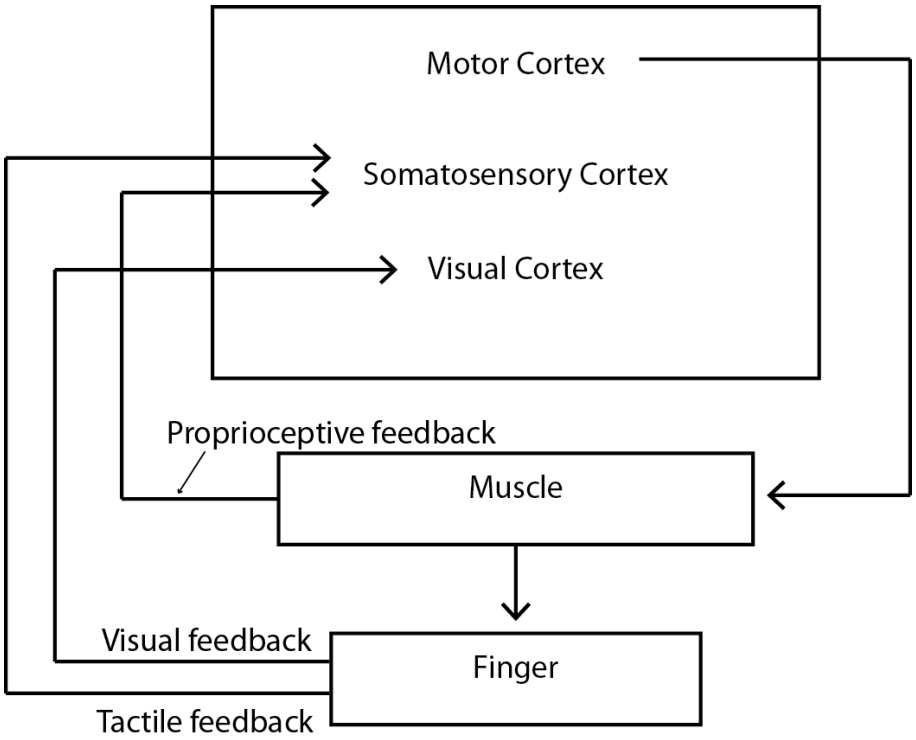

Figure 56: Sensorimotor feedback during motor task.

- A future goal of the dissertation work is for the methodology to be used in practice by physiologists, general practitioners, and rehabilitation therapist. Testing of the methodology in real-time setting using a brain computer interface would enable development of the approach and testing the timing efficiency. The necessary hardware is suggested in Aim 3 through the use of IBM's InfoSphere Stream computing software.

8.3 Contributions

The objective of the research was to develop a methodology to understand the neural control of movement with aging, and applications to the stroke population. The results of the work support the National Institute on Aging's aim to "understand the mechanisms involved in normal brain aging; the role of cognition in everyday functioning; protective factors for sensory, motor, emotional, and cognitive function;

and the pathogenesis of Alzheimer's Disease and other neurodegenerative disorders of aging within health disparity populations" [98]. It is of hope that the results can also support the National Institute of Neurological Disorders and Stroke's goals to "understand how the normal brain and nervous system develop and work, and what goes wrong in disease" and to "translate basic and clinical discoveries into better ways to prevent and treat neurological disorders" [99].

Contributions

- Demonstration of the change in correlated activity between muscle and brain with fine motor simple and complex dual tasks with healthy aging
- Demonstration of the application and optimization of cepstral analysis for analysis of muscle and brain activity
- A quantitative-based feature library for characterizing the neural control of movement with aging during unilateral, bilateral, and motor cognitive tasks
- A methodology for the selection and classification of time, frequency, information theory, nonlinear and cepstral features to characterize the neural control of movement. In turn providing future potential contributions for: 1) a methodology for physiologist to analyze and interpret data; 2) a computational tool to provide early detection of neuromuscular disorders in healthy populations; 3) a methodology for assessing the status and rehabilitation of patient populations.
- Functional explanations for the association of features with aging during unilateral, bilateral, and motor cognitive tasks.

The research in this dissertation has been published in following forms:
Journal(s):

- **A.N. Johnson** and Shinohara, M. "Corticomuscular coherence with and without additional task in elderly," *Journal of Applied Physiology,* in press.

- **A.N. Johnson**, Wheaton, L. and Shinohara, M. "Attenuation of corticomuscular coherence with additional motor or non-motor task," *Clinical Neurophysiology,* vol. 122, pp. 356-363, 2011.

Peer-reviewed proceedings:

- **A.N. Johnson**, Sow, D. and Biem, A. "A Discriminative Approach to EEG Seizure Detection," *Proceedings of the American Medical Informatics Association (AMIA 2011),* pp. 1309-1317, 2011.

- **A.N. Johnson**, Vachtsevanos, G. and Shinohara, M. "Feature subset selection for age-related changes in EEG and EMG during motor tasks," *Proceedings of the 2010 International Conference of the IEEE Engineering in Medicine and Biology Society,* pp. 3285-3288, 2010.

Additional studies supporting the dissertation work:
Journal(s):

- **A.N. Johnson**, Huo, X., Ghovanloo, M. and Shinohara, M. "Dual-task motor performance with a tongue-operated assistive technology compared with hand operations," *Journal of NeuroEngineering and Rehabilitation,* in press.

Peer-reviewed proceedings:

- J. Fairley, **Johnson, A.N.**, Georgoulas, G. and Vachtsevanos, G. "Automated polysomnogram artifact compensation using the generalized singular value decomposition algorithm," *Proceedings of the 2010 International Conference of the IEEE Engineering in Medicine and Biology Society,* pp. 5097-5100, 2010.

- **A.N. Johnson**, Huo, X., Cheng, C., Ghovanloo, M. and Shinohara, M. "Effects of additional workload on hand and tongue performance," *Proceedings of the 2010 International Conference of the IEEE Engineering in Medicine and Biology Society,* pp. 6611-6614, 2010.

APPENDIX A

EDINBURGH HANDEDNESS INVENTORY

Subject ID:_____

Please indicate your preferences in the use of hands in the following activities by putting + in the appropriate column. Where the preference is so strong that you would never try to use the other hand unless absolutely forced to, put ++. If in any case you are really indifferent put + in both columns. Some of the activities require both hands. In these cases the part of the task, or object, for which hand preference is wanted is indicated in brackets. Please try to answer all of the questions, and only leave a blank if you have no experience at all of the object or task.

Table 27: Handedness Inventory.

		Left	Right
1	Writing		
2	Drawing		
3	Throwing		
4	Scissors		
5	Toothbrush		
6	Knife (without fork)		
7	Spoon		
8	Broom (upper hand)		
9	Striking Match (match)		
10	Opening box (lid)		
11	Which foot do you prefer to kick with?		
12	Which eye do you use when using only one?		

Laterality quotient (L.Q.) value* = _____

* the L.Q. value is the total number of +'s for the RIGHT hand boxes, less the total number of +'s for the LEFT hand boxes, divided by the total +'s in both RIGHT and LEFT hand boxes.

APPENDIX B

MINI-MENTAL STATE EXAM

Table 28: Mini-Mental State Exam.

Maximum	Score	
5		What is the (year) (season) (date) (day) (month)?
5		Where are we (state) (country) (town/city) (campus of) (floor)?
3		Name 3 objects: 1 second to say each. Then ask the subject all 3 after you have said them.
5		Count by serial 7's and stop after 5 answers.
3		What were the three objects learned above?
2		Name a pencil and watch.
1		Repeat the following "No ifs, ands, or buts"
3		Follow a 3-stage command:"Take a paper in your hand, fold it in half, and put it on the floor."
1		Read and obey the following: CLOSE YOUR EYES
1		Write a sentence.
1		Copy the design shown.

/30 Total Score Alert Overtly Anxious Concentration Difficulty Drowsy

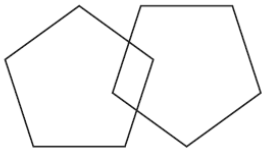

Figure 57: Mini-Mental State Exam design.

APPENDIX C

FEATURE LIBRARY

Table 29: Feature Library Part 1

Feature Name	Feature Equation	Channels	Feature Domain
Coherence	$\mid C_{xy}(f) \mid^2 = \frac{\mid P_{xy}(f) \mid^2}{P_{xx}(f)P_{yy}(f)}$	EMG-C3, EMG-F3, EMG-FC3, C3-C4, F3-F4, FC3-FC4	Frequency
Power Spectral Density (maximum)	$max(\mid FFT(x_i) \mid^2)$	All 7 channels	Frequency
Power Spectral Density (relative)	$\frac{\mid FFT(x_i) \mid^2_{subband}}{\mid FFT(x_i) \mid^2_{total}}$	All 7 channels	Frequency
Wavelet Coherence	$Coh_W(a,b) = \frac{\left\mid \sum_{i=1}^{n} \overline{W_\psi x_i(a,b)} W_\psi y_i(a,b) \right\mid^2}{\sum_{i=1}^{n} \left\mid W_\psi x_i(a,b) \right\mid^2 \sum_{i=1}^{n} \left\mid W_\psi y_i(a,b) \right\mid^2}$	EMG-C3, EMG-F3, EMG-FC3, C3-C4, F3-F4, FC3-FC4	Frequency
Mean Absolute Value	$\frac{1}{n} \sum_i^n \mid x_i \mid$	All 7 channels	Time
Standard Deviation	$\sqrt{\frac{1}{n} \sum_i^n (x_i - \bar{x})^2}$	All 7 channels	Time
Zero-crossing	$ZC'_i =$ $1, x_i \leq 0 \cap x_{i+1}$ $1, x_i \geq 0 \cap x_{i+1}$ $0, otherwise$ $ZC = \sum_i^{n-1} ZC'_i$	All 7 channels	Time

Table 30: Feature Library Part 2

Feature Name	Feature Equation	Channels	Feature Domain
Mutual Information	$\sum_{y \in Y} \sum_{x \in X} p(x,y) log\left(\frac{p(x,y)}{p(x)p(y)}\right)$	EMG-C3, EMG-F3, EMG-FC3, C3-C4, F3-F4, FC3-FC4	Information Theory
Kurtosis	$\frac{\frac{1}{n}\sum_i^n (x_i - \bar{x})^4}{\left(\sqrt{\frac{1}{n}\sum_i^n (x_i - \bar{x})^2}\right)^4}$	All 7 channels	Information Theory
Complexity	$\sqrt{\frac{a_4}{a_0}}$ a_4, variance of 2nd derivative of signal a_0, variance of signal	All 7 channels	Information Theory
Sample Entropy	$-ln\left(\frac{A}{B}\right)$ $\frac{A}{B}$, conditional probability that two sequences within a particular tolerance remain in that tolerance at the next point	All 7 channels	Information Theory
Shannon Entropy	$-\sum_i^n (pdf(x_i) * log(pdf(x_i)))$	All 7 channels	Information Theory
Nonlinear Energy	$\sum_i^n x_i^2 - x_{i+1}x_{i-1}$	All 7 channels	Nonlinear
Katz Fractal Dimension	$\sum_i^n \frac{log(n-1)}{log\left(\frac{max\left(\sum \sqrt{(x_i - x_1)^2 + i^2}\right)}{\sum \sqrt{(x_{i+1} - x_i)^2 + 1}}\right) + log(n-1)}$	All 7 channels	Nonlinear
Real Cepstrum	$FFT^{-1}(log\lvert FFT(x)\rvert)$	All 7 channels	Cepstral (Nonlinear)
Mel-Frequency Cepstrum	$DCT(log(FFT(x)))$	All 7 channels	Cepstral (Nonlinear)

REFERENCES

[1] Allen, P., Polizzi, G., Krakow, K., Fish, D., and Lemieux, L., "Identification of EEG events in the MR scanner: the problem of pulse artifact and a method for its subtraction," *Neuroimage*, vol. 8, no. 3, pp. 229–239, 1998.

[2] Baker, S. N., Olivier, E., and Lemon, R. N., "Coherent oscillations in monkey motor cortex and hand muscle EMG show task-dependent modulation," *Journal of Physiology*, vol. 501 (Pt 1), pp. 225–41, 1997.

[3] Baker, S., "Oscillatory interactions between sensorimotor cortex and the periphery," *Current Opinion in Neurobiology*, vol. 17, no. 6, pp. 649–655, 2007.

[4] Basmajian, J. and de Luca, C., *Muscles alive. Their functions revealed by electromyography.* 1985.

[5] Baweja, H., Patel, B., Martinkewiz, J., Vu, J., and Christou, E., "Removal of visual feedback alters muscle activity and reduces force variability during constant isometric contractions," *Experimental Brain Research*, vol. 197, no. 1, pp. 35–47, 2009.

[6] Bayraktaroglu, Z., von Carlowitz-Ghori, K., Losch, F., Nolte, G., Curio, G., and Nikulin, V., "Optimal imaging of cortico-muscular coherence through a novel regression technique based on multi-channel EEG and un-rectified EMG," *NeuroImage*, 2011.

[7] Beauchet, O., Dubost, V., Herrmann, F., Rabilloud, M., Gonthier, G., and Kressig, R., "Relationship between dual-task related gait changes and intrinsic risk factors for falls among transitional frail older adults," *Aging Clinical and Experimental Research*, vol. 17, no. 4, pp. 270–275, 2005.

[8] Begg, R., Palaniswami, M., and Owen, B., "Support vector machines for automated gait classification," *IEEE Transactions on Biomedical Engineering*, vol. 52, no. 5, pp. 828–838, 2005.

[9] Begic, D., Hotujac, L., and Jokic-Begic, N., "Electroencephalographic comparison of veterans with combat-related post-traumatic stress disorder and healthy subjects," *International Journal of Psychophysiology*, vol. 40, no. 2, pp. 167–172, 2001.

[10] Biem, A., "Minimum classification error training of hidden markov models for handwriting recognition," in *Proceedings of IEEE International Conference on Acoustics Speech and Signal Processing (ICASSP)*, vol. 3, 2001.

[11] Biem, A., "Minimum classification error training for online handwriting recognition," *IEEE Transactions on Pattern Analysis and Machine Intelligence*, pp. 1041–1051, 2006.

[12] Biem, A., Katagiri, S., McDermott, E., and Juang, B.-H., "An application of discriminative feature extraction to filter-bank-based speech recognition," *IEEE Transactions on Speech and Audio Processing*, vol. 9, pp. 96–110, Feb. 2001.

[13] Blum, A. L. and Langley, P., "Selection of relevant features and examples in machine learning," *Artificial Intelligence*, vol. 97, no. 1-2, pp. 245–271, 1997.

[14] Boonstra, T., van Wijk, B., Praamstra, P., and Daffertshofer, A., "Corticomuscular and bilateral emg coherence reflect distinct aspects of neural synchronization," *Neuroscience Letters*, vol. 463, no. 1, pp. 17–21, 2009.

[15] Burrell, L. S., Smart, O. L., , G., and Vachtsevanos, G. J., "Evaluation of Feature Selection Techniques for Analysis of Functional MRI and EEG," in *IEEE International Conference on Data Mining*, June 2007.

[16] Cabeza, R., Anderson, N., Locantore, J., and McIntosh, A., "Aging gracefully: compensatory brain activity in high-performing older adults," *Neuroimage*, vol. 17, no. 3, pp. 1394–1402, 2002.

[17] Chakarov, V., Naranjo, J., Schulte-Monting, J., Omlor, W., Huethe, F., and Kristeva, R., "Beta-range EEG-EMG coherence with isometric compensation for increasing modulated low-level forces," *Journal of Neurophysiology*, vol. 102, no. 2, p. 1115, 2009.

[18] Chao, E., *Biomechanics of the hand: a basic research study*. World Scientific Publication Co. Inc., 1989.

[19] Christensen, H., Mackinnon, A., Korten, A., Jorm, A., Henderson, A., Jacomb, P., and Rodgers, B., "An analysis of diversity in the cognitive performance of elderly community dwellers: Individual differences in change scores as a function of age," *Psychology and Aging*, vol. 14, no. 3, p. 365, 1999.

[20] Conway, B. A., Halliday, D. M., Farmer, S. F., Shahani, U., Maas, P., Weir, A. I., and Rosenberg, J. R., "Synchronization between motor cortex and spinal motoneuronal pool during the performance of a maintained motor task in man," *Journal of Physiology*, vol. 489, no. 3, pp. 917–924, 1995.

[21] Conway, B. A., Reid, C., and Halliday, D. M., "Low frequency corticomuscular coherence during voluntary rapid movements of the wrist joint," *Brain Topography*, vol. 16, no. 4, pp. 221–224, 2004.

[22] Craik, F. and Salthouse, T., *The handbook of aging and cognition*. Lawrence Erlbaum, 2000.

[23] Cramer, S., Nelles, G., Benson, R., Kaplan, J., Parker, R., Kwong, K., Kennedy, D., Finklestein, S., and Rosen, B., "A functional MRI study of subjects recovered from hemiparetic stroke," *Stroke*, vol. 28, no. 12, pp. 2518–2527, 1997.

[24] Duda, R., Hart, P., and Stork, D., *Pattern Classification (2nd Edition)*. Wiley-Interscience, 2000.

[25] Duffy, F., Albert, M., Mcanulty, G., and Garvey, A., "Age-related differences in brain electrical activity of healthy subjects," *Annals of Neurology*, vol. 16, no. 4, pp. 430–438, 1984.

[26] Duffy, F., McAnulty, G., and Albert, M., "The pattern of age-related differences in electrophysiological activity of healthy males and females," *Neurobiology of Aging*, vol. 14, no. 1, pp. 73–84, 1993.

[27] Enoka, R., Christou, E., Hunter, S., Kornatz, K., Semmler, J., Taylor, A., and Tracy, B., "Mechanisms that contribute to differences in motor performance between young and old adults," *Journal of Electromyography and Kinesiology*, vol. 13, no. 1, pp. 1–12, 2003.

[28] Esteller, R., Vachtsevanos, G., Echauz, J., and Litt, B., "A comparison of waveform fractal dimension algorithms," *Circuits and Systems I: Fundamental Theory and Applications, IEEE Transactions on*, vol. 48, no. 2, pp. 177–183, 2001.

[29] Fang, Y., Daly, J. J., Sun, J., Hvorat, K., Fredrickson, E., Pundik, S., Sahgal, V., and Yue, G. H., "Functional corticomuscular connection during reaching is weakened following stroke," *Clinical Neurophysiology*, vol. 120, no. 5, pp. 994–1002, 2009.

[30] Farina, D., Merletti, R., and Enoka, R., "The extraction of neural strategies from the surface emg," *Journal of Applied Physiology*, vol. 96, no. 4, p. 1486, 2004.

[31] Farmer, S., Gibbs, J., Halliday, D., Harrison, L., James, L., Mayston, M., and Stephens, J., "Changes in emg coherence between long and short thumb abductor muscles during human development," *Journal of Physiology*, vol. 579, no. 2, pp. 389–402, 2007.

[32] Faul, S., Gregorcic, G., Boylan, G., Marnane, W., Lightbody, G., and Connolly, S., "Gaussian Process Modeling of EEG for the Detection of Neonatal Seizures," *Biomedical Engineering, IEEE Transactions on*, vol. 54, no. 12, pp. 2151 –2162, 2007.

[33] Feige, B., Aertsen, A., and Kristeva-Feige, R., "Dynamic synchronization between multiple cortical motor areas and muscle activity in phasic voluntary movements," *Journal of Neurophysiology*, vol. 84, no. 5, pp. 2622–9, 2000.

[34] Fleury, A., Vacher, M., and Noury, N., "SVM-based multimodal classification of activities of daily living in health smart homes: sensors, algorithms, and first experimental results," *IEEE Transactions on Information Technology in Biomedicine*, vol. 14, no. 2, pp. 274–283, 2010.

[35] Folstein, M., Folstein, S., and McHugh, P., "Mini-mental state: a practical method for grading the cognitive state of patients for the clinician," *Journal of Psychiatric Research*, 1975.

[36] Galganski, M., Fuglevand, A., and Enoka, R., "Reduced control of motor output in a human hand muscle of elderly subjects during submaximal contractions," *Journal of Neurophysiology*, vol. 69, no. 6, p. 2108, 1993.

[37] Garry, M., van Steenis, R., and Summers, J., "Interlimb coordination following stroke," *Human Movement Science*, vol. 24, no. 5-6, pp. 849–864, 2005.

[38] Goble, D., Coxon, J., Van Impe, A., De Vos, J., Wenderoth, N., and Swinnen, S., "The neural control of bimanual movements in the elderly: Brain regions exhibiting age-related increases in activity, frequency-induced neural modulation, and task-specific compensatory recruitment," *Human Brain Mapping*, vol. 31, no. 8, pp. 1281–1295, 2010.

[39] Goldberger, A., Amaral, L., Glass, L., Hausdorff, J., Ivanov, P., Mark, R., Mietus, J., Moody, G., Peng, C., and Stanley, H., "PhysioBank, PhysioToolkit, and PhysioNet: Components of a new research resource for complex physiologic signals," *Circulation*, vol. 101, no. 23, p. e215, 2000.

[40] Goldberger, A., Amaral, L., Hausdorff, J., Ivanov, P., Peng, C., and Stanley, H., "Fractal dynamics in physiology: alterations with disease and aging," *Proceedings of the National Academy of Sciences of the United States of America*, vol. 99, no. Suppl 1, p. 2466, 2002.

[41] Gotman, J., Flanagan, D., Zhang, J., and Rosenblatt, B., "Automatic seizure detection in the newborn: methods and initial evaluation," *Electroencephalography and Clinical Neurophysiology*, vol. 103, no. 3, pp. 356 – 362, 1997.

[42] Graziadio, S., Basu, A., Tomasevic, L., Zappasodi, F., Tecchio, F., and Eyre, J., "Developmental tuning and decay in senescence of oscillations linking the corticospinal system," *Journal of Neuroscience*, vol. 30, no. 10, p. 3663, 2010.

[43] Grosse, P., Guerrini, R., Parmeggiani, L., Bonanni, P., Pogosyan, A., and Brown, P., "Abnormal corticomuscular and intermuscular coupling in high-frequency rhythmic myoclonus," *Brain*, vol. 126, no. Pt 2, pp. 326–42, 2003.

[44] Halliday, D. M., Conway, B. A., Farmer, S. F., and Rosenberg, J. R., "Using electroencephalography to study functional coupling between cortical activity and electromyograms during voluntary contractions in humans," *Neuroscience Letters*, vol. 241, no. 1, pp. 5–8, 1998.

[45] Halliday, D. M., Rosenberg, J. R., Amjad, A. M., Breeze, P., Conway, B. A., and Farmer, S. F., "A framework for the analysis of mixed time series/point process data–theory and application to the study of physiological tremor, single motor unit discharges and electromyograms," *Prog Biophys Mol Biol*, vol. 64, no. 2-3, pp. 237–78, 1995.

[46] Halliday, D. and Rosenberg, J., "On the application, estimation and interpretation of coherence and pooled coherence," *Journal of Neuroscience Methods*, vol. 100, no. 1-2, p. 173, 2000.

[47] Henderson, G., Ifeachor, E., Wimalaratna, H., Allen, T., and Hudson, R., "Prospects for routine detection of dementia using the fractal dimension of the human electroencephalogram," in *Science, Measurement and Technology, IEE Proceedings*, vol. 147, pp. 321–326, IET, 2000.

[48] Heuninckx, S., Wenderoth, N., and Swinnen, S., "Systems neuroplasticity in the aging brain: recruiting additional neural resources for successful motor performance in elderly persons," *Journal of Neuroscience*, vol. 28, no. 1, p. 91, 2008.

[49] Hiraga, C., Garry, M., Carson, R., and Summers, J., "Dual-task interference: attentional and neurophysiolgical influences," *Behavioral Brain Research*, vol. 205, no. 1, pp. 10–18, 2009.

[50] Hortobágyi, T., Solnik, S., Gruber, A., Rider, P., Steinweg, K., Helseth, J., and DeVita, P., "Interaction between age and gait velocity in the amplitude and timing of antagonist muscle coactivation," *Gait & Posture*, vol. 29, no. 4, pp. 558–564, 2009.

[51] Hu, X. and Keilholz, S., "Class notes for ECE 6786 - Medical Imaging Systems." A study of the principles and design of medical imaging systems.

[52] Hughes, J. and Cayaffa, J., "The EEG in patients at different ages without organic cerebral disease," *Electroencephalography and Clinical Neurophysiology*, vol. 42, no. 6, pp. 776–784, 1977.

[53] James, L. M., Halliday, D. M., Stephens, J. A., and Farmer, S. F., "On the development of human corticospinal oscillations: age-related changes in eeg-emg coherence and cumulant," *European Journal of Neuroscience*, vol. 27, no. 12, pp. 3369–79, 2008.

[54] Jasper, H., "The ten-twenty electrode system of the international federation," *Clinical Neurophysiology*, vol. 10, pp. 370–75, 1958.

[55] Johansson, B. B., "Brain plasticity and stroke rehabilitation. the willis lecture," *Stroke*, vol. 31, no. 1, pp. 223–30, 2000.

[56] Johnson, A. N., Huo, X., Ghovanloo, M., and Shinohara, M., "Dual-task motor performance with a tongue-operated assistive technology compared with hand operations," *Journal of NeuroEngineering and Rehabilitation*, vol. 9, 2012.

[57] Johnson, A. N. and Shinohara, M., "Beta band corticomuscular coherence with an additional motor or non-motor task in healthy elderly adults," *40th Annual Meeting of the Society for Neuroscience*, 2010.

[58] Johnson, A. N. and Shinohara, M., "Corticomuscular coherence with and without additional task in elderly," *Journal of Applied Physiology*, in press.

[59] Johnson, A. N., Sow, D., and Biem, A., "A discriminative approach to eeg seizure detection," in *Proc. of the American Medical Informatics Association (AMIA 2011)*, pp. 1309–1317, AMIA, 2011.

[60] Johnson, A. N., Vohra, S., and Shinohara, M., "Distinct neural strategies underlie increased emg and force variability between cognitive and motor tasks in young and elderly adults," *39th Annual Meeting of the Society for Neuroscience*, 2009.

[61] Johnson, A. N., Wheaton, L., and Shinohara, M., "Attenuation of corticomuscular coherence with additional motor or non-motor task," *Clinical Neurophysiology*, vol. 122, no. 2, pp. 356–363, 2011.

[62] Johnson, A. N., V. G. J. and Shinohara, M., "Feature subset selection for age-related changes in EEG and EMG during motor tasks," in *Proceedings of the 2010 International Conference of the IEEE Engineering in Medicine and Biology Society*, pp. 3285–3288, 2010.

[63] Juang, B.-H. and S.Katagiri, "Discriminative learning for minimum error classification," *IEEE Trans. on Acoustics, Speech, and Signal Processing*, vol. 40, no. 12, pp. 3042–3054, 1992.

[64] Kandel, E., Schwartz, J., Jessell, T., Mack, S., and Dodd, J., *Principles of Neural Science*, vol. 3. Elsevier New York, 1991.

[65] Kattla, S. and Lowery, M., "Fatigue related changes in electromyographic coherence between synergistic hand muscles," *Experimental Brain Research*, vol. 202, no. 1, pp. 89–99, 2010.

[66] Katz, R. and Horowitz, G., "Electroencephalogram in the septuagenarian: studies in a normal geriatric population.," *Journal of the American Geriatrics Society*, vol. 30, no. 4, p. 273, 1982.

[67] Kawashima, R., Taira, M., Okita, K., Inoue, K., Tajima, N., Yoshida, H., Sasaki, T., Sugiura, M., Watanabe, J., and Fukuda, H., "A functional mri study of simple arithmetic–a comparison between children and adults," *Cognitive Brain Research*, vol. 18, no. 3, pp. 227–233, 2004.

[68] Keen, D., Yue, G., and Enoka, R., "Training-related enhancement in the control of motor output in elderly humans," *Journal of Applied Physiology*, vol. 77, no. 6, p. 2648, 1994.

[69] Kelly-Hayes, M., Beiser, A., Kase, C., Scaramucci, A., D'Agostino, R., and Wolf, P., "The influence of gender and age on disability following ischemic stroke: the framingham study* 1," *Journal of Stroke and Cerebrovascular Diseases*, vol. 12, no. 3, pp. 119–126, 2003.

[70] Kern, D., Semmler, J., and Enoka, R., "Long-term activity in upper-and lower-limb muscles of humans," *Journal of Applied Physiology*, vol. 91, no. 5, p. 2224, 2001.

[71] Kil, D. and Shin, F. B., *Pattern Recognition and Predictions with Applications to Signal Characterization*. AIP Press, 1996.

[72] Kilner, J. M., Baker, S. N., Salenius, S., Hari, R., and Lemon, R. N., "Human cortical muscle coherence is directly related to specific motor parameters," *Journal of Neuroscience*, vol. 20, no. 23, pp. 8838–45, 2000.

[73] Kilner, J. M., Baker, S. N., Salenius, S., Jousmaki, V., Hari, R., and Lemon, R. N., "Task-dependent modulation of 15-30 hz coherence between rectified emgs from human hand and forearm muscles," *Journal of Physiolology*, vol. 516 (Pt 2), pp. 559–70, 1999.

[74] Kilner, J. M., Salenius, S., Baker, S. N., Jackson, A., Hari, R., and Lemon, R. N., "Task-dependent modulations of cortical oscillatory activity in human subjects during a bimanual precision grip task," *Neuroimage*, vol. 18, no. 1, pp. 67–73, 2003.

[75] Koyama, K., Hirasawa, H., Okubo, Y., and Karasawa, A., "Quantitative EEG correlates of normal aging in the elderly.," *Clinical Electroencephalography*, vol. 28, no. 3, p. 160, 1997.

[76] Kristeva, R., Patino, L., and Omlor, W., "Beta-range cortical motor spectral power and corticomuscular coherence as a mechanism for effective corticospinal interaction during steady-state motor output," *Neuroimage*, vol. 36, no. 3, pp. 785–92, 2007.

[77] Kristeva-Feige, R., Fritsch, C., Timmer, J., and Lucking, C. H., "Effects of attention and precision of exerted force on beta range eeg-emg synchronization during a maintained motor contraction task," *Clinical Neurophysiology*, vol. 113, no. 1, pp. 124–31, 2002.

[78] Lauer, R. and Prosser, L., "Use of the teager-kaiser energy operator for muscle activity detection in children," *Annals of Biomedical Engineering*, vol. 37, no. 8, pp. 1584–1593, 2009.

[79] Lewis, G. and Bybow, W., "Bimanual coordination dynamics in poststroke hemiparetics," *Journal of Motor Behavior*, vol. 36, no. 2, pp. 174–188, 2004.

[80] Lipsitz, L. and Goldberger, A., "Loss of'complexity'and aging," *Journal of the American Medical Association*, vol. 267, no. 13, p. 1806, 1992.

[81] Logan, B., "Mel frequency cepstral coefficients for music modeling," in *International Symposium on Music Information Retrieval*, vol. 28, Citeseer, 2000.

[82] Lundbye-Jensen, J. and Nielsen, J. B., "Central nervous adaptations following 1 wk of wrist and hand immobilization," *Journal of Applied Physiology*, vol. 105, no. 1, pp. 139–51, 2008.

[83] Marshall, R., Perera, G., Lazar, R., Krakauer, J., Constantine, R., and DeLaPaz, R., "Evolution of cortical activation during recovery from corticospinal tract infarction," *Stroke*, vol. 31, no. 3, pp. 656–661, 2000.

[84] Mattay, V., Fera, F., Tessitore, A., Hariri, A., Das, S., Callicott, J., and Weinberger, D., "Neurophysiological correlates of age-related changes in human motor function," *Neurology*, vol. 58, no. 4, p. 630, 2002.

[85] McDermott, E. and Katagiri, S., "Minimum Classification Error for Large Scale Speech Recognition Tasks using Weighted Finite State Transducers," in *Proceedings of ICASSP*, vol. 1, pp. 113–116, March 2005.

[86] McDowd, J. and Craik, F., "Effects of aging and task difficulty on divided attention performance," *Journal of Experimental Psychology: Human Perception and Performance*, vol. 14, pp. 267–280, 1988.

[87] Mima, T. and Hallett, M., "Corticomuscular coherence: a review," *Journal of Clinical Neurophysiology*, vol. 16, no. 6, pp. 501–11, 1999.

[88] Mima, T., Simpkins, N., Oluwatimilehin, T., and Hallett, M., "Force level modulates human cortical oscillatory activities," *Neuroscience Letters*, vol. 275, no. 2, pp. 77–80, 1999.

[89] Mima, T., Toma, K., Koshy, B., and Hallett, M., "Coherence between cortical and muscular activities after subcortical stroke," *Neuroscience Letters*, vol. 32, no. 11, pp. 2597–2601, 2001.

[90] Murthy, V. N. and Fetz, E. E., "Coherent 25- to 35-Hz oscillations in the sensorimotor cortex of awake behaving monkeys," *Proc. of the National Academy of Science U S A*, vol. 89, no. 12, pp. 5670–4, 1992.

[91] Murthy, V. N. and Fetz, E. E., "Oscillatory activity in sensorimotor cortex of awake monkeys: synchronization of local field potentials and relation to behavior," *Journal Neurophysiology*, vol. 76, no. 6, pp. 3949–67, 1996a.

[92] Myers, L., Lowery, M., O'Malley, M., Vaughan, C., Heneghan, C., Gibson, A., Harley, Y., and Sreenivasan, R., "Rectification and non-linear pre-processing of emg signals for cortico-muscular analysis," *Journal of Neuroscience Methods*, vol. 124, no. 2, pp. 157–165, 2003.

[93] Neto, O., Baweja, H., and Christou, E., "Increased voluntary drive is associated with changes in common oscillations from 13 to 60 Hz of interference but not rectified electromyography," *Muscle & Nerve*, 2010.

[94] Neto, O. and Christou, E., "Rectification of the EMG signal impairs the identification of oscillatory input to the muscle," *Journal of Neurophysiology*, vol. 103, no. 2, p. 1093, 2010.

[95] Neuper, C. and Pfurtscheller, G., "Evidence for distinct beta resonance frequencies in human eeg related to specific sensorimotor cortical areas," *Clinical Neurophysiology*, vol. 112, no. 11, pp. 2084–2097, 2001.

[96] Niedermeyer, E. and Da Silva, F., *Electroencephalography: basic principles, clinical applications, and related fields*. Lippincott Williams & Wilkins, 2005.

[97] Nunez, P. and Srinivasan, R., *Electric fields of the brain: the neurophysics of EEG*. Oxford University Press, USA, 2006.

[98] of Health: National Institute of Aging, U. S. N. I., "Health disparities strategic plan: Fiscal years 2009-2013," April 2010.

[99] of Health: National Institute of Neurological Disorders, U. S. N. I. and Stroke, "Ninds strategic plan: Priorities and plans for the national institute of neurological disorders and stroke," June 2010.

[100] Oldfield, R. C., "The assessment and analysis of handedness: The Edinburgh inventory," *Neuropsychologia*, vol. 9, no. 1, pp. 97–113, 1971.

[101] Perez, M. A., Lundbye-Jensen, J., and Nielsen, J. B., "Changes in corticospinal drive to spinal motoneurones following visuo-motor skill learning in humans," *Journal of Physiology*, vol. 573, no. Pt 3, pp. 843–55, 2006.

[102] Pfurtscheller, G. and Neuper, C., "Event-related synchronization of mu rhythm in the EEG over the cortical hand area in man," *Neuroscience letters*, vol. 174, no. 1, pp. 93–96, 1994.

[103] Pikkujämsä, S., Mäkikallio, T., Sourander, L., Räihä, I., Puukka, P., Skyttä, J., Peng, C., Goldberger, A., and Huikuri, H., "Cardiac

interbeat interval dynamics from childhood to senescence: comparison of conventional and new measures based on fractals and chaos theory," *Circulation*, vol. 100, no. 4, pp. 393–399, 1999.

[104] Plonsey, R. and Barr, R., *Bioelectricity: A quantitative approach*. Springer, 2007.

[105] Pols, L., "Spectral analysis and identification of dutch vowels in monosyllabic words," *Doctoral dissertion, Free University, Amsterdam, The Netherlands*, 1977.

[106] Rabiner, L. and Juang, B., *Fundamentals of speech recognition*. Prentice hall Englewood Cliffs, New Jersey, 1993.

[107] Rankin, J., Woollacott, M., Shumway-Cook, A., and Brown, L., "Cognitive influence on postural stability," *The Journals of Gerontology Series A: Biological Sciences and Medical Sciences*, vol. 55, no. 3, pp. M112–M119, 2000.

[108] Rosamond, W., Flegal, K., Friday, G., Furie, K., Go, A., Greenlund, K., Haase, N., Ho, M., Howard, V., Kissela, B., and others, "Heart disease and stroke statistics–2007 update: a report from the american heart association statistics committee and stroke statistics subcommittee," *Circulation*, vol. 115, no. 5, p. e69, 2007.

[109] Rosenberg, J. R., Amjad, A. M., Breeze, P., Brillinger, D. R., and Halliday, D. M., "The fourier approach to the identification of functional coupling between neuronal spike trains," *Progress in Biophysics and Molecular Biology*, vol. 53, no. 1, pp. 1–31, 1989.

[110] Roubicek, J., "The electroencephalogram in the middle-aged and the elderly.," *Journal of the American Geriatrics Society*, vol. 25, no. 4, p. 145, 1977.

[111] Sadato, N., Yonekura, Y., Waki, A., Yamada, H., and Ishii, Y., "Role of the supplementary motor area and the right premotor cortex in the coordination of bimanual finger movements," *Journal of Neuroscience*, vol. 17, no. 24, p. 9667, 1997.

[112] Safri, N. M., Murayama, N., Igasaki, T., and Hayashida, Y., "Effects of visual stimulation on cortico-spinal coherence during isometric hand contraction in humans," *International Journal of Psychophysiology*, vol. 61, no. 2, pp. 288–93, 2006.

[113] Sailer, A., Dichgans, J., and Gerloff, C., "The influence of normal aging on the cortical processing of a simple motor task," *Neurology*, vol. 55, no. 7, p. 979, 2000.

[114] Schmied, A., Pagni, S., Sturm, H., and Vedel, J. P., "Selective enhancement of motoneurone short-term synchrony during an attention-demanding task," *Experimental Brain Research*, vol. 133, no. 3, pp. 377–390, 2000.

[115] Semmler, J., Kornatz, K., and Enoka, R., "Motor-unit coherence during isometric contractions is greater in a hand muscle of older adults," *Journal of Neurophysiology*, vol. 90, no. 2, p. 1346, 2003.

[116] Semmler, J., Kornatz, K., Meyer, F., and Enoka, R., "Diminished task-related adjustments of common inputs to hand muscle motor neurons in older adults," *Experimental Brain Research*, vol. 172, no. 4, pp. 507–518, 2006.

[117] Shahid, S. and Smith, L., "Cepstrum of bispectrum spike detection on extracellular signals with concurrent intracellular signals," *BMC Neuroscience*, vol. 10, no. Suppl 1, p. P59, 2009.

[118] Shinohara, M., "Adaptations in motor unit behavior in elderly adults.," *Current Aging Science*, vol. 4, pp. 200–208.

[119] Shinohara, M., Scholz, J., Zatsiorsky, V., and Latash, M., "Finger interaction during accurate multi-finger force production tasks in young and elderly persons," *Experimental Brain Research*, vol. 156, no. 3, pp. 282–292, 2004.

[120] Shoeb, A., "Application of machine learning to epileptic seizure onset detection and treatment," *PhD Thesis, Massachusetts Institute of Technology*, 2009.

[121] Si, Y., Gotman, J., Pasupathy, A., Flanagan, D., Rosenblatt, B., and Gottesman, R., "An expert system for EEG monitoring in the pediatric intensive care unit," *Electroencephalography and Clinical Neurophysiology*, vol. 106, no. 6, pp. 488–500, 1998.

[122] Solnik, S., DeVita, P., Rider, P., Long, B., and Hortobágyi, T., "Teager–kaiser operator improves the accuracy of emg onset detection independent of signal-to-noise ratio," *Acta of bioengineering and biomechanics/Wroclaw University of Technology*, vol. 10, no. 2, p. 65, 2008.

[123] Somol, P., Pudil, P., and Kittler, J., "Fast branch and bound algorithms for optimal feature selection," *IEEE Trans. on Pattern Analysis and Machine Intelligence*, vol. 26, pp. 900–912, 2004.

[124] Sosnoff, J., Vaillancourt, D., and Newell, K., "Aging and rhythmical force output: loss of adaptive control of multiple neural oscillators," *Journal of Neurophysiology*, vol. 91, no. 1, p. 172, 2004.

[125] "SPSS, Data Mining, Statistical Analysis Software, Predictive Analytics, Decision Support Systems." http://www.spss.com.

[126] Stegeman, D., van de Ven, W., van Elswijk, G., Oostenveld, R., and Kleine, B., "The alpha-motoneuron pool as transmitter of rhythmicities in cortical motor drive," *Clinical Neurophysiology*, 2010.

[127] Stelmach, G. E., Amrhein, P. C., and Goggin, N. L., "Age differences in bimanual coordination," *Journal of Gerontology*, vol. 43, no. 1, pp. P18–23, 1988.

[128] Temko, A., Boylan, G., Marnane, W., and Lightbody, G. in *Engineering in Medicine and Biology Society, Proceedings of the 2010 International Conference of the IEEE*, pp. 3281–3284, 2010.

[129] Thomas, E., Temko, A., Lightbody, G., Marnane, W., and Boylan, G., "Gaussian mixture models for classification of neonatal seizures using EEG," *Physiological Measurement*, vol. 31, p. 1047, 2010.

[130] Ushiyama, J., Takahashi, Y., and Ushiba, J., "Muscle dependency of corticomuscular coherence in upper and lower limb muscles and training-related alterations in ballet dancers and weightlifters," *Journal of Applied Physiology*, vol. 109, no. 4, p. 1086, 2010.

[131] Vaillancourt, D. E., Larsson, L., and Newell, K. M., "Effects of aging on force variability, single motor unit discharge patterns, and the structure of 10, 20, and 40 hz emg activity," *Neurobiology of Aging*, vol. 24, no. 1, pp. 25–35, 2003.

[132] Vaillancourt, D. and Newell, K., "Changing complexity in human behavior and physiology through aging and disease," *Neurobiology of Aging*, vol. 23, no. 1, pp. 1–11, 2002.

[133] Vallesi, A., McIntosh, A., Kovacevic, N., Chan, S., and Stuss, D., "Age effects on the asymmetry of the motor system: Evidence from cortical oscillatory activity," *Biological Psychology*, 2010.

[134] Van der Heijden, F., Duin, R., De Ridder, D., and Tax, D., *Classification, Parameter Estimation and State Estimation*. Wiley Online Library, 2004.

[135] Vanneste, S., "Timing in aging: The role of attention," *Experimental Aging Research*, vol. 25, no. 1, pp. 49–67, 1999.

[136] Verhaeghen, P. and Cerella, J., "Aging, executive control, and attention: A review of meta-analyses," *Neuroscience & Biobehavioral Reviews*, vol. 26, no. 7, pp. 849–857, 2002.

[137] Verhaeghen, P., Steitz, D., Sliwinski, M., and Cerella, J., "Aging and dual-task performance: A meta-analysis.," *Psychology and Aging*, vol. 18, no. 3, p. 443, 2003.

[138] Voelcker-Regage, C. and Alberts, J. L., "Effects of motor practice on dual-task performance in older adults," *Journal of Gerontology*, vol. 62, no. 3, pp. 141–148, 2007.

[139] "Weka 3 - Data Mining with Open Source Machine Learning Software in Java." http://www.cs.waikato.ac.nz/ml/weka/.

[140] Welsh, S., Dinenno, D., and Tracy, B., "Variability of quadriceps femoris motor neuron discharge and muscle force in human aging," *Experimental Brain Research*, vol. 179, no. 2, pp. 219–233, 2007.

[141] Wheaton, L. A., Bohlhalter, S., Nolte, G., Shibasaki, H., Hattori, N., Fridman, E., Vorbach, S., Grafman, J., and Hallett, M., "Cortico-cortical networks in patients with ideomotor apraxia as revealed by eeg coherence analysis," *Neuroscience Letters*, vol. 433, no. 2, pp. 87–92, 2008.

[142] Wu, T. and Hallett, M., "Neural correlates of dual task performance in patients with parkinson's disease," *Journal of Neurology Neurosurgery Psychiatry*, vol. 79, no. 7, pp. 760–6, 2008.

[143] Yao, B., Salenius, S., Yue, G. H., Brown, R. W., and Liu, J. Z., "Effects of surface emg rectification on power and coherence analyses: An eeg and meg study," *Journal of Neuroscience Methods*, vol. 159, no. 2, pp. 215–223, 2007.

[144] Yu, X., Zhang, J., Xie, D., Wang, J., and Zhang, C., "Relationship between scalp potential and autonomic nervous activity during a mental arithmetic task," *Autonomic Neuroscience*, vol. 146, no. 1-2, pp. 81–86, 2009.

[145] Zhang, Y., Chen, Y., Bressler, S., and Ding, M., "Response preparation and inhibition: the role of the cortical sensorimotor beta rhythm," *Neuroscience*, vol. 156, no. 1, pp. 238–246, 2008.

[146] Zijdewind, I., van Duinen, H., Zielman, R., and Lorist, M. M., "Interaction between force production and cognitive performance in humans," *Clinical Neurophysiology*, vol. 117, no. 3, pp. 660–667, 2006.